TEXTILE RESEARCH JOURNAL

Publication of

TEXTILE RESEARCH INSTITUTE

OCTOBER 1961 NUMBER 10

One of a series

"NO, IT ISN'T OUR SOFTENER. IT'S JUST THEIR BUGS."

The accompanying sigh of relief was heard throughout the sales service lab. The 20x glass had shown that some indeterminate insects indigenous to southern Texas had ended their existence in the thousand dozen sweaters. When a scour didn't free the fragments from a sample, an enzyme did: the protease loosened the juice that held the bugs to the fibers, and the goods worked clean.

Has it ever occurred to you that soils of many sorts are stuck on with "juices"? It has — to the dry cleaner. From vests, rompers and summer slip covers, he removes gravy, egg and other stains we'd rather not mention — all with the help of an enzymatic digester. The reason we bring this whole matter up, of course, is that Wallerstein makes RSR, the **standard** dry cleaning digester. In fact, when it comes to making **many** chemical aids for the unromantic but necessary dry cleaning industry, Wallerstein's name is as significant as it is in textiles.

The significance for you? This: constant searching for better digesters has stocked our shelves with commercial, development and experimental enzymes of many types. Purity ranges from AR on down. Could some of these enzymes prove useful in your R&D? Perhaps if you dropped us a line detailing your needs, we might be able to help you work out some "bugs" from your problems. (And remember, please, we make Rapidase® and Serizyme® too.)

WALLERSTEIN COMPANY
Division of Baxter Laboratories, Inc.
Staten Island 3, N.Y.

Interested in alginate-solubilizing enzyme preparations? Write Dept. R-10.

TEXTILE RESEARCH JOURNAL

Volume 31 — *October 1961* — Number 10

Editor:
Richard K. Toner

Production Editor:
Dorothy Dana Hollmann

Advisory Board

Herbert J. Ball
Earl E. Berkley
John Boulton
C. H. Fisher
Walter J. Hamburger
Milton Harris
R. M. Hoffman
Harold P. Lundgren
Herman Mark
George Switlyk
Helmut Zahn

TEXTILE RESEARCH JOURNAL, published monthly at Prince and Lemon Streets, Lancaster, Pa., is devoted to the interest of research in textile and allied industries. It is published by Textile Research Institute.

Manuscripts and communications should be sent to the Publications Department, P.O. Box 625, Princeton, N. J.

Second-class postage paid at Lancaster, Pa.

Subscription rates: $25.00 per year; additional for postage, 50 cents to Canada, $1.00 to all other countries. Single copies, $2.50 each.

Contents copyright © 1961 by Textile Research Institute. Advertising rates supplied on request.

IN THIS ISSUE

Studies of High Fastness to Light in Coloring Matters in Hydrophilic Substrates. *Charles H. Giles, George Baxter, and Syed M. K. Rahman* 831

The Statistical Interpretation of Fiber Counts in Yarn Cross-Sections. *D. N. E. Cooper* 845

The Relationship of Fine Structure to Mechanical Properties of Stretched Saponified Acetate Fibers. *B. Sheldon Sprague and Herman D. Noether* 858

The Effect of the Short Fibers in a Cotton on Its Processing Efficiency and Product Quality. Part III: Pilot-Scale Processing of Yarns. *John D. Tallant, Louis A. Fiori, David M. Alberson, and Walter E. Chapman* 866

A Statistical Procedure for Determining End Breakage Rate in Spinning. *E. Fred Schultz, Jr., Herschel W. Little, John D. Tallant, and Louis A. Fiori* 872

Quantitative Investigation of the X-Ray Diffraction Picture of Some Typical Rayon Specimens, Part II. *P. H. Hermans and A. Weidinger* 875

Cross-Linking Etherified Cottons with Dimethylol Ethyleneurea. *Russell M. H. Kullman, John G. Frick, Jr., Robert M. Reinhardt, and J. David Reid* 877

A Quantitative Study of Differential Dyeing of Cotton as a Means of Elucidating Fiber Structure. *L. Rebenfeld and Hong Wu* 886

Adsorption of Calcium and Polyphosphates on Cotton Cellulose and Its Effect on Soil Deposition. *Beverly J. Rutkowski and Albert R. Martin* 892

Physical Properties of Wool Fibers at Various Regains. Part III: Study of the State of Water in Wool by N.M.R. Techniques. *G. W. West, A. R. Haly, and M. Feughelman* 899

Some Aspects of Capillary Absorption in Fibrous Textile Wicking. *R. D. Laughlin and J. E. Davies* 904

LETTERS TO THE EDITOR

The Molecular Configuration of Wool Keratin. *K. J. Whiteley* 911

Non-Lint Content Measurement by the One-Pass Shirley Analyzer Procedure. *R. L. N. Iyengar* 912

Molecular Conformation in Oriented Fibers. *A. V. Tobolsky and V. D. Gupta* 913

Chlorine Retention of Resin-Treated Cotton Fabrics. *M. K. Gokhale and P. C. Mehta* 915

REPRINT REQUESTS SHOULD BE DIRECTED TO THE AUTHORS

SEE ARTICLES FOR ADDRESSES

LAB. BLENDER—NEP COUNT

Developed by the United States Dept. of Agriculture

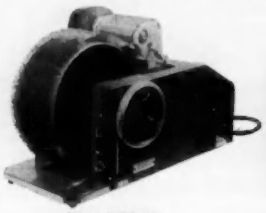

Model CS-45

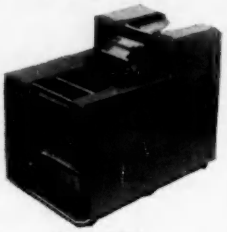

Model CS-69

The *Mechanical Cotton Blender* effectively blends cotton samples 20 times faster than by hand. The principal feature is an adjustable feed plate in combination with a fluted feed roll which feeds a sample into a rotary blending cylinder. Blending or carding of dyed samples for color combination is another use of this unit. (ASTM D1441-54).

The *Nep Test Machine* provides a rapid and satisfactory method of preparing specimens of raw cotton for nep evaluation. The design of this machine incorporates the principal mechanical assemblies of textile carding machines in order to simulate commercial production method (ASTM D1446-50T).

Folders and price upon request

As our name implies we also welcome the opportunity to work on custom design and manufacture of testing instruments of all types for individual and general needs.

CUSTOM SCIENTIFIC INSTRUMENTS, INC.

541 Devon Street **Kearny, N. J.**

OCTOBER 1961
VOL. 31 NO. 10

TEXTILE RESEARCH JOURNAL

Studies of High Fastness to Light in Coloring Matters in Hydrophilic Substrates

Charles H. Giles, George Baxter, and Syed M. K. Rahman

Colour Chemistry Research Laboratory, The Royal College of Science and Technology, Glasgow, C.1., Scotland

Abstract

A variety of dyes of high lightfastness, *viz.*, metal-complex and mordanted dyes on protein and cellulosic substrates, basic dye lakes, and reactive dyes, on cellulose, have been examined by fading-rate and CF (characteristic fastness) measurements. Apparently in all cases the dye is highly aggregated.

Normally with water-soluble dyes lightfastness improves with rise in concentration; theoretically this should not occur with pigments applied in substance, but in practice it does do so. The cause is shown to be aggregation of particles by capillary attraction before the fluid matrix sets to a solid.

It is shown that, on account of the relation between the association of a dye and its absorption spectrum, fading may tend to cause a reddening of shade of water-soluble dyes, and a blueing of water-insoluble ones.

The heat of illumination can break down dye aggregates and thus cause an apparent rise in depth of color. This effect, which occasionally masks fading in the early stages, is sometimes favored by dry conditions. The accelerated fading produced by rise in atmospheric humidity is due in some cases partly to the absence of this compensating factor; but it is also probably due to the mass action effect of an increase in concentration of the moisture that enters into the fading reaction.

THIS paper examines in detail some of the factors contributing to the improvement of the lightfastness of organic coloring matters. Previous papers from this laboratory [3, 4, 7, 9, 10, 11, 12] have emphasized that lightfastness in hydrophilic substrates is largely determined by the physical form of the dye, and the results have suggested that dyes of high lightfastness are likely to be more highly aggregated than those of low fastness. This suggestion has been confirmed by Weissbein and Coven in electron micrographic tests on a number of direct dyes in regenerated cellulose film [20]: they found that dyes of high fastness are present as aggregates, but those of low fastness are not, or at least, if aggregates are present, they are too small to be seen. In the present paper a number of lightfast dyes of different types are examined to determine whether aggregation is responsible for their fastness, and factors other than aggregation which influence fastness are also considered.

Three general methods are here used to detect qualitatively the presence of particulate dye: (a) spectrophotometric absorption tests; (b) examination of CF curves; (c) examination of fading-rate curves.

(a) The *absorption spectrum* of most dyes in the visible region shows two bands, the short-wave (γ) band representing associated dye and the long-wave

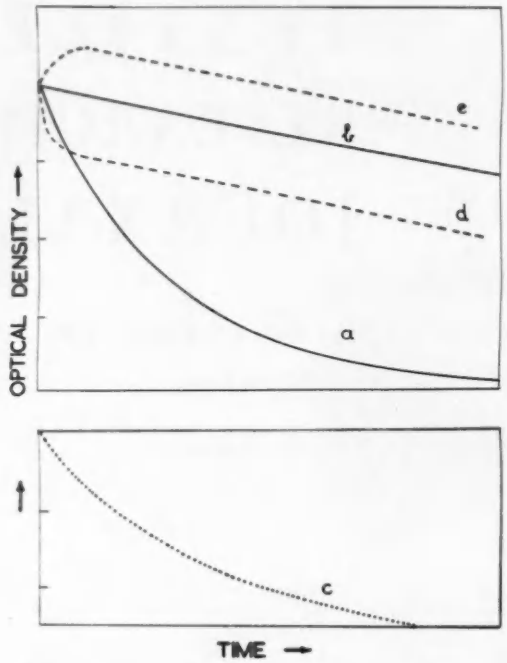

Fig. 1. Types of fading-rate curve given by dyes and pigments: a, first-order curve—dye in molecular dispersion; b, zero-order curve—dye or pigment in large particles; c, second-order curve—dye in molecular dispersion, substrate dry (?); d, first-order, followed by zero-order curve—dye partly in molecular dispersion and partly in large particles; e, zero-order curve with maximum—dye or pigment in large particles: partly disaggregating in heat of illuminant. Note. In some cases the first part of the falling section of the curve may be of first- or second-order type.

(x) band, representing monodisperse dye. An increase in the ratio of y/x extinctions represents an increase in degree of association [7, 14].

(b) The slope of the *CF (characteristic fading) curve* (log of time for a given loss of dye vs. log of initial concentration) gives qualitative information on the state of association of dye in the substrate. This is discussed briefly in a previous paper [11], and elsewhere in more detail [4, 10]. It has been shown [10] that in place of log t_F (t_F = time for a given loss of dye), the fastness grade number may be plotted, and similar (CFG, or "characteristic fastness grade") curves obtained. These also can give information on the physical state of the dye, but their detailed theory, which is complicated by effects of visual judgment of dye content, has not been worked out.

(c) The shape of the *fading-rate curve* is also informative upon the physical state of the dye [3]. Since a number of conclusions reached in this paper are based on interpretation of this type of curve, it is desirable to examine the significance of its shape in detail.

Theoretically, a truly monodisperse dye should fade at a rate that decreases exponentially with time (Figure 1a), i.e., a first-order reaction rate. In practice this type of fading is only rarely observed [3] and the types of fading-rate curve most often observed are shown in Figure 1 b, d, and e.[1]

Type b is a zero-order curve in which the rate remains constant with time. A true zero order would occur, in theory, only when the total area of dye surface exposed to air, moisture, and light, *remains constant throughout.* This obviously cannot occur if the dye is dispersed entirely as single molecules or small aggregates, all freely exposed; so that if a truly linear curve is obtained, the latter conditions do not hold. The reason, in the case of hydrophilic substrates, is most probably that only large aggregated particles of dye are present. Even so, if these particles are exposed on all sides, and so can fade over most of their surface, their total surface area will decrease as the dye fades and the decomposition products break away. It has been pointed out to us by a referee that in the case of freely exposed spherical dye particles fading at a rate proportional to the outer surface, the cube root of the weight will decrease proportionately with time; the fading-rate curve will then have a slowly decreasing slope and will be difficult to distinguish from a straight line over short ranges of fading.

There are, however, two complicating factors here. (i) Optical density is not proportional to dye weight if the particle size is not constant; for a constant weight of dye the optical density rises with decrease in particle size [6]. Thus as the particles become smaller on fading, this effect will tend to compensate for the loss of surface area of dye, and thus will tend to reduce the curvature of the fading-rate curve. (ii) The dye particles are never completely exposed; they must be to some extent trapped in the molecular chains of the (air-dye) substrate, and only a proportion of their external surface is accessible to

[1] The shapes of the respective curves for the y and x bands of most dyes are usually very similar, probably because of considerable overlapping of the absorptions of the associated and the monomeric forms.

oxygen, water, and light, and therefore susceptible to fading. (Indeed for this reason, the lightfastness of dye in aggregated particles may be much higher than expected from a mere decrease in the proportion of external surface to total weight.) A true zero-order fade could thus be observed in practice, because the area of *accessible* surface of dye could remain virtually constant over the period of observation. This situation is similar to that illustrated diagrammatically by Baxter et al. [4, Fig. 1c [2]].

In theory, of course, an apparently linear fading rate could be obtained from a molecular dispersion of a dye that is extremely resistant to photochemical decomposition, rendering impracticable an exposure long enough to show recognizable curvature. This does not seem to occur in practice. All cases of virtually linear fading so far encountered fall into one of two classes, described in this paper, *viz.*, those (i) in which the coloring matter is known to be present mainly as large particles, as in the case of pigment dispersions, or a direct dye shown by electron micrography to be highly aggregated, or (ii) in which there is other evidence that the dye is likely to be highly aggregated, as in some basic dye lakes and metal-complex dyes. It seems therefore reasonable to assume, as will be done in this paper, that a linear fade is evidence of a high degree of aggregation.

Water-soluble dyes usually give a curve of type d (Figure 1), or a form somewhere intermediate between d and a, in which an initial rapid fade occurs, nearly first-order; but this persists for only a short period, and the rate then quickly slows down, and may sometimes become almost zero-order. The most reasonable interpretation of this type of curve appears to be that a small proportion of the dye is highly dispersed, but most of it is aggregated.

An interesting type of curve (Figure 1e) is sometimes observed, in which there is an initial *negative fade*, i.e., the amount of dye present appears actually to increase with exposure, at first, because the optical density rises. It was earlier stated [3], and is further demonstrated below, that the probable cause is the initial breakup of large dye particles in the heat of the illumination. Indeed, in view of the points brought out in the discussion above, it is likely that this type of curve is probably the best indication given by fading tests of the presence of aggregated dye particles, because there does not appear to be any way in which it could be produced by a normal monodisperse dye.[3]

A unique type of curve, not shown here, was encountered earlier [3]. In this, the rate of fading steadily *increases*. The only system so far found giving this curve is an insoluble azo dye in methylethylcellulose films. The effect was attributed to a steady breakdown of large dye particles to small ones in the heat of the lamp; the small ones fade the more rapidly. (Presumably fading is rapid enough to neutralize any increase in optical density caused by the disaggregation itself—see above.) This effect is probably the cause of the very rapid breakdown that some azoic dyes on cellulose show in the final stages of the fading [*cf.* 18a].

It has been reported (Hirashima et al., private communication) that some direct cotton dyes fade according to a second-order law (linear relation between time and the reciprocal of optical density, or nearly constant curvature of the graph of optical density against time, Figure 1c). We have so far observed very few fades of this type. A possible cause of this type of fade may be that the destruction of a rapid-fading molecularly dispersed dye is retarded by a low moisture content of the substrate.

Pigments

It has already been pointed out [4, 10] that the CF curves of a pigment (over ranges of concentration in which not all the light is absorbed) should be horizontal, i.e., the lightfastness should be the same at all depths, because the particle-size distribution is constant. This comment applies strictly only to fastness measured by optical density; complications may occur in expressing this in terms of visual appearance of a pigmented opaque surface. Figure 2 shows that in practice a dye applied as a pigment gives a CF curve which, while not actually hori-

[2] The case shown applies when the accessible area of dye is the same for all concentrations, as well as remaining constant during fading. This gives a CF curve of maximum slope. If the accessible area, which is determined by a variety of physical conditions during dyeing and subsequent drying, is greater the greater the initial weight of dye, but once established, remains constant during fading, then a zero-order fade will still be observed at all concentrations, but the CF curve could have a lower slope than the maximum, indeed it could have any value down to zero (higher concentrations then fade more rapidly than in the conditions shown in the diagram).

[3] Morton [18a] suggested that some phototropic dyes might fade in this manner.

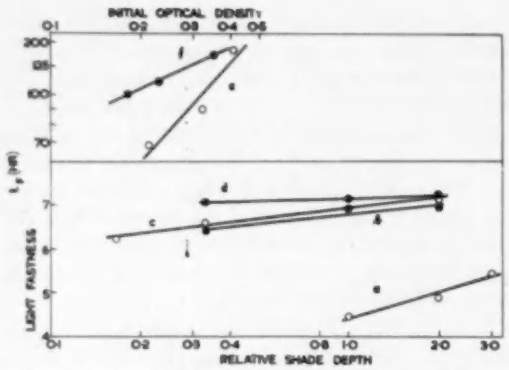

Fig. 2. CF and CFG curves for pigments and dyeings. (a) Azoic dyes applied by normal method. (b) Azoic dyes applied as resin-bonded pigments. Data for (a) and (b) supplied by the same manufacturer. (c) Vat dyes applied by normal method. (d) Vat and phthalocyanine dyes applied as resin-bonded pigments. Data for (c) and (d) supplied by the same manufacturer. Microfix Blue RX (Ciba) applied to gelatin films, (e) by vatting and dyeing on hardened gelatin, (f) by incorporation in gelatin solution as a pigment, with binder, and baking. (Gelatin solution was used because it was found impracticable to obtain even coloration by using a cellophane film.)

zontal, has a lower slope than that given when it is applied from a solution and afterwards insolubilized on the substrate (*cf.* also Figure 4 in [4]). This slope difference appears also in technical systems. Thus CFG curves for fabrics colored with commercial resin-bonded pigments have lower slope than those for fabrics dyed with insolubilized dyes of the same manufacturer (*cf.* Figure 19 in [10]). Other similar information (supplied in confidence by another manufacturer) is given in Table I.

One daylight figure appears to be anomalous. This may be the result of changes in atmospheric humidity (which was not controlled). In our own tests (Figure 2e, f), however, the CF curve slope for vat dyeings was not significantly affected by change in humidity, and that for the pigmented shades became slightly steeper under wet conditions.

TABLE I. Characteristic-Fastness-Grade (CFG) Curve Slopes * of an Identical Series of Coloring Matters Applied to Cellulose by Different Methods

Method of application	Exposure by Fade-Ometer	Exposure by Daylight	
Padding and resin-bonding	0.5	1.9(?)	0.25
Dyeing by vat method	1.3	1.1	

Bracketed data are from tests run simultaneously

* The slope given is the increase in mean fastness grade number for a ten-fold increase in shade depth.

Capillary Effects and Pigment Fastness

The cause of the positive slope of the CF curve for pigments must now be considered. Basically, of course, it means that the particle-size distribution is not constant over all concentrations; with rise in concentration the proportion of larger particles increases. It was suggested [4] that migration effects might be the cause of this positive slope. Experiments now confirm this and demonstrate the effect of capillary attraction between the pigment particles. This attraction draws together particles to form clusters before the base has set solid, and obviously the nearer the particles are together at first, i.e., the higher the concentration, the greater is the tendency for this to happen (Figure 3). This was confirmed by tests with a pigment exposed in cast films of different mobility (Figure 4). For films of ethylmethylcellulose the curve is steepest (Figure 4a); this material does not set until quite dry, and therefore the pigment particles have the longest period of time to migrate and have the best chance of forming clusters. For gelatin films the curve is less steep (Figure 4c). These films set rapidly after pouring out, and remain as gels while being dried; thus migration is retarded and clustering is reduced. When, however, the gelatin films are frozen immediately after pouring, so that particle migration is almost prevented, the CF curve is nearly horizontal (Figure 4d).

When the pigment is incorporated by stirring into hot gelatin solution the curve is both flatter and

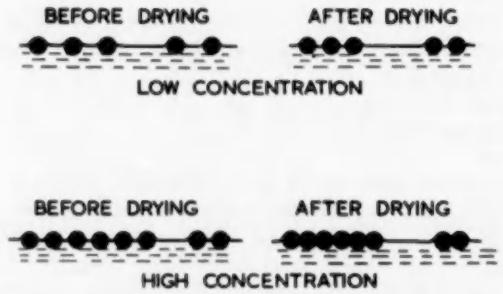

Fig. 3. Diagram showing suggested aggregation, by capillary action, of pigment particles suspended in a viscous fluid during drying. Before the fluid sets solid, particles more readily aggregate in high than in low concentrations. (In real cases aggregation will take place in three dimensions, not in two as shown here.)

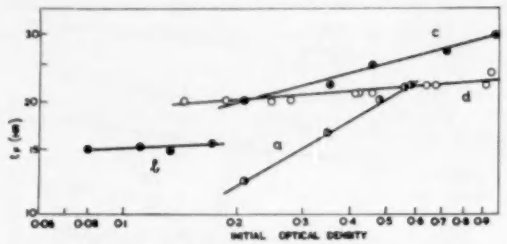

Fig. 4. Characteristic Fading (CF) curves for the pigment C.I. Azoic Diazo Component 5 → C.I. Azoic Coupling Component 5 incorporated in fluid substrates under different conditions. (a) Ethylmethylcellulose solution, incorporated cold, film dried by heat; (b) gelatin solution, incorporated by stirring at 50° C. for 1 hr., film set and dried cold; (c) gelatin solution, incorporated cold, film set and dried by heat; (d) gelatin solution, incorporated cold, film first set by freezing, then dried by heat. (No correction has been made here to the optical density values to allow for their possible small variation with particle size, for a given concentration, between the different series of films.)

much lower (Figure 4b), because individual conglomerates of pigment particles are broken up and dispersed by being penetrated slowly by the gelatin solution, and their specific surface area is thus increased. The process takes place also to some extent even in the gelatin films mixed cold. This can be seen by comparing the curves for normal-set films (Figure 4c) with the frozen ones (Figure 4d). At low concentrations the fastness in normal films falls below that in the frozen films, because of some slow penetration and breakdown of particle conglomerates at normal temperatures. Thus there are two opposing effects tending to alter particle-size distribution.

Pigments in Rayon

An attempt was made to demonstrate the effects just described by using viscose rayon colored with an azoic dye applied in two forms: (a) by naphtholation and coupling, and (b) by incorporation as a pigment in the spinning dope. The laboratory-spun yarn was exposed and its reflectance values determined, in the form of knitted fabric. A number of trials were made with different preparations of rayon. Though the pigmented material always tended to have the higher fastness, great difficulty was experienced in obtaining reproducible results. Figure 5 shows the results of one of the best runs. Because of the disaggregating effect of the heat of the illumination, there is an apparent increase initially in depth of color, as mentioned earlier. (See legend to Figure 5.)

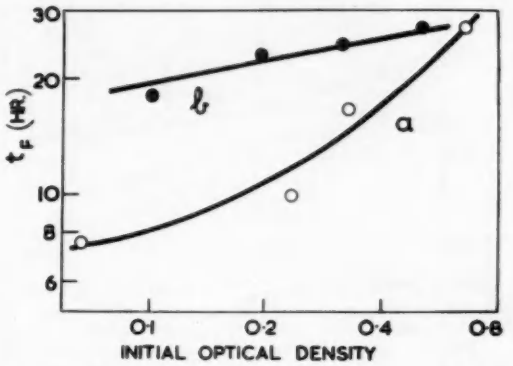

Fig. 5. CF curves for viscose rayon fabrics colored with C.I. Azoic Diazo Component 5 → C.I. Azoic Coupling Component 5, (a) by the normal dyeing method; (b) by incorporation of the pre-formed pigment in the spinning dope. (t_F values calculated from points on fading-rate curves at which the apparent depth increase, due to heat, has ceased: "initial concentration" values are optical densities of original dyed fabrics in aqueous sulfuric acid.)

Mordanted Dyes

The high lightfastness of many mordanted dyes may be attributed to a high photochemical resistance of dye–metal chelate molecules, or to a pronounced tendency to associate in the fiber. It seems very possible that complexing with a metal may assist the association or polymerization of dye molecules. Thus it has been shown [1] that the chromium lake of hematein, the coloring principle of logwood, prob-

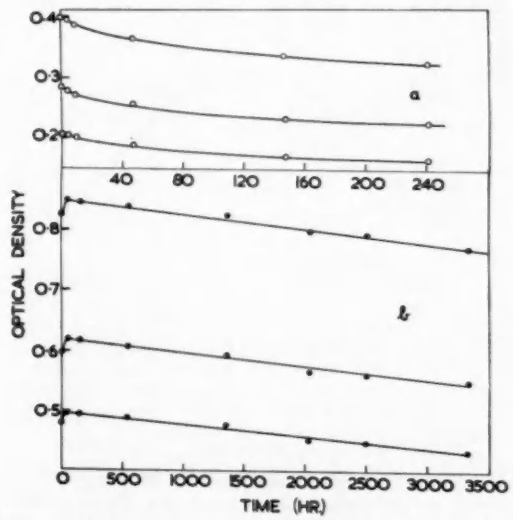

Fig. 6. Fading-rate curves of C.I. Mordant Black 11 in gelatin films, (a) unmordanted; (b) afterchromed.

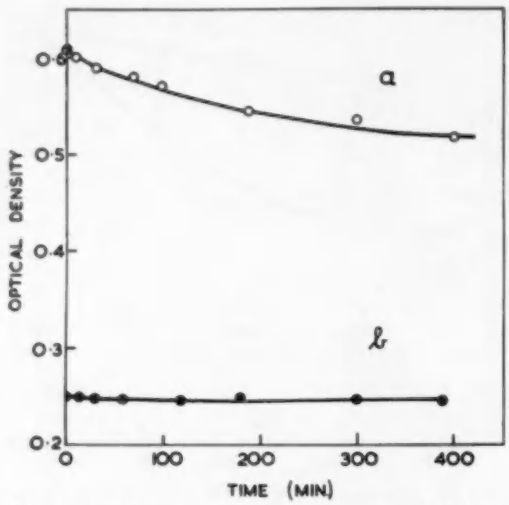

Fig. 7. Fading-rate curves of C.I. Direct Red 173 in Cellophane films, (a) direct; (b) aftercoppered, irradiated at high humidity, and 10° C.

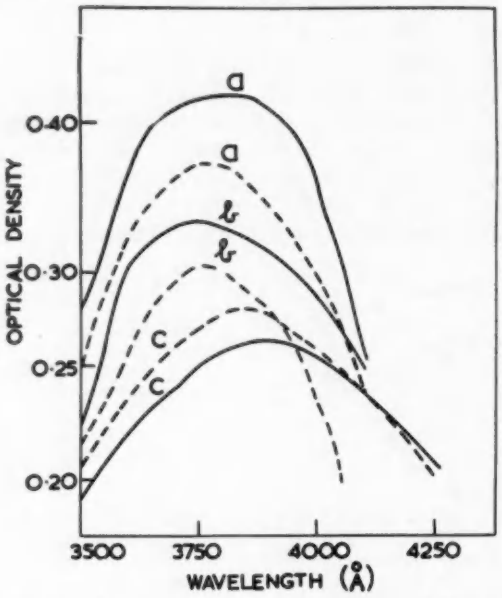

Fig. 8. Absorption spectra of C.I. Mordant Yellow 20: (a) untreated; (b) aftertreated with aluminum; (c) aftertreated with chromium. Full lines, dye in gelatin films; broken lines, dye in aqueous pyridine extracts (in which aggregation is assumed to be minimized).

ably has a polymeric structure. In the present work several representative chelate-complex forming dyes were chosen, and the shape of their fading-rate curves, the position of their CF curves, and in some

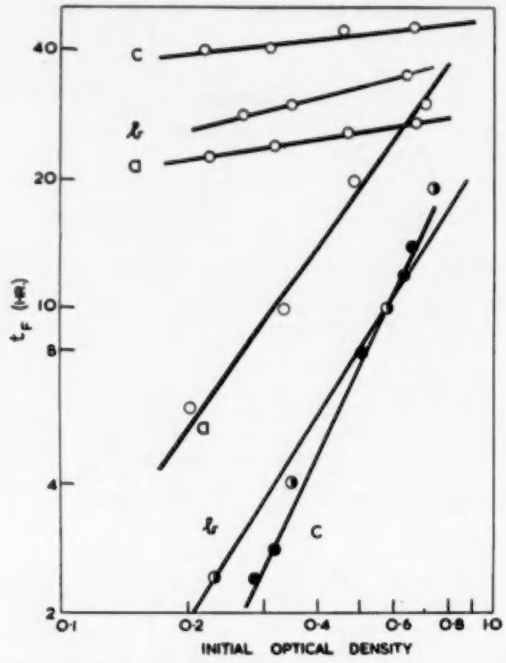

Fig. 9. CF curves for mordant dyes in gelatin films: (a) untreated; (b) aftertreated with aluminum; (c) aftertreated with chromium. Top curves: C.I. Mordant Yellow 20; bottom curves: C.I. Mordant Red 3 (soluble alizarin).

cases their absorption spectra, were determined before and after treatment with a complexing metal (Figures 6–9). In nearly all cases, the straightening of the rate curves (e.g., Figures 6 and 7) gives evidence that the dye becomes more highly associated by being complexed.

The absorption spectra of C.I. Mordant Yellow 20 lakes indicate that in gelatin the aluminum lake is more highly associated than the chromium lake (Figure 8: in pyridine, a powerful disaggregating agent, the absorption band of the aluminum lake is narrower than in gelatin, but there is little difference between the spectra of the chromium lake in the two media), and the CF curves (Figure 9) show that the aluminum lake has the higher lightfastness of the two. Comparison of the relative fastness of some of the other dyes, before and after complexing, is difficult because of the greater shift of their absorption bands brought about by complexing; the shift may itself affect fastness because the illumination has not a continuous spectrum. The degree of association of Alizarine Red S (C.I. 58005) is apparently not increased by complexing (as judged by the shape of

the fading-rate curves—not shown here); the fastness is reduced,[4] but this may be due partly to the absorption spectrum shift.

[4] These CF curves are very unusual in having greater slopes than the theoretical for zero-order fades [4]. Presumably the available active surface of the dye actually decreases with increase in concentration, for some unknown reason.

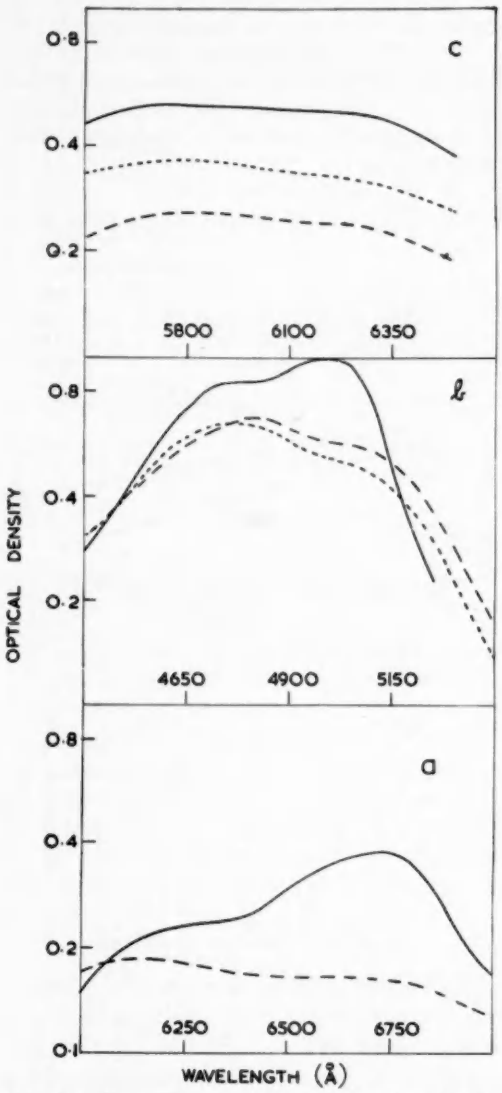

Fig. 10. Absorption spectra of basic dyes in Cellophane films. (a) Methylene Blue B (C.I. Basic Blue 9); (b) Acridine Orange R (C.I. Basic Orange 14); (c) Victoria Pure Blue BO (C.I. Basic Blue 7). Full lines, untreated; broken lines, aftertreated with phosphomolybdic acid; dotted lines, aftertreated with phosphotungstic acid.

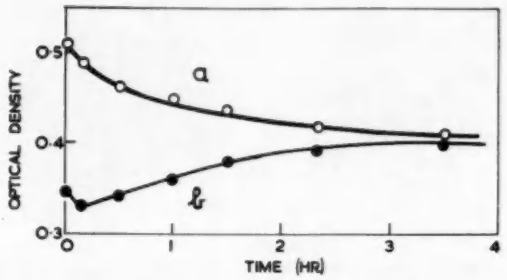

Fig. 11. Fading-rate curves of C.I. Basic Orange 14 on Cellophane film, (a) untreated; (b) aftertreated with phosphomolybdic acid. The slow rise in optical density of (b) is attributable to aggregate breakdown.

Complex Lakes of Basic Dyes

It was suggested earlier, on the evidence of CF curves, that the improvement in fastness of basic dyes produced by laking them with certain complex inorganic acids may be due to the resultant increase in particle size [4]. This is now confirmed by examination of absorption spectra (Figure 10) and by fading-rate measurements (Figure 11). After laking, the extinction of the *y*-band [14] of the spectrum is increased relative to that of the *x*-band, indicative of increased association of the dye molecules. The fading-rate curves are nonlinear for the uncomplexed dye, indicating the presence of some monodisperse dye, and have an initial rise for the complexed dye, indicating the presence of aggregated particles.

Water-soluble Dyes of High Lightfastness

Metal-Complex Dyes for Wool

The unsulfonated 2:1-metal complex (neutral dyeing) dyes are distinguished by their high light-

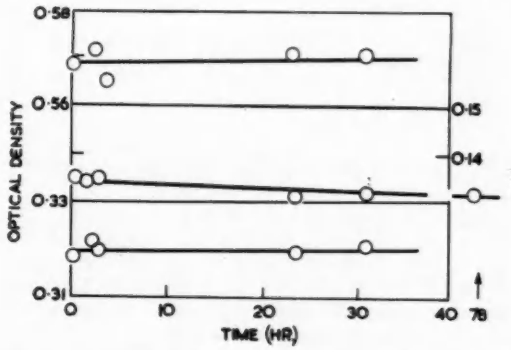

Fig. 12. Fading-rate curves of three typical unsulfonated 2:1 dye–metal complexes in gelatin film (from [13]).

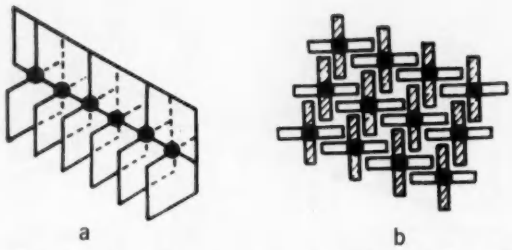

Fig. 13. Suggested structure of micelle of 2:1 metal complex (neutral dyeing) dye (after Giles and MacEwan [13]). (a) Isometric projection (schematic) of one line of associated complex molecules in the micelle. (Azo dye units shown as plain rectangles for clarity. Metal atoms shown as black circles.) (b) Plan (schematic) of one part of a layer of the micelle, showing interlocking of azo dye units by planar association. Hatched rectangles show units below, and white rectangles show units above, the line of metal atoms.

fastness. Fading-rate curves (Figure 12) show the typical zero-order rate of aggregated dye, with, in some cases, an initial increase in density. For this and other reasons Giles and MacEwan [13] suggested that these dyes are present in the fiber as large aggregates, and an examination of their molecular geometry shows that the most likely form of aggregate is a unique type of micelle consisting of interlocked molecules with surface "fins" of aromatic nuclei (Figure 13).

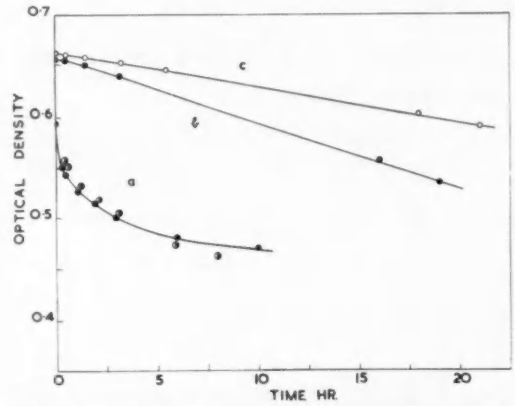

Fig. 14. Fading-rate curves of direct cotton dyes in Cellophane: (a) C.I. Direct Blue 1 at high humidity; (b) copper complex of Direct Blue 1 at high humidity; (c) as (b), at low humidity; (d) as (b), but dyed film aftertreated at b.p. for 1 hr. with copper sulphate (5% on film weight). Half-filled circles on Curve a show results in cool atmosphere (10° C.); all others were obtained without cooling (55° C).

Metal-Complex Dyes for Cotton

Weissbein and Coven [20] confirmed, by electron micrography, that there are aggregates of the copper complex of Sky Blue FF (C.I. 24410) in dyed regenerated cellulose film. In the present work this observation is supported by the characteristic shape of the fading-rate curve of this dye (Figure 14 b, c) in comparison with that of its uncomplexed form (Figure 14a). This is a direct confirmation that a linear fading rate curve can indicate a high degree of association in the case of a water-soluble dye; previously direct confirmation could be obtained only with insoluble dyes [3].

High Lightfastness Direct Cotton Dye, Not Metal-Complexed

A typical dye of this class, Solar Green BL (C.I. 34045) shows a fading curve characteristic of aggregated dye (Figure 15).

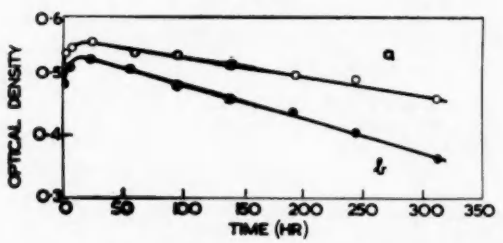

Fig. 15. Fading-rate curves of C.I. Direct Green 26 in Cellophane, (a) at low humidity; (b) at high humidity.

Acid Wool Dyes

Fading-rate curves for two anthraquinone acid wool dyes [Figure 7 of Ref. 3] show an initial rise characteristic of aggregated particles, and X-ray diffraction data on other dyes of this class on wool give evidence of the presence of crystallites [2].

Reactive Dyes on Cellulose

Two lines of evidence demonstrate that reactive dyes are aggregated in cellulose: the fading-rate curve [Figures 14, 15 of Ref. 3] and the change of x/y band extinction ratio with concentration [14]. In the present work more fading-rate curves for reactive dyes have been obtained (Figure 16), and these show clearly the initial increase in density which indicates that particulate dye is present.

Reduction in Humidity

Hedges [15] was probably the first investigator to study quantitatively and in detail the effect of atmospheric humidity (and of temperature) on the lightfastness of dyed fabrics. He found that rise in humidity accelerates fading in all cases. Later, Morris et al. [18] studied the effects of change in humidity and temperature on the fading of dyes on a variety of fibers, using more than 1300 samples.

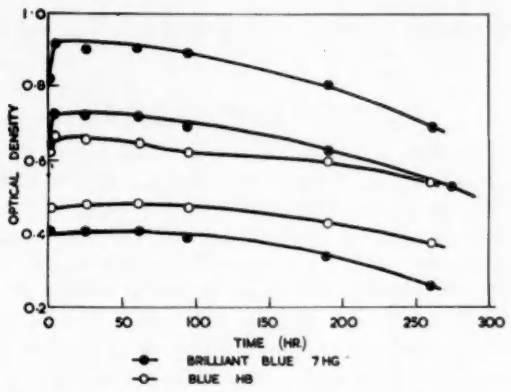

Fig. 16. Fading-rate curves of Procion (I.C.I.) reactive dyes in Cellophane.

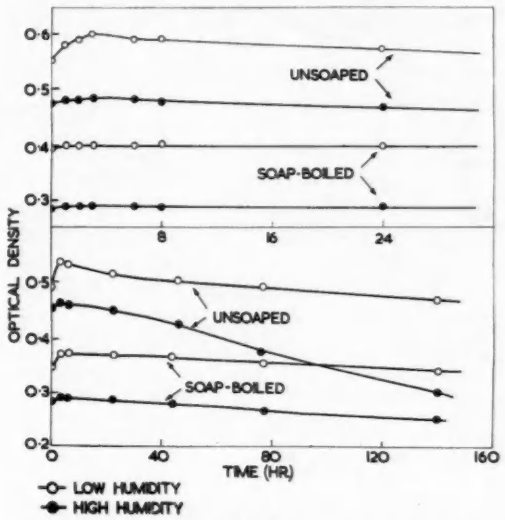

Fig. 17. Fading-rate curves for azoic combinations in cellophane. Top: C.I. Azoic Diazo Component 11 → C.I. Azoic Coupling Component 4. Bottom: C.I. Azoic Diazo Component 13 → C.I. Azoic Coupling Component 4.

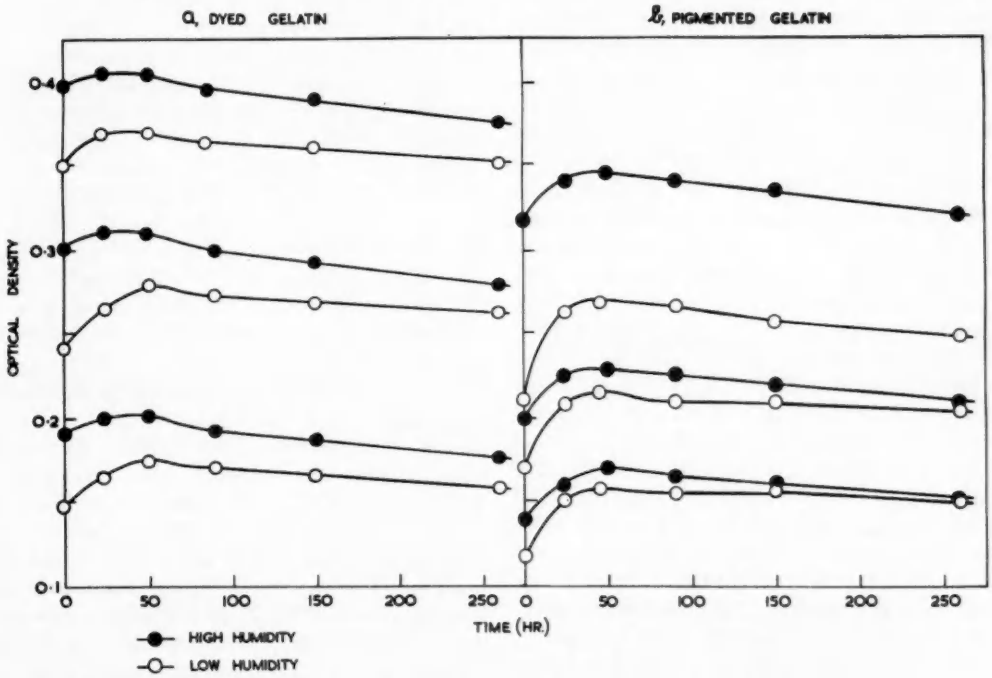

Fig. 18. Fading-rate curves for Microfix Blue in gelatin, applied by pigmentation or dyeing.

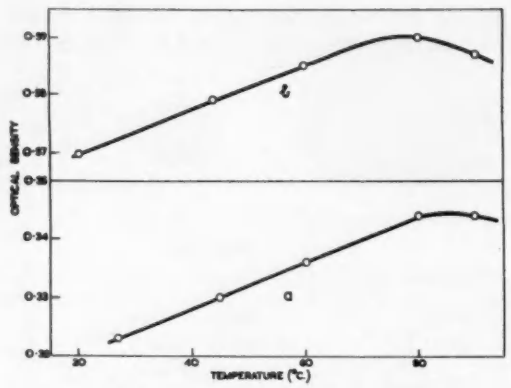

Fig. 19. Effect of ambient temperature on optical density of aggregated dyes in Cellophane films. (a) C.I. Azoic Diazo Component 13 → C.I. Azoic Coupling Component 4; (b) C.I. Direct Green 26. Films heated in the dark 20 min. at the given temperature before measurement. Rate measurements showed that the increase in density was in all cases complete in *ca.* 10 min.

They found that dyes on Acrilan, cellulose acetate, Dacron,[5] Dynel, Orlon,[3] and wool are very little affected by variations in humidity: those on nylon and Vicara are moderately affected. In general, fading on all the fibers was affected much more by increase in temperature than by increase in RH. McLaren [17] has recently examined the effect of humidity on fading of dyes on cellulose, and has found that the fading of one azoic dye in particular is markedly accelerated by rise in humidity. In general trend these observations agree with expectation. They may simply be due to a mass action effect. It is known that water takes part in the fading reaction [16], and therefore it is expected that fading will occur more rapidly at high humidities than low. Unfortunately the present data and those given by the earlier investigators are not suitable for a direct test of the mass action hypothesis. One difficulty, e.g., lies in the determination of the amount of the adsorbed moisture actually available for the fading reaction. Mass action does not however account entirely for the observed effects. If it did, then all dyes should be affected similarly by changes in humidity, but they are not. Some are much more affected than others. A further discussion on this matter will be given in a later paper.

Tests made in the present work show that reduction of humidity affects fading rate in two ways. In most cases it retards fading to a constant degree throughout the period of test (Figures 14–18); no doubt this is a normal mass action effect. In *some* cases where an initial increase in density occurs due to aggregate breakdown (see above), the increase is greater under dry conditions than under wet; this seems to apply only to azoic dyes. Dry conditions therefore can improve lightfastness by a two-fold action: by retarding access of moisture to the dye, and sometimes by facilitating breakdown of large dye aggregates,[6] whereby the apparent depth of color tends to increase.

[5] Du Pont trademark.

Heat and Aggregation Effects

The data in Figure 14 indicate that with a dye of rapid fading rate on cellophane, there is little difference, in the present methods of irradiation, between the results obtained in a hot and a cold atmosphere. Indeed in the cold atmosphere, fading is very slightly more rapid, probably because the substrate then contains more moisture.

The initial rise in optical density on irradiation of many aggregated dyes ([3] and above) is now shown to be most probably due to heat, because it occurs when the films are heated in the dark, whereby the density rises linearly with temperature, up to a limiting temperature (Figure 19), and when films are irradiated in a cooled atmosphere the initial rise is less than when they are irradiated hot. Heat breaks down the aggregated dye particles. Thus, in the first stages of irradiation of Methylene Blue in ethylmethylcellulose there is a fall in extinction of the absorption band representing aggregated dye, but a rise in that representing monomeric dye. The amount of aggregated dye is thus decreasing and that of disaggregated dye increasing [Figure 4 of Ref. 7]. (Chipalkatti et al. [8] found that gelatin films required about 1 hr. to reach the maximum temperature, 65–75° C., in the lamp used here.)

Further, the effect is now shown to be reversible (Figure 20). On cooling in the dark the optical density falls, but rises again when the lamp is switched on. (Both changes are much greater at high humidity than at low humidity.) Thus there is an apparently continuing fade in the dark (with one exception, see Figure 20). This type of effect has sometimes been attributed to a continuing chemical action caused by peroxide produced photochemically during the irradiation, but the reversibility of

[6] Bean and Rowe observed that dry heating breaks down aggregates of azoic dyes in cellulose [5].

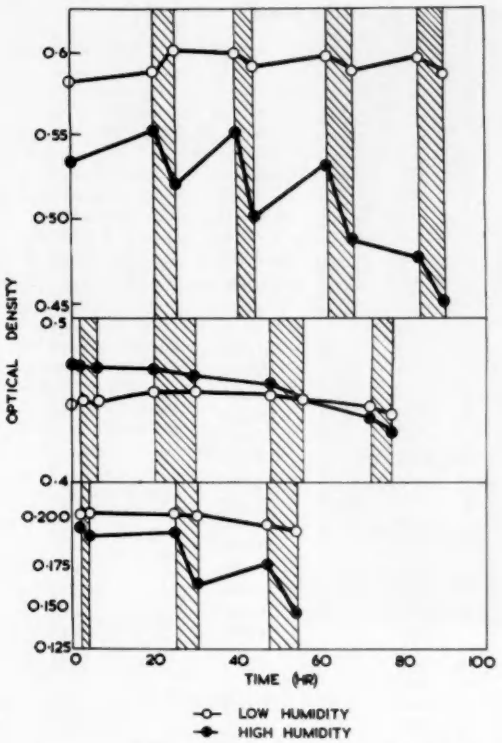

Fig. 20. Effect on dyed Cellophane fading rates, of alternating irradiation and storage in the dark. Top: C.I. Direct Green 26 (*ca.* 55° C.); middle: C.I. Direct Green 26 (*ca.* 10° C.); bottom: C.I. Azoic Diazo Component 11 → C.I. Azoic Coupling Component 4 (*ca.* 55° C.). Hatched areas show times during which the lamp was switched off. Ambient temperatures shown in parenthesis.

the change in the present cases shows that such an explanation is untenable here. (Perhaps the very slight "dark fade" in the cooled atmosphere may have been caused by peroxide.)

Evidence of Nature of Fading from Absorption Spectra

It has been found that nearly all water-soluble dyes in transparent dyed substrates give an increased y/x band extinction ratio with increase in concentration; this is evidence of aggregation [14]. If monodisperse dye fades more rapidly than aggregated or micellar dye, the y/x band ratio should increase when the dye is faded. Data in Table II show that it does so with water-soluble dyes. With insolubilized dyes the opposite effect sometimes occurs, the y/x band ratio falling with exposure. Presumably this is the result of the breakdown, in the heat of illumination, of some of the large dye crystals to give a small proportion of monodisperse dye, possibly a vaporization or sublimation process.

Experimental

Materials, etc.

The general methods of preparing the dyed films have previously been described [3, 4, 8]. After-treatments with mordanting solutions were made by standard procedures. Fading was followed spectrophotometrically by a Unicam instrument at the wavelength of maximum absorption of the unexposed sample. To freeze the gelatin films (see Figure 4) the freshly bound films (on glass) were placed on glass plates supported 2 in. above a flat vessel containing solid carbon dioxide. The films set within 5 min. and were then removed and left to dry at room temperature.

Apparatus

The apparatus used for irradiation in these and previously reported experiments is shown in Figure 21. The colored films are cut to fit the cell holder of the spectrophotometer and for protection and to ensure flatness are bound as a sandwich between two pieces of photographic glass plate cut to the same size. The irregular, slight buckling of the film that occurs in all cases allows air channels to form between the slides, which appear sufficient to ensure access of air and moisture (no difference in results is observed when film is bound to one glass only, with one side fully exposed to air). They are then suspended by threads, in the tubes shown, at the level of the arc, which has a shield of aluminum sheet, centered on the arc. These tubes have ground-glass stoppers and contain a few grams of calcium chloride for tests in a dry atmosphere or a few cubic centimeters of water for tests in a damp atmosphere. The tubes are water-jacketed, and tap water may be circulated around them to maintain a low temperature (*ca.* 10° C.) at the film surface. In open air the temperature (with a 400 W Hg lamp) rises to *ca.* 56° C. at the exposed glass surface, to 65° C. inside an undyed gelatin film, and to 67–70° C. inside a dyed one [8].

For many types of test it appears unnecessary to maintain these controlled conditions, and the film slides are then rested unprotected on a shelf encircling the inside of the aluminum shield.

TABLE II. Change of Absorption Spectra of Dyes when Faded

	Time of exposure, hr.	λ_{max}	*y*-band O.D.	*y*/*x* extinction ratio
I. Water-soluble dyes				
(in Cellophane, except where shown)				
Benzopurpurine 4B	0	5200	0.775	0.70
(C.I. 23500)	1.0	5120	0.710	0.75
	20	5100	0.620	0.83
	93	5070	0.510	0.85
	288	5070	0.373	0.85
Methylene Blue 2B	0	6300	0.690	0.81
(C.I. 52015)	0.5	6300	0.750	0.61
	1.0	6300	0.580	0.63
	2.0	6300	0.460	0.74
	3.0	6300	0.380	0.83
Chlorazol Azurine G	0	6350(?)	0.684	1.24
(C.I. 24140)	0.17	6350(?)	0.649	1.29
	0.50	6350(?)	0.649	1.29
	48	6350(?)	0.272	1.51
Victoria Pure Blue BO	0	6250	0.276	1.15
(C.I. 42595)	2.0	6250	0.226	1.19
	4.0	6250	0.184	1.22
	6.0	6250	0.142	1.26
Chlorazol Sky Blue FF	0	6600	1.440	0.89
(C.I. 24410)	0.8	6600	1.360	0.93
	5.0	6600	1.150	1.08
	46	6600	1.010	1.12
Chlorazol Sky Blue FF	0	6600	0.800	0.60
	5.0*	6600	0.770	0.60
	15*	6600	0.740	0.65
	25*	6600	0.725	0.70
Azo Geranine 2G	0	5400	0.162	0.95
(C.I. 18050)	24*	5400	0.157	0.95
in gelatin	48*	5400	0.154	0.97
	96*	5400	0.158	0.98
II. Water-insoluble dyes				
(in Cellophane)				
Acridine Orange R	0	5150	0.670	1.08
(C.I. 46005)	2.3	5150	0.540	1.17
(Phosphomolybdic acid lake)	11.6	5150	0.510	1.17
Base 2 → naphthol 4†	0	5400	0.310	1.16
	35	5400	0.320	1.14
	55	5400	0.295	1.20
Base 2 → naphthol 10†	0	5300	0.261	1.17
	18.5	5300	0.271	1.17
	42	5300	0.260	1.16
	75	5300	0.248	1.14
	165	5300	0.177	1.13
Base 2 → naphthol 19†	0	5300	0.181	1.25
	18.5‡	5300	0.194	1.21
	48.5‡	5300	0.185	1.23
Victoria Pure Blue BO	0	6250	0.757	1.20
(Phosphotungstic acid lake)	24‡	6250	0.840	1.09
	72‡	6250	0.840	1.06

* Xenon lamp; all others exposed to mercury vapor lamp.
† Base = C.I. Azoic Diazo Component; Naphthol = C.I. Azoic Coupling Component.
‡ In these cases the extinction increase, due to heat, had not ceased at the end of the experiment.

Fig. 21. Setup of irradiation apparatus. The films, attached to glass slides cut (12 × 50 mm.) to fit the spectrophotometer optical cell housing, are suspended by threads in the jacketted tubes equidistant from the arc. Cooling water may be circulated through the jackets, as shown. Solid calcium chloride or water may be placed at the bottom of each tube to give low or high humidity conditions. If temperature or humidity control is not required, the slides are rested on a ledge around the inside of the cylindrical aluminum shield. A 400 W mercury vapor lamp is shown; when a source of continuous radiation is required a xenon arc lamp is used.

Fading tests made over calcium chloride cannot be considered as made under quite dry conditions, because moisture is not completely desorbed from the films by holding them in a dry atmosphere at room temperature, even if they are held thus for a considerable time in the dark before irradiation (this was not done here). In any case small amounts of moisture are re-adsorbed during the few minutes when the slides are removed from the tubes for measurement in the spectrophotometer.

The device used for obtaining uniformly dyed Cellophane films is shown in Figure 22. The film is wound round the glass rod former, which is rotated at 20 r.p.m. by an electric clock motor.

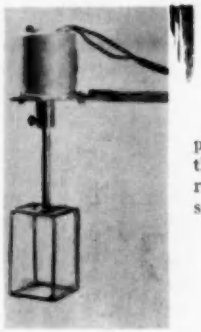

Fig. 22. Device for dyeing Cellophane film. The film is bound round the lacquered brass wire frame and rotated in the dyebath by the slow-speed (clock) motor.

Conclusions

Dyes of high lightfastness of all the classes examined appear to owe this property to their high degree of association. Aggregated dye particles appear often to break down when heated and to reform on cooling; the relative humidity of the atmosphere can influence this action. Pigment particles can be aggregated by capillary action in a fluid matrix, and their lightfastness after drying is thus improved.

Acknowledgments

The authors thank Professor P. D. Ritchie for his interest and encouragement, Mr. G. H. Dowse and Courtaulds Ltd. for preparing the samples of pigmented and colored viscose rayon (Figure 5), several manufacturers for gifts of dyes and for information, the Wool Textile Research Council for a Scholarship (to G. B.), and Mrs. P. Catchpole and Messrs. C. M. Brown and J. M. McGrath for experimental assistance.

Note Added in Proof

Phototropy. It should be added that the effects shown in the tests in alternating light and darkness (Figure 20) are almost certainly due to heat and not to phototropy (*cf.* [18a] and footnote 2 above),

because, as can be seen in Figure 20, they almost disappear when the sample is irradiated in a cool atmosphere. Moreover Eigenmann and Kern [21] have recently shown, in tests with a number of phthalocyanine dyes in cellulose, that phototropic sensitivity decreases linearly with increase in degree of aggregation (as measured by the y/x spectral ratio).

Literature Cited

1. Arshid, F. M., Connelly, R. F., Desai, J. N., Fulton, R. G., Giles, C. H., and Kefalas, J. C., *J. Soc. Dyers Colourists* **70**, 402 (1954).
2. Astbury, W. T. and Dawson, J. A. T., *J. Soc. Dyers Colourists* **54**, 6 (1938).
3. Baxter, G., Giles, C. H., and Lewington, W. J., *J. Soc. Dyers Colourists* **73**, 386 (1957).
4. Baxter, G., Giles, C. H., McKee, M. N., and Macaulay, N., *J. Soc. Dyers Colourists* **71**, 218 (1955).
5. Bean, P. and Rowe, F. M., *J. Soc. Dyers Colourists* **45**, 67 (1929).
6. Campbell, D. S. E., Cathcart, D., Giles, C. H., and Rahman, S. M. K., *Trans. Faraday Soc.* **55**, 1631 (1959).
7. Campbell, D. S. E. and Giles, C. H., *J. Soc. Dyers Colourists* **74**, 164 (1958).
8. Chipalkatti, H. R., Desai, N. F., Giles, C. H., and Macaulay, N., *J. Soc. Dyers Colourists* **70**, 487 (1954).
9. Eaton, J. C., Gordon, M., and Giles, C. H., *J. Soc. Dyers Colourists* **68**, 394 (1952).
10. Giles, C. H., *J. Soc. Dyers Colourists* **73**, 127 (1957); p. 130, in Fig. 3e, A, B should read "nylon, Terylene," respectively; p. 139, add ref. 37y to Table IV; in Fig. 12, names of each pair in the first three cases to be reversed; p. 143, Vat dyes (BASF) relative shade depths are ⅙, ⅓, 1, slope 0.85; p. 147 footnote ‡, line 3, for "cotton" read "viscose rayon"; p. 149, last par., 1st col., line 6, for "(without carrier)" read "data for heavy depths given for fibre dyed with Tumescal D (ICI) as carrier; this does not affect fastness, cf. Table IV."
11. Giles, C. H., Baxter, G., Macaulay, N., and Rahman, S. M. K., TEXTILE RESEARCH JOURNAL **30**, 934 (1960). In figure 2, abscissa scales are 0.1–1.0 for top left, top center, and middle center boxes. Since this paper went to press a notice has appeared of another investigation of the effect of alkylation upon the fastness to light, etc. of acid wool dyes; see Nikolenko, L. N., Eremina, O. I., Karpova, E. N., Mikhaĭlova, I. F., and Kobrina, L. S., *Zhur. Priklad. Khim.* **33**, 1617 (1960); through *J. Soc. Dyers Colourists* **76**, 636 (1960).
12. Giles, C. H. and Macaulay, N., *Royal Photographic Soc., Cent. Conf.* 309 (1953).
13. Giles, C. H. and MacEwan, T. H., *J. Chem. Soc.* 1791 (1959).
14. Giles, C. H. and Rahman, S. M. K., *J. Chem. Soc.* 1209 (March 1961).
15. Hedges, J. J., *J. Soc. Dyers Colourists* **43**, 261 (1927); **44**, 52, 341 (1928).
16. Hillson, P. J. and Rideal, E., *Proc. Roy. Soc.* **A216**, 458 (1953).
17. McLaren, K., *J. Soc. Dyers Colourists* **72**, 527 (1956); **73**, 121 (1957).
18. Morris, M. G., Anderson, D. A., Ericson, H. W., Hultber, A. I., Jaeger, W. H., Jones, J. H., Kelley, J. G., and Norton, J. E., *Am. Dyestuff Reptr.* **43**, P497 (1954).

18a. Morton, T. H., *J. Soc. Dyers Colourists* **65**, 597 (1949).

19. Schwen, G. and Schmidt, G., *J. Soc. Dyers Colourists* **75**, 101 (1959).
20. Weissbein, L. and Coven, G. E., TEXTILE RESEARCH JOURNAL **30**, 58, 62 (1960).
21. Eigenmann, G. and Kern, F., *Textil-Rundschau* **16**, 167 (April 1961).

Manuscript received February 14, 1961.

The Statistical Interpretation of Fiber Counts in Yarn Cross-Sections

D. N. E. Cooper

Courtaulds, Limited, Textile Research Laboratory, Bocking, Braintree, Essex, England

Abstract

Part I. In a model yarn spun from two components differing only in color, the factors affecting yarn irregularity may be divided into two classes, only one of which affects the regularity of blend proportions. The published tests for random mixing are reviewed and it is shown that the correct test for randomness is one based on the variance of blend proportions.

Part II. When tests based on the theory of blending are applied to blends of dissimilar fibers, the results must be interpreted with caution. Departures from randomness may be safely detected, but these departures may be caused by the physical differences between the fibers rather than by insufficient processing.

Part III. The mixing of components within the cross-section must be considered separately, and special attention should be paid to effects in the yarn surface. The number of apparent groups along an arbitrary line in the section provides the most sensitive test for departures from randomness, but information about the behavior of the individual components must be obtained by other means.

Introduction

Spun yarns are manufactured by processes inevitably leading to variations in the number of fibers in the cross-section and, in blended yarns, in the proportions of the various components. These variations have received considerable attention, as they can have an appreciable effect on the appearance and mechanical properties of the yarn. A complete investigation of the problem would have to cover three aspects: (i) the comparison of the arrangement of fibers obtained with that expected in a random system; (ii) the correlation of this arrangement with the appearance and other properties of the final product; and (iii) the modification of spinning conditions in the light of the information obtained.

This paper is concerned with the first aspect only, which is obviously necessary for realistic study of the other two. In Part I we shall make an elementary approach to the theory of blend irregularity, in Part II discuss its application to real yarns, and in Part III consider the distinct but related problem of the arrangement of fibers within the cross-section. Although the statistical theory must be applied with some reserve, based as it is on models simplified both mechanically and statistically, it will be found to provide a useful basis for the interpretation of fiber counts in the cross-sections of blended yarns. Throughout the paper only binary blends are considered, but the same principles would be equally applicable where a greater number of components is present.

In the formulation of this approach to the statistics of blending, the author is indebted to the work of Coplan and Klein [2, 3], Cox [8], and de Barr and Walker [9], referred to many times in the paper, and to his colleague Mr. J. B. Hamilton for making his experimental data available for use in illustrating the approach. Thanks are also due to Mr. E. J. Whyte for reading the manuscript and making a number of very helpful suggestions.

Part I: Elementary Theory of Blend Irregularity

Factors Affecting Irregularity in a Model Yarn

Let a yarn be produced by mixing, drafting, and spinning Ω slivers of similar mean fiber number and irregularity. If all the fibers used were identical, except that those in one sliver were marked in some way (e.g. by color), it would be observed that the frequency with which the marked fibers occurred

in the yarn was subject to continual fluctuation. The possible causes of this fluctuation may be considered in two groups, as follows.

Group A. Factors affecting marked and unmarked fibers independently: (i) purely random influences on the individual fibers during their passage through the system; (ii) separate groups of fibers from one sliver moving through the system together; and (iii) substantial irregularities in the original slivers.

Group B. Factors affecting marked and unmarked fibers together: (i) fibers drafted together being subject to the same irregularities of motion; (ii) the formation of entangled groups of fibers (irrespective of origin) which remain thereafter associated; (iii) possible limitations on the numbers of fibers passing various points in the system; and (iv) other mechanical irregularities in the process.

These factors will be considered in more detail later, but for the time being we shall distinguish only between the effects of the two groups. Let the fibers in a substantial number, Ω_1, of the slivers now be marked, and the number of marked fibers, f_1, appearing in yarn cross-sections be noted. If we may assume that the average blend proportions are approximately constant throughout the system, we may divide the variance of f_1 into two components corresponding to the two groups of factors. The effects of the A factors on the fibers from the various slivers will be independent, and hence additive, but the effects of the B factors will be correlated and the total contribution proportional to the square of the number of slivers. (Any other factor affecting the process in a more complex manner may be resolved similarly into A and B components.)

Let x_i be the number of fibers appearing in a cross-section from the ith colored sliver, where $i = 1, 2, \ldots, n$.

Total number of colored fibers in the cross-section

$$f_1 = \sum_{i=1}^{n} x_i$$

and

$$\text{var } (f_1) = \sum \text{var } (x_i) + \sum_{i \neq j} \text{cov. } (x_i, x_j)$$

$$= n \text{ var } (x_i) + n (n - 1) \text{ cov. } (x_i, x_j)$$

For large n we may write as a close approximation

$$\text{var } (f_1) = n \text{ var } (x_i) + n^2 \text{ cov. } (x_i, x_j)$$

Putting

$$A = \frac{\text{var } (x_i)}{\bar{x}} \quad \text{and} \quad B = \frac{\text{cov. } (x_i, x_j)}{(\bar{x})^2},$$

$$\text{var } (f_1) = A (\bar{f}_1) + B (\bar{f}_1)^2 \tag{1}$$

with A and B constants *for the given yarn.*

In many cases, blending would take place before the first draw-frame and a slightly different model would have to be used. Factor A(iii) would then relate to the irregularity of feeding in the components at the first stage of mixing, and would be less important because of the randomization effected by the preliminary processes.

General Expressions

Let f = number of fibers in cross-section
f_1 = number of marked fibers in cross-section
$f_2 = f - f_1$, $p_x = f_1/f$, $q_x = 1 - p_x$
$p = \bar{f}_1/\bar{f}$, $q = 1 - p$.

Then from Equation 1

$$\text{var } (f_1) = Ap (\bar{f}) + Bp^2 (\bar{f})^2 \tag{2}$$

$$\text{var } (f_2) = Aq (\bar{f}) + Bq^2 (\bar{f})^2 \tag{3}$$

$$\text{var } (f) = A (\bar{f}) + B (\bar{f})^2 \tag{4}$$

Whence it may be shown that

$$\text{cov. } (f_1, f_2) = Bpq (\bar{f})^2 \tag{5}$$

and

$$\text{var } (p_x) = \frac{Apq}{\bar{f}} \tag{6}$$

It will be noted that only group A factors contribute to the irregularity of blend proportions, although both groups contribute to the over-all yarn irregularity. Within the calculable statistical uncertainties, it is therefore possible to assess the effects of the two groups separately. In the following sections we shall compare this general treatment with those which seek to take account of specific factors, and it will be seen that the equations deduced are in fact special cases of those given above.

Random Variations

A number of authors [16, 21, 22] have considered the consequences of the occurrence of fibers in the yarn being purely random. If the fibers are regarded as independent units, the Poisson distribution shows that

$$\text{var } (f) = (\bar{f}) \tag{7}$$

In practice, however, it is observed that

$$\text{var } (f) > (\bar{f})$$

This could be due to the fibers associating in groups of ν individuals, when

$$\text{var } (f) = \nu\,(\bar{f}) \tag{7a}$$

If each group were composed of fibers from the same original assembly,

$$\text{var } f_1 = \nu p\,(\bar{f})$$
$$\text{cov. } (f_1, f_2) = 0$$
$$\text{var } (p_x) = \frac{\nu pq}{\bar{f}}$$

i.e., in our notation, $A = \nu$, $B = 0$.

If, however, the groups are random mixtures of fibers from different sources, by considering groups of size ν made up randomly (according to the binomial distribution) from white and colored fibers, the groups moving thereafter as independent units, it may be shown that

$$\text{var } (f_1) = p\bar{f}\,[1 + (\nu - 1)p]$$
$$\text{cov. } (f_1, f_2) = (\nu - 1)pq\bar{f}$$
$$\text{var } (p_x) = \frac{pq}{\bar{f}}$$

i.e.,

$$A = 1, \quad B = \frac{\nu - 1}{\bar{f}}$$

If a range of group size is possible, and the number of groups containing a given number of individuals was determined by a Poisson probability, similar results would be obtained, ν being replaced by a parameter which is closely related to the mean group size when $\bar{\nu}$ is close to unity.

It is therefore possible to interpret both yarn irregularity and blend regularity by assuming various grouping tendencies in the system. In a real system, however, there is no doubt that a number of other factors must be taken into account.

Additional Factors

Foster [11] and Cox and Ingham [7] have independently developed theories leading to similar expressions for yarn irregularity. The two theories have been compared by Foster [11]. Cox and Ingham consider the movement of small groups of fibers during drafting, while Foster considers the formation of drafting waves. Cox and Ingham consider also certain machine faults; but for our purposes these may be taken to supplement our group B factors.

Both treatments take account of gross irregularity in top or sliver. For general application to blending, the effect of mixing before the draw-frame would have to be considered; qualitatively this may be seen to reduce blend irregularity, but an exact treatment would demand knowledge of the movement of fibers during carding, etc., which is not yet available. In the present discussion we shall follow the simple case of mixing at the draw-frame discussed by Cox [8].

The results of both treatments may be expressed as follows.

$$\text{var } (f) = \nu\,(\bar{f}) + B\,(\bar{f})^2 + \frac{V_T^2\,(\bar{f})^2}{\Omega} \tag{8}$$

where V_T is the coefficient of variation of each top.

Cox, however, follows Foster in taking $\nu = 1$, and writes

$$\text{var } (f) = k\,(\bar{f}) + \frac{V_T^2\,(\bar{f})^2}{\Omega} \tag{9}$$

For large Ω, he shows that

$$\text{cov. } (f_1, f_2) = (k - 1)pq\bar{f} \tag{10}$$

and writing $R = f_1/f_2$ and assuming the covariance is unaffected by the initial irregularities, he finds that

$$\text{var } (\log_e R) = \frac{\text{var } (f_1)}{(\bar{f}_1)^2} + \frac{\text{var } (f_2)}{(\bar{f}_2)^2} - \frac{2\,\text{cov. } (f_1, f_2)}{(\bar{f}_1)(\bar{f}_2)} \tag{11}$$

i.e.,

$$\frac{1}{pq\,(\bar{f})} + \frac{(V_T)^2}{\Omega}\left(\frac{1}{p} + \frac{1}{q}\right) \tag{12}$$

(ignoring Cox's implied distinction between the irregularities of the white and colored slivers). Equation 12 shows that the yarn irregularity is affected by the irregularities of the original slivers, but that the effect should be inversely proportional to the number Ω. In our notation these results correspond to

$$A = 1 + D\,(V_T)^2 \tag{13}$$

$$B = \frac{k - 1}{\bar{f}} \tag{14}$$

where $D = \bar{f}/\Omega$, a constant for a given setting of the apparatus.

In practice, Cox's formula appears to underestimate yarn irregularity [8, 20, 25] for small Ω. This might be due to oversimplification in the theoretical model. It seems quite possible that fiber groups from the original tops might persist during the first few doublings, and the unity in Equations 12 and 13 above would then have to be replaced by ν_Ω, itself a function of Ω.

The Effect of Limitations on Fiber Movement

In the treatments mentioned so far, the yarn is considered to be formed by the superposition of a number of assemblies subject to random and systematic variations. This approach has been criticized by some writers on the grounds that in practice the occurrence of fibers in the yarn is subject to certain limitations.

Vanden Abeele [23] considers a continuous-filament yarn in which the spinning of each filament is interrupted from time to time. In the ideal case he shows that

$$\text{var } (f) < (\bar{f})$$

although variations affecting the whole yarn simultaneously may prevent this being observed in practice. Hannah and Rodden [18], after briefly discussing Vanden Abeele's treatment, impose a further limitation, assuming that the position of each fiber is restricted along the yarn. Although this seems a valid consideration, their treatment is difficult to follow and has been strongly critized by Breny [1]. Breny's criticisms, moreover, were accepted by Hannah and Rodden [19], and further discussion of this restriction must await a more satisfactory treatment.

Coplan and Klein [2] have developed a theory formally similar to Vanden Abeele's. Grains (representing fibers) are thrown against a grid (representing the spinning system) and the composition of the model yarn is determined by those grains passing through the grid. Although at first sight such a model may seem inappropriate, it is an attempt to take account of an element of competition among the fibers which the authors find lacking in the other theories.

When grains are considered to move individually, in our notation we could write their conclusions as

$$A = 1, \quad B = \frac{Q - 1}{\bar{f}}$$

If, however, grouping occurs, $A = \nu$, rather than unity. Q is the probability that a hole in the grid will not pass at a given toss. B is thus seen to be negative. Once again, over-all variations will supplement this factor, tending to make it positive, without contributing to blend irregularity.

Coplan and Klein have suggested a very useful Index of Blend Irregularity, defined by

$$\text{IBI} = \sqrt{\frac{1}{n} \sum \frac{(f_1 - pf)^2}{pqf}} \tag{15}$$

where n is the number of observations made. Walker has pointed out that this index is a form of χ^2 test [3, 24], i.e.,

$$\text{IBI} = \sqrt{\chi^2/n}$$

Now

$$\frac{\chi^2}{n - 1} = \frac{\text{actual var } (p_x)}{\text{random var } (p_x)} = \frac{\bar{f} \text{ var } p_x}{pq} = A \tag{16}$$

For large n, the square of the IBI may thus be used as an estimate of A, which if no other factors contribute may be regarded as a group size [2], and the significance and confidence limits of the estimate may be calculated from χ^2.

Practical Application

The expressions proposed by various authors appear to be special cases of Equation 1. Unless other information is available, therefore, the most that can be deduced from fiber counts alone is a value for the constants A and B. A detailed investigation of the theory of drafting would involve a very great deal of work, as is shown by the paper on the theory of drafting by Grishin [12]. The main use of the theory in its present state is to give guidance in testing for significant departures from random blending.

Although both groups of factors contribute to yarn irregularity, only Group A contributes to the irregularity of blend proportions (Equation 6). The minimum theoretical value of A is unity; it may exceed this value either because of fiber grouping or because of the persistence of initial irregularities in blending. The test for blend regularity should therefore be designed to establish a value of A and its statistical significance.

Tests have been proposed by Coplan and Klein [2, 5], Cox [8], and Hampson and Onions [16]. These have been compared by Hannah [17]. This comparison, however, is somewhat unsatisfactory, as the criterion applied seems inappropriate and there are obvious errors in its application. We have seen that both Coplan and Klein's test and Cox's are methods of estimating A. Hampson and Onions' test, however, confuses irregularity of blending with yarn irregularity. Satisfactory proportions may therefore be rejected [5] because of yarn irregularity, which should be regarded as a separate problem.

The choice of tests therefore lies between Cox's and Coplan and Klein's. These may not yield exactly the same information, because of differences between the distributions of $\log_e R$ and p_x; as the theoretical distribution of χ^2 is known exactly, Walker's modification of Coplan and Klein's test is probably preferable.

Conclusions

The factors contributing to yarn irregularity may be divided into two groups, the effects of which may be distinguished in yarns spun from two components differing only in color. While one group of factors controls the blend regularity, the other controls the common variation of the two components.

The effects of the individual factors within each group cannot be separated in the same way. Provided therefore that a theory takes account of one factor in each group, an expression of the correct form will be obtained, but this may lead to misleading conclusions.

The most satisfactory test for randomness of blending is the type of test developed by Coplan and Klein, used either in the original form (IBI) or as a χ^2 test.

Part II: General Application to Real Yarns

Effect of Differences between Components

The theory developed so far applies only to blends of fibers of similar mechanical properties. Most blended yarns are composed of components differing in dimensions, elasticity, and coefficient of friction, all of which might affect the interaction between the fibers and the processing machinery. Before applying the simple theory to such yarns, it is therefore necessary to test the data obtained from them for consistency with the relationships obtained in Part I.[1] We shall now consider how far any observed inconsistencies may be interpreted on the basis of the same approach.

Following the original argument of Part I, we might expect relationships of the following type.

$$\text{var } (f_1) = A_1 p(\bar{f}) + B_1 p^2 (\bar{f})^2 \qquad (17)$$

$$\text{var } (f_2) = A_2 q (\bar{f}) + B_2 q^2 (\bar{f})^2 \qquad (18)$$

(where p and q are blend proportions by fiber number). It is impossible, however, to form expressions for var (f), cov. (f_1, f_2), or var (p_x) without further assumption.

(i) If $A_1 = A_2$, $B_1 = B_2$, the treatment of Part I may be applied directly, and the consistency of the assumption (within the statistical errors) demonstrated in Equations 2–6.

(ii) If $A_1 \neq A_2$ but $B_1 = B_2$, the two components are treated alike by the system, but differences in behavior are due to initial irregularities or tendencies to grouping. If grouping is the only difference, we may still write

$$\text{cov. } (f_1, f_2) = Bpq\ (\bar{f})^2$$

and this assumption seems reasonable also when initial irregularities differ, as these should not be correlated.

It follows that

$$\text{var } f = (A_1 p + A_2 q)(\bar{f}) + B\ (\bar{f})^2 \qquad (19)$$

and[2]

$$\text{var } p_x = (A_1 q + A_2 p)\frac{pq}{\bar{f}} \qquad (20)$$

[1] It is important to emphasize here the distinction between the apparent significance of an observed statistic and the confidence with which its true value may be estimated. Suppose in the estimation of group size from $\chi^2/(n-1)$ a value 1.1 is obtained by averaging 10 cross-sections. A significant departure from the random expectation of unity would have been assumed only if the 5% probability level of 1.9 had been attained, but the observed value of 1.1 also allows a 5% probability of the true value being as great as 3. If, however, the same value of 1.1 were obtained from 120 cross-sections, although the departure from unity would be relatively more significant (5% level now 1.2), it is now practically certain that the true value lies below 1.5. In order to justify the use of the simple theory of Part I it is necessary for sufficient observations to be made to enable the true values of the statistics to be estimated with a reasonable degree of confidence; it is not sufficient simply to show that no significant departures from expectation occur in a small number of cross-sections.

[2] Var p_x [= var (f_1/f_2)] must be calculated from $p^2q^2 \times \left\{ \frac{\text{var } (f_1)}{(\bar{f}_1)^2} + \frac{\text{var } (f_2)}{(\bar{f}_2)^2} - \frac{2 \text{ cov. } (f_1, f_2)}{(\bar{f}_1)(\bar{f}_2)} \right\}$ rather than (var $(f_1) - p^2$ var $(f))/(\bar{f})^2$, as p_x and f are now likely to be correlated and hence cov. (p_x, f) would exist.

It is now possible to solve for A_1, A_2, and B, but there is no check on the assumptions involved, other than the reasonableness of the answers obtained.

(iii) If $B_1 \neq B_2$, the two components are not controlled by the system in the same way, and the elementary theory is inapplicable.

Application of Theory

All yarns, especially those made from natural fibers, will contain fibers of a range of dimensions and mechanical properties. The elementary theory should therefore be applied with reservations, but if in blended yarns sensible answers are obtained for A and B, it seems reasonable to use the theory in interpreting the data.

If it may be assumed that the components differ only in their grouping, the values of A_1 and A_2 may be interpreted as mean group sizes for the two components (see Part I). In such a case, direct estimation of A_1 and A_2 is preferable to the method of calculating group size suggested by Coplan and Klein [2], as their method, though ingenious, is only applicable when there is no correlation between p_x and f. Such a correlation is possible when the two components differ markedly in their tendencies to group, and application of the method may sometimes lead to imaginary values of group size, even though interpretation in terms of real values of A_1 and A_2 is possible.

The tests for random mixing discussed in Part I may still be applied when components differ, but the departures from randomness must now be interpreted in the light of the foregoing discussion. It may of course be impossible to achieve randomness, even by prolonged mixing, if the components are not controlled by the system in the same way (i.e., $B_1 \neq B_2$).

Examination of Some Data

Data were available of fiber counts on the binary blended yarns whose compositions are detailed in the Appendix, and these will now be examined in the light of the theory developed so far. Only approximate conclusions may be drawn, however, as only 50 sections from each yarn were available; the standard errors of the estimate of variance are therefore about ± 20% (this value being that expected for a normal distribution). The standard error of a covariance is known even less exactly, but for a normal distribution from 50 cross-sections would be approximately $\pm (15/\rho)\%$, where ρ, the correlation coefficient between the variables, is small.[3] Both these estimates of variance have been found to be approximately correct for the actual data, and may be therefore used to estimate very roughly the

[3] By substitution in the formula given in standard texts on mathematical statistics, e.g., reference [26].

TABLE I. Summary of Data Derived from Fiber Counts

Yarn	p	$\bar{f}_1$	$\bar{f}_2$	$\bar{f}$	var (p_x)	var (f_1)	var (f_2)	cov. (f_1, f_2)	var (f)	$\frac{\chi^2}{n-1}$
1	0.505	55.3	54.2	109.5	0.00416	260	129	94	577	1.62
2	0.524	60.2	54.6	114.9	0.00373	131	97	19	265	1.66
3	0.543	62.6	52.8	115.4	0.00298	77	86	5	173	1.34
4	0.513	70.3	66.9	137.2	0.00255	122	142	36	335	1.24
5	0.508	70.4	68.1	138.5	0.00201	138	175	87	487	0.97
6	0.546	63.1	52.6	115.6	0.00234	182	235	151	719	1.09
7	0.472	50.8	57.7	107.6	0.00411	371	205	190	957	1.77
8	0.520	69.7	64.4	134.1	0.00472	131	334	65	595	2.55
9	0.446	54.7	67.9	122.6	0.00481	248	225	129	732	2.03
10	0.542	59.5	50.3	109.8	0.00664	140	263	79	561	2.62
11	0.491	67.2	69.6	136.9	0.00443	419	106	91	708	2.40
12	0.538	66.3	57.0	123.4	0.00535	184	396	142	863	2.38
13	0.398	40.5	61.2	101.7	0.00431	184	164	108	564	1.69
14	0.753	133.0	43.7	176.7	0.00397	829	308	243	1623	3.87
15	0.316	41.0	88.5	129.5	0.00403	172	201	63	499	2.46
16	0.674	102.4	49.5	151.9	0.00390	444	263	206	1120	2.39
17	0.581	86.3	62.2	148.5	0.00254	296	205	140	781	1.53
18	0.367	39.5	68.1	107.6	0.00263	43	194	29	294	1.17
19	0 296	31.8	75.6	107.4	0.00228	43	236	28	335	1.31

accuracy with which conclusions may be drawn from the present results.

The statistics calculated from the fiber counts are given in Tables I and II. Because of the large probable errors, those in Table II are rounded off to the first decimal place. The following comments may be made.

The calculation of χ^2 shows that that variation of blend proportions is significantly greater than the random expectation (5% probability) for all yarns except numbers 3, 4, 5, 6, 18, and 19. The estimates of A obtained from var (p_x) rather than χ^2 are seen to be slightly different in some cases; this is because in the calculation of χ^2 the variation in f between cross-sections is allowed for, whereas this has been neglected in the derivation of Equation 6. The discrepancies are, however, much smaller than the probable errors.

A departure from randomness of blend proportions does not in itself imply a difference in behavior between the two components. If we assume that $A_1 = A_2$ and $B_1 = B_2$, we may calculate A and B from Equations 5 and 6 and hence predict values of var (f_1) and var (f_2) expected for similarly-behaving components. There is no rigorous statistical method of testing whether the observed values are consistent with these predictions, but consideration of the approximate standard errors suggests that they are certainly consistent in Yarns 2, 3, 4, 5, and 17 and inconsistent in Yarns 7, 8, 10, 11, 12, 15, and 16. Yarns 1, 6, 9, 14, 18, and 19 must be considered doubtful.

Having established that some differences probably exist, values of A_1 and A_2 may be estimated from Equations 17 and 18 by assuming

TABLE II. Analysis of Data

(with estimated approximate standard errors)

Yarn	Obs. $\frac{\text{var}(f_1)}{(f_1)}$	Obs. $\frac{\text{var}(f_2)}{(f_2)}$	Obs. $\frac{\text{var}(f)}{(f)}$	Calculated A	Calculated $B(f)$	Exp. $\frac{\text{var}(f_1)}{(f_1)}$	Exp. $\frac{\text{var}(f_2)}{(f_2)}$	Exp. $\frac{\text{var}(f)}{(f)}$	Estimated A_1	Estimated A_2
1	4.7	2.4	5.3	1.8 ± 0.4	3.4 ± 1.0	3.6 ± 0.6	3.5 ± 0.6	5.2 ± 1.0	3.0 ± 1.1	0.7 ± 0.6
2	2.2	1.8	2.3	1.7 ± 0.3	0.7 ± 0.6	2.1 ± 0.4	2.0 ± 0.4	2.4 ± 0.6	1.8 ± 0.6	1.5 ± 0.3
3	1.2	1.6	1.5	1.4 ± 0.3	0.2 ± 0.4	1.5 ± 0.4	1.5 ± 0.5	1.6 ± 0.6	1.1 ± 0.4	1.5 ± 0.4
4	1.7	2.1	2.4	1.4 ± 0.3	1.0 ± 0.6	1.9 ± 0.4	1.9 ± 0.4	2.4 ± 0.6	1.2 ± 0.4	1.6 ± 0.4
5	2.0	2.6	3.5	1.1 ± 0.2	2.5 ± 0.6	2.4 ± 0.4	2.3 ± 0.4	3.6 ± 0.7	0.7 ± 1.0	1.3 ± 0.8
6	2.9	4.5	6.2	1.0 ± 0.2	5.3 ± 1.0	4.0 ± 0.6	3.5 ± 0.6	6.4 ± 1.0	0.0 ± 0.8	2.1 ± 1.0
7	7.3	3.6	8.9	1.8 ± 0.4	7.1 ± 1.5	5.1 ± 0.8	5.5 ± 0.8	8.9 ± 1.6	3.9 ± 1.6	−0.1* ± 1.0
8	1.9	5.2	4.4	2.5 ± 0.5	2.0 ± 1.0	3.6 ± 0.7	3.5 ± 0.6	4.5 ± 1.0	0.9* ± 0.6	4.2 ± 1.2
9	4.5	3.3	6.0	2.4 ± 0.5	4.3 ± 1.2	4.3 ± 0.7	4.8 ± 0.8	6.7 ± 1.2	2.6 ± 1.0	1.0* ± 0.9
10	2.4	5.2	5.1	2.9 ± 0.6	2.9 ± 1.0	4.5 ± 0.8	4.3 ± 0.8	5.8 ± 1.2	0.8* ± 1.0	3.9 ± 1.2
11	6.2	1.5	5.2	2.4 ± 0.5	2.7 ± 1.0	3.7 ± 0.6	3.8 ± 0.7	5.1 ± 1.0	4.9 ± 1.3	0.2* ± 0.6
12	2.8	6.9	7.0	2.7 ± 0.5	4.6 ± 1.3	5.1 ± 0.8	3.8 ± 0.8	7.3 ± 1.4	0.3* ± 0.8	4.8 ± 1.4
13	4.5	2.7	5.5	1.8 ± 0.4	4.4 ± 1.0	3.6 ± 0.6	4.5 ± 0.8	6.2 ± 1.1	2.8† ± 1.0	0* ± 0.8
14	6.2	7.0	9.2	3.8 ± 0.8	7.4 ± 2.3	9.3 ± 1.8	5.6 ± 1.0	11.2 ± 2.4	0.7* ± 2.1	5.2† ± 1.5
15	4.2	2.3	3.9	2.4 ± 0.5	2.2 ± 1.0	3.1 ± 0.6	4.0 ± 0.8	4.6 ± 1.1	3.5† ± 0.9	0.8* ± 0.8
16	4.3	5.3	7.4	2.7 ± 0.5	6.2 ± 1.6	6.8 ± 1.2	3.8 ± 0.8	8.9 ± 1.6	0.7* ± 1.2	3.3† ± 1.2
17	3.4	3.3	5.3	1.5 ± 0.3	3.9 ± 1.0	3.8 ± 0.6	3.2 ± 0.6	5.4 ± 1.0	1.2 ± 0.8	1.7† ± 0.8
18	1.1	2.8	2.7	1.2 ± 0.2	1.2 ± 0.6	1.6 ± 0.3	2.0 ± 0.4	2.4 ± 0.6	0.7 ± 0.3	2.1 ± 0.6
19	1.4	3.1	3.1	1.2 ± 0.2	1.2 ± 0.6	1.5 ± 0.3	2.1 ± 0.6	2.4 ± 0.7	1.0† ± 0.4	2.2 ± 0.7

* Longer component.
† Coarser component.

$$B_1 = B_2 = \frac{\text{cov. } (f_1, f_2)}{pq\ (\bar{f})^2} \quad \text{(from Equation 6)}$$

The results are necessarily very approximate, and once again there is no rigorous statistical method of testing the apparent differences. On the whole, the conclusions already reached are confirmed, with Yarns 2, 3, 4, 5, and 17 showing differences which are probably negligible. Because of the large expected errors in this test most of the remaining yarns appear as borderline cases.

Discussion of Results

Although the data have been analyzed principally in order to illustrate the application of the theory and were not obtained originally with any such purpose in mind, a number of very interesting points emerge.

Yarns 1–6 were blends of fibers of similar length and denier. These appear to be consistent with the simple theory, although in Yarn 6 it seems unlikely that $A_1 = 0$; the interpretation of the data is necessarily approximate, and this zero value is probably spurious. The alternative hypothesis, that $A_1 = A_2 = 1$ (i.e., we have similarly-behaving components distributed randomly) seems to be more reasonable.

Yarns 17–19 were blends of fibers differing in denier but not in length. Again, reasonable results are obtained by application of the theory. Reference to details of yarn preparation (Appendix) suggests that in both sets the effects of initial irregularity should be small, and the values of A_1 and A_2 may probably be interpreted as estimates of mean group size.

In Yarns 7–16, however, the fibers differed in staple length (in 13–16 in denier also) and a very interesting effect is observed. In each case there is a very large difference between the estimated A_1 and A_2. The value associated with the longer component, moreover, is almost invariably less than unity, while that for the shorter component is greater than 2.5. The mean values (with standard errors) are 3.9 ± 0.2 and $0.4(5) \pm 0.1$, respectively, compared with 1.4 ± 0.3 for the components in all the other yarns. Thus not only is there a highly significant difference between the values for the longer and shorter components, but also the mean of the former is very significantly less than unity.

A value less than unity is inconsistent with the theory developed here. It must therefore be concluded that the theory is inapplicable when there is a difference between the lengths of the components.

It is worth while, however, to inquire whether the theory is capable of suggesting how such a discrepancy could occur. The significant point is that on the average less than half the expected independent variation occurs in the longer component. If the two components were simply controlled by the system to different extents, this would be expected to reduce their common variation and supplement their independent variations. In this case the opposite is observed, and it seems that part of the expected random variation in the longer component has in fact contributed to the common variation. This implies that the longer component is in some way controlling the occurrence of the shorter component. Consideration of the processes suggests that the behavior of the sliver in the drafting zone would be largely determined by the occurrence of the longer fibers, and it is therefore not surprising that the theory breaks down in this case.

These results suggest that the effect of length differences on the statistics of blending is a subject needing further investigation.

Conclusions

The elementary theory of blend irregularity may only be applied to real yarns with some reservations. Reasonable results have been obtained when components were similar in length and denier or differed only in denier, but the theory appears to be inapplicable where there are differences in length, although it is possible to put forward a reasonable explanation for the observed anomalies.

The tests for random mixing are still useful as an assessment of the blend regularity achieved, but the attainment of randomness may not always be possible in practice.

Part III: Arrangement of Fibers within the Cross-Section

Possible Means of Assessment

Parts I and II were concerned with the distribution of fibers along the length of the yarn. Randomness in this sense, however, may not always be associated with a random arrangement of fibers within any cross-section, and it is necessary now to consider what guidance theory can give us in testing for departures from randomness of this type.

Possible aspects of the observed arrangement which may be tested are as follows: (i) the variation of blend proportions within the cross-section; (ii) the number of apparent groups of each component; and (iii) the sizes of the apparent groups. In an irregular two-dimensional arrangement, it is not always clear what is meant by a "group" of fibers, but we shall see that there are a number of ways in which this difficulty may be avoided.

Before applying any of these tests it is necessary to decide whether they should be applied to the surface zone of the yarn alone, which is primarily responsible for its appearance, or to the cross-section as a whole. In a blend of fibers differing only in color, it may be reasonable to regard the surface zone as merely an unbiased sample from the whole cross-section; consideration of the whole section then makes the tests more sensitive because of the greater number of fibers involved. When the components differ physically, however, it is a well-established fact that some radial separation of components takes place [4, 10, 14], and the composition of the blend may vary by as much as 30% from core to surface. In such a case there are strong arguments for applying the tests to the surface zone alone.

In the application of the tests, a useful fiber-counting technique suggested by Coplan and Klein [3] has the twofold advantage of yielding a linear array to which simple binomial statistics may be applied and enabling different zones of the cross-section to be studied separately. A point in the center of the section is chosen, and a continuous line is drawn from this point to the surface in the form of a rough spiral, taking in one layer of fibers (as far as possible) in each revolution. The arrangement of fibers along this spiral is then recorded.

If only the surface zone is to be examined, a counting method used by Hamilton [15] is appropriate. On the projection of the cross-section (prepared as described elsewhere [13]) the fibers round the edge are marked, together with those touching them. (These fibers are possible surface fibers before the laying-in of hairiness.) The marked fibers are then joined consecutively by a zig-zag line, along which the arrangement of fibers is studied. In a truly random arrangement the configuration of the chosen line is immaterial provided that it is drawn without reference to the nature of the individual fibers, and this procedure should therefore lead to the same conclusion as the study of Coplan and Klein's two outer layers. The data used to illustrate this part of the paper were obtained by this method.

We shall now show how the three possible methods of assessment may be applied to the data.

Variation of Blend Proportions

The variation of blend proportions within the cross-section may be studied simply by dividing the section arbitrarily, the actual arrangement of fibers within each division being ignored. Coplan and Klein have used this method to obtain a within-section IBI [2, 3]. If it may be assumed that grouping together of similar fibers is the only factor affecting mixing within the section and that the groups are statistical units randomly distributed, a mean group size may be deduced from the mean $(IBI)^2$ within the individual cross-sections. Alternatively the mean variance of proportions between the divisions may be calculated and Equation 6 modified to include the mean number of fibers in the arbitrary divisions. The expected errors may be roughly calculated in the same manner as before. Group sizes have been estimated by the latter method from data for three blended yarns (Nos. 17–19 in Appendix), and it will be seen that none of the three yarns shows departures from randomness in this respect which are of certain statistical significance (the standard error of the group size being at least $\pm$ 0.2).

The figure obtained in this way is an over-all estimate for the whole section. It is quite possible that the two components would exhibit different grouping tendencies. As in the test for variations between sections, Coplan and Klein's method of calculating component group sizes is not universally applicable, and the following alternative method is suggested. The only assumption made is that the groups are statistical units randomly distributed.

Let f', p', etc. be defined by the number of groups of size ν_1 and ν_2 of the respective components. Then

$$\text{var } (p_x') = p'q'/\bar{f}'$$

$$\text{var } (f_1') = (p')^2 \text{ var } (f') + (\bar{f}')^2 \text{ var } (p_x')$$

$$\text{var } (f_2') = (q')^2 \text{ var } (f') + (\bar{f}')^2 \text{ var } (q_x')$$

$$\therefore (q')^2 \text{ var } (f_1') - (p')^2 \text{ var } (f_2') = p'q' (q' - p')\bar{f}'$$

TABLE III. Group Sizes Estimated from Fiber Counts in Semi-Zones

Yarn	p	$\bar{f}_1$	$\bar{f}_2$	$\bar{f}$	Var p_x	Var f_1	Var f_2	ν	ν_1	ν_2
17	0.409	11.8	17.0	28.8	0.01123	9.52	8.77	1.34	1.36	1.31
18	0.274	7.1	18.9	26.0	0.01038	6.98	6.89	1.35	1.35	1.36
19	0.243	6.3	19.7	26.0	0.00780	4.76	4.76	1.02	1.01	1.05

Converting to fiber numbers and simplifying,

$$q^2 \text{ var } (f_1) - p^2 \text{ var } (f_2) = pq\,(\nu_1 q - \nu_2 p)\bar{f}$$

$$\therefore\ \nu_1 q - \nu_2 p = q\,\frac{\text{var } (f_1)}{\bar{f}_1} - p\,\frac{\text{var } (f_2)}{\bar{f}_2}$$

Now

$$\nu_1 q + \nu_2 p = \frac{\bar{f} \text{ var } (p_x)}{pq} \quad \text{(Equation 20)}$$

Whence

$$\nu_1 = \frac{1}{2q}\left\{\frac{\bar{f} \text{ var } (p_x)}{pq} + \frac{q \text{ var } (f_1)}{\bar{f}_1} - \frac{p \text{ var } (f_2)}{\bar{f}_2}\right\} \quad (21a)$$

$$\nu_2 = \frac{1}{2p}\left\{\frac{\bar{f} \text{ var } (p_x)}{pq} + \frac{p \text{ var } (f_2)}{\bar{f}_2} - \frac{q \text{ var } (f_1)}{\bar{f}_1}\right\} \quad (21b)$$

Equations 21a and 21b show how the sizes of the fiber groups distributed in the cross-section can be deduced from the variation of fiber numbers and blend proportions. The calculated values of ν_1 and ν_2 for the present yarns are given in Table III. There is no suggestion of any difference between the components in any of the yarns.

Number of Apparent Groups

In order to assess the number of apparent groups of similar fibers it is necessary to convert the irregular arrangement of fibers in the cross-section into an ordered arrangement which can be treated statistically. The assumption of regular close packing, suggested by some authors [16], would seem to be improper in many cases [5].

Cox [8] developed a theory of blending in which he considered parallel "sub-slivers" within the roving being spun. He assumed that no lateral mixing occurred (*cf.* Coplan and Klein's assumption of a random arrangement), and he developed a test for the arrangement of fibers in slivers or rovings which may be opened out into a plane web. In its original form the test is not applicable to yarns after spinning.

De Barr and Walker [9] have shown that the number of apparent groups (g) of each component in the plane web predicted by Cox's theory is

$$g = \Omega pq\{1 - \exp(-f/\Omega)\} \quad (22)$$

while for random mixing (f being large, i.e., at least 50)

$$g_x \approx fpq \quad (23)$$

They define a quantity γ as the ratio of the observed g to the theoretical g_x. Cox's theory predicts

$$\gamma = \frac{\Omega}{f}\{1 - \exp(-f/\Omega)\} \quad (24)$$

In practice, however, they find that random mixing is achieved more rapidly than Cox's theory would predict, and conclude that appreciable lateral mixing must take place.

Coplan [6] has pointed out that if fiber groups are assumed to be distributed at random, γ may be taken as the reciprocal of a mean group size. In addition to providing a possible explanation of the discrepancies between observation and Cox's theory, this interpretation of γ allows it to be used to characterize the arrangement of fibers along any arbitrary line in the cross-section of the spun yarn. The statistical distribution of γ in random systems may be calculated as follows.

Imagine marks made between each fiber in the linear array, these marks differing according to the composition of the pair they separate. The observed and expected frequencies of each type of mark may then be calculated as in Table IV. We may thus form

$$\chi^2_{(1)} = \frac{(g - g_x)^2}{p^2q^2f} \quad (25)$$

It will be noted that this expression differs from that given by Coplan and Klein [3]. The expression given here is considered preferable, because we have considered distribution of individuals between classes, which is the correct use of χ^2. In the well-known coin-tossing problem, for example, χ^2 is calculated not from the occurrence of "heads" alone, but (observed − expected)^2/expected is calculated for both "heads" and "tails" and $\chi^2_{(1)}$ obtained by addition. Unless such a procedure can be employed, the calculation of (observed − expected)^2/expected becomes meaningless. The number of classes which can be assigned independently shows

TABLE IV. Formation of χ^2 for Neighboring Fibers

Class	I	II	III	IV
Neighbors	a, a	a, b	b, a	b, b
Expected	$pf-g_x$	g_x	g_x	$qf-g_x$
Observed	$pf-g$	g	g	$qf-g$

the number of degrees of freedom for which χ^2 must be calculated—in this case, one only. It will be seen below that the result obtained here is more appropriate in practice than Coplan and Klein's.

For a given level of $\chi^2_{(1)}$, we may calculate the distribution of γ_i for individual cross-sections.

$$|g - g_x| = \sqrt{\chi^2_{(1)} p^2 q^2 f}$$
$$\therefore |\gamma_i - 1| = \sqrt{\chi^2_{(1)}/f} \qquad (26)$$

If n sections are available,

$$|\gamma' - 1| = \sqrt{\chi^2_{(1)}/\Sigma f} \qquad (27)$$

where γ' is calculated for the complete set of data. In practice, γ' will be indistinguishable from the mean of γ_i. These results may be used to test whether an observed result is significantly less than the unity expected in a random arrangement. Assuming a symmetrical distribution of γ_i (seen below to be true in practice), 5% probability levels may be calculated from the 10% level of $\chi^2_{(1)}$. To avoid confusing effects within the section with blend variations along the yarn, g and g_x must be determined for each section individually [3].

Confidence limits may be set for an observed value of γ, 5% levels now corresponding to the 5% level of $\chi^2_{(1)}$. If the observed γ is significantly less than unity, it may be assumed that the number of independent units in each section is γf and Equations 26 and 27 modified accordingly.

It will be noted that the error in the estimation of group size from γ is much smaller than in that calculated from the variance of blend proportions, the ratio being of the order of $1/\sqrt{f}$ when both are calculated from 50 sections. This means that γ should provide a more sensitive test for departures from randomness.

The results of group counts in the surface zones of Yarns 17, 18, and 19 are shown in Table V. Only No. 17 gives a significantly low γ, No. 19 is a borderline case, and No. 18 well within the limit.

Values of γ_i for each individual section have been calculated, and compared with the theoretical distribution derived from Equation 26 and with Cop-

TABLE V. Calculation of γ

Yarn	17	18	19
Mean no. of fibers, $\hat{f}_1$	34.0	37.7	39.4
$\hat{f}_2$	23.5	14.3	12.6
Mean no. of groups of each, $\hat{g}$	12.7	10.0	9.1
Mean proportion (by number), p	0.591	0.274	0.243
Total observed groups of each, Σg	635	499	453
Total expected number, Σg_x	669	505	467
Ratio, γ'	0.948	0.989	0.967
5% lower limit	0.969	0.968	0.968
Estimated mean group size, $1/\gamma'$	1.055	1.011	1.034
95% limits	±0.038	±0.040	±0.040

TABLE VI. Distribution of γ_i

Yarn	% Levels of $\chi^2_{(1)}$	Expected number	Observed number for limits calculated from: Equation 26	Observed number for limits calculated from: C. & K.
17	0–20	10	9	4
	20–50	15	16	12
	50–80	15	14	16
	80–100	10	11	18
18	0–20	10	12	4
	20–50	15	14	12
	50–80	15	15	17
	80–100	10	9	17
19	0–20	10	18	6
	20–50	15	9	14
	50–80	15	14	13
	80–100	10	9	17
Total $\chi^2_{(3)}$			9.9	26.9
Probability			>30%	<1%

TABLE VII. Symmetry of γ_i

Yarn	% Levels of $\chi^2_{(1)}$	Between limits below mean	Between limits above mean
17	0–20	5	4
	20–50	7	9
	50–80	5	9
	80–100	5	6
18	0–20	7	5
	20–50	4	10
	50–80	9	6
	80–100	6	3
19	0–20	9	9
	20–50	5	4
	50–80	5	9
	80–100	5	4
Total $\chi^2_{(3)}$ (for expected symmetry)		2.0	
Probability		>99%	

lan and Klein's suggested test. It is seen from Table VI that while the deviations from the former could easily occur by chance, those from the latter are unlikely. Table VII shows the validity of our assumption of symmetry of γ_i about $\bar{\gamma}$.

Sizes of Apparent Groups

The distribution of the sizes of apparent groups in a random linear arrangement of fibers of two types drawn from an infinite population of known blend proportions may be calculated from the binomial probability. The expected number (E) of groups of the first component containing just x individuals is given by

$$E\,(r = x) = fp^x q^2$$

and of those containing not less than x by

$$E\,(r \geqslant x) = fp^x q$$

Appreciable anomalies in grouping may thus be detected by comparison of observed and expected distributions.

It should be possible to test this distribution by a form of χ^2 test (though indirectly, as the groups themselves are not distributable units) but this would give no indication of the nature of the deviation. The most important type of deviation would be the existence of an unexpected number of very large accumulations of one component, to which a test analogous to Hampson and Onions' large cluster test [16] could be applied. The largest accumulations of each component in Yarns 17, 18, and 19 are listed in Table VIII, together with the appropriate $E\,(r \geqslant x)$ for the combined 50 sections of each. It will be seen that the only group for which $E\,(r \geqslant x) < 5 \times 10^{-2}$ occurs in Yarn 17. (This yarn was the only one of the three which contained significantly fewer groups than expected.)

Further examination shows a tendency for Tricel to form an appreciable number of very large groups in all three yarns. This is shown in Table IX, and its significance is not quite clear. It seems possible that it might have some effect on the appearance of the yarn if the components differed in color, but this could be decided only by further investigation.

TABLE VIII. Largest Accumulations in the Observed Surface Zones

Yarn		Size of largest groups, r_m	Total number expected $\geqslant r_m$
17	Tricel	16	2×10^{-1}
	Fibro	12	4×10^{-2}
18	Tricel	29	6×10^{-2}
	Fibro	7	2×10^{-1}
19	Tricel	32	9×10^{-2}
	Fibro	5	1.3

TABLE IX. Large Accumulations of Tricel

Yarn	$r \geqslant 10$ Observed no. of groups	$r \geqslant 10$ Expected no. of groups
17	16	6.2
18	33	28.8
19	46	39.2

Discussion

It has been shown how tests of three different types may be used to assess the randomness of arrangement of fibers within the cross-sections of blended yarns. It must be emphasized that each test is concerned with different aspects of randomness, and it is therefore not surprising that they do not always lead to exactly the same conclusion. For example, in the three yarns considered, while Yarn 17 shows a significantly low value of γ and a highly unlikely large cluster, the variation of blend proportions is within the expected limits. Yarns which are borderline cases in any one test should either be given the benefit of the doubt or be subjected to a different type of test before a decision is reached.

Two of the tests considered enable an estimate to be made of a mean group size. This, however, is not the mean size of the apparent groups, but the size of equal groups which when distributed randomly would give a value of the parameter considered equal to that observed in the array considered. When an arbitrary linear arrangement in a section cutting fibers of finite length is considered, it is obvious that even if such groups are distributed randomly in the yarn, the tests applied will not give a true picture of their nature. The results of the tests should not be regarded as descriptions of the actual arrangement of fibers so much as estimations of the probability of the observed arrangements occurring in a random system. The existence of fiber groups is only one of the possible explanations of departures from randomness, as may be seen by comparing the interpretations of γ given by De Barr and Walker on the one hand and Coplan and Klein on the other.

In many ways, γ is the most convenient of the possible statistics, leading to a very accurate estimate of a mean group size; but differences in behavior between the components, although sometimes detectable in a study of apparent group sizes, may usually be estimated only by the less sensitive test involving the variation of blend proportions. Small-scale tests, of the type suggested by Hampson and Onions, although useful as spot tests where a rapid assessment is essential, are in general less satisfactory in their results.

Although in a given yarn, the less probable arrangement would be the less regular in its blending, there are obvious dangers in using statistical parameters to compare the arrangements of fibers in different yarns, especially if the appearance of the yarn is being studied. Some parameter which describes the actual arrangement, perhaps some weighted mean of the apparent group sizes, would then be preferable.

In illustrating the different types of test, data from real yarns have been used. It was also considered to be of interest to apply the test to model systems constructed from tables of random numbers. As would be expected, these systems showed variance of blend proportions and component grouping tendencies within the expected limits, the predicted distribution of γ_i, and no significantly large accumulations of either component.

Conclusions

The most sensitive test for a departure from a random arrangement along a line in the cross-section is that based on the number of apparent groups. If it is desired to investigate the separate behavior of the two components, the less sensitive method, based on the variation of blend proportions, must be used. Additional information obtained from the study of large clusters may be important as regards the appearance of the fabric. All these tests, however, are means of assessing departures from randomness rather than describing the actual arrangement of fibers.

Appendix

Composition of Yarns

No.	1st Component	2nd Component	(1st Component) by number
1	Fibro 3 den. 2½″	Celafibre 3 den. 2½″	0.50
2	Fibro 3 den. 2½″	Tricel 3 den. 2½″	0.52
3	Fibro 3 den. 2½″	Courtelle 3 den. 2½″	0.54
4	Fibro 3 den. 2½″	nylon 3 den. 2½″	0.51
5	Fibro 3 den. 2½″	Dacron[1] 3 den. 2½″	0.51
6	Celafibre 3 den. 2½″	nylon 3 den. 2½″	0.55
7	Fibro 3 den. 1 7/16″	Celafibre 3 den. 2½″	0.48
8	Fibro 3 den. 2½″	Celafibre 3 den. 1 7/16″	0.52
9	Fibro 3 den. 1 7/16″	nylon 3 den. 2½″	0.45
10	Fibro 3 den. 2½″	nylon 3 den. 1 7/16″	0.54
11	Celafibre 3 den. 1 7/16″	nylon 3 den. 2½″	0.49
12	Celafibre 3 den. 2½″	nylon 3 den. 1 7/16″	0.54
13	Fibro 4½ den. 1 7/16″	Celafibre 3 den. 2½″	0.40
14	Fibro 4½ den. 1 7/16″	Celafibre 4½ den. 1 7/16″	0.75
15	Fibro 4½ den. 1 7/16″	nylon 1½ den. 2½″	0.32
16	Fibro 1½ den. 2½″	nylon 3 den. 1 7/16″	0.67
17	Fibro 1½ den. 2″	Tricel 4½ den. 2″	0.58
18	Fibro 3 den. 2½″	Tricel 3 den. 2½″	0.37
19	Fibro 4½ den. 2″	Tricel 2 den. 2″	0.30

[1] DuPont Polyester fiber.

Spinning

All the yarns were 12/1 cotton count. The components were blended at the opener and passed once through the beater to form blend laps. Four laps were then passed twice through the beater to form finished laps, which were then carded. The slivers were drawn six-ends-up with a draft of six, three heads of drawing being used to produce the final sliver. This was fed one-end-up to the intermediate frame and spun two-end-up on the ring

frame. The spinning was superintended by Dr. G. M. Jeffrey.

Components

Fibro[2]	Viscose rayon staple (Courtaulds Ltd.)
Celafibre[2]	Acetate staple (British Celanese Ltd.)
Tricel[2]	Triacetate staple (British Celanese Ltd.)
Courtelle[2]	Acrylic fiber (Courtaulds Ltd.)
Nylon	Polyamide fiber (British Nylon Spinners Ltd.)
Dacron[2]	Polyester fiber (E. I. du Pont de Nemours Inc.)

[2] Regd. Trade Marks.

Literature Cited

1. Breny, H., *J. Textile Inst.* **49**, T48 (1958).
2. Coplan, M. J. and Klein, W. G., TEXTILE RESEARCH JOURNAL **25**, 743 (1955). (Note corrections on p. 968.)
3. Coplan, M. J. and Klein, W. G., TEXTILE RESEARCH JOURNAL **29**, 632 (1959).
4. Coplan, M. J. and Bloch, M. G., TEXTILE RESEARCH JOURNAL **25**, 902 (1955).
5. Coplan, M. J. and Klein, W. G., *J. Textile Inst.* **47**, T232 (1956).
6. Coplan, M. J., *J. Textile Inst.* **49**, P 392 (1958).
7. Cox, D. R. and Ingham, J., *J. Textile Inst.* **41**, P 376 (1950).
8. Cox, D. R., *J. Textile Inst.* **45**, T113 (1954).
9. de Barr, A. E. and Walker, P. G., *J. Textile Inst.* **48**, T405 (1957).
10. Ford, J. E., *J. Textile Inst.* **49**, T608 (1958).
11. Foster, G. A. R., *J. Textile Inst.* **41**, P398 (1950).
12. Grishin, P. F., *J. Textile Inst.* **45**, T167 (1954).
13. Hamilton, J. B., *J. Textile Inst.* **49**, T411 (1958).
14. Hamilton, J. B., *J. Textile Inst.* **49**, T687 (1958).
15. Hamilton, J. B., private communication.
16. Hampson, A. G. and Onions, W. J., *J. Textile Inst.* **46**, T377 (1955).
17. Hannah, M., *J. Textile Inst.* **47**, T236 (1956).
18. Hannah, M. and Rodden, S., *J. Textile Inst.* **47**, T402 (1956).
19. Hannah, M. and Rodden, S., *J. Textile Inst.* **49**, T52 (1958).
20. Ingham, J., *J. Textile Inst.* **49**, P364 (1958).
21. Lund, G. V., TEXTILE RESEARCH JOURNAL **24**, 759 (1954).
22. Martindale, J. G., *J. Textile Inst.* **41**, P340 (1950).
23. vanden Abeele, A. M., *J. Textile Inst.* **42**, P162 (1951).
24. Walker, P. G., *J. Textile Inst.* **48**, T133 (1957).
25. Walker, P. G., *J. Textile Inst.* **49**, P365 (1958).
26. Weatherburn, C. E., "A First Course in Mathematical Statistics," Cambridge, 1947, Chapter VII.

Manuscript received February 17, 1961.

The Relationship of Fine Structure to Mechanical Properties of Stretched Saponified Acetate Fibers[1]

B. Sheldon Sprague and Herman D. Noether

Celanese Corporation of America, Summit Research Laboratories, Summit, N. J.

Introduction

The relationship of fine structure to mechanical properties of viscose rayon has been the subject of considerable investigation and discussion. Hermans [1], Ingersoll [4], Howsman [3a], and Sisson [7], to mention only a few, have investigated the dependence of mechanical properties on crystallite orientation and crystallinity. However, these investigations have been primarily concerned with the rupture properties of the fibers, rather than with more general aspects of stress–strain behavior, and have been complicated by the difficulty in separating the effects of orientation and crystallinity [3b].

Little information has been published, however, on the relationship of fine structure to mechanical properties of rayons prepared by the saponification of stretched cellulose acetate, the only major study being due to Work [11]. These fibers have special interest because, while highly oriented and crystalline, their acetate precursors are highly oriented but noncrystalline. By studying both the regenerated rayon and

[1] Presented at the 139th Annual Meeting, American Chemical Society, Division of Cellulose Chemistry, St. Louis, Missouri, March 22, 1961.

the acetate precursor, therefore, it is possible to separate to some degree the effects of orientation and crystallinity.

It is the purpose of this study to determine the fine structure and mechanical properties of a series of stretched acetate fibers and the corresponding rayons prepared by saponification, as a function of degree of stretching. The relationship of fine structure to mechanical properties will be examined, and a qualitative explanation of the observed effects will be presented.

Materials and Methods

Preparation of Yarns

Nominal 560 denier cellulose acetate yarn, prepared from acetate of approximately 54% combined acetic acid by normal dry spinning from acetone, was stretched to various levels from 50–2000% in saturated steam at a gauge pressure of 50 lb./in.^{2} and sampled. The stretched acetates were cake saponified in 1% caustic and 10% sodium acetate for one hour at 65° C., washed, and dried. These conditions were chosen specifically to prevent loss of orientation during saponification, by suppressing swelling and solvation, and although it cannot be proved conclusively that some disordering did not occur, the properties and fine structure of the resulting rayons, to be discussed below, indicate that any such disordering must have been very minor indeed.

Mechanical Properties

Tensile tests were performed on an Instron tensile tester operating at a rate of specimen extension of 60%/min. with a gauge length of 3.33 in. Except where noted, all testing was carried out at 23° C. and 65% RH. Where wet testing was performed, the specimens were tested fully immersed. Tenacity, elongation, initial modulus, and yield stress were calculated from the stress–strain curves.

Fine Structure

X-ray data were obtained on a North American Philips X-ray diffractometer, using nickel filtered CuKα radiation. Flat plate fiber diagrams were obtained using a film-to-specimen distance of 5.00 cm., with the specimens irradiated perpendicular to the fiber axis.

Crystallite orientation values were obtained by examining the azimuthal intensity distributions of the 10$\bar{1}$ and 10$\bar{1}$ diffractions for cellulose II (specimen rotating perpendicular to beam). The orientation was calculated as the angular width of the diffraction arc at one-half maximum intensity.

Relative percent crystallinity [2] was determined from goniometer curves obtained with a geiger counter diffractometer and a well randomized specimen. The specimen preparation has been described previously [10]. The relative percent crystallinity was calculated as the ratio of the area between the diffractometer curve for the specimen and an assumed curve for amorphous cellulose to the total area under the diffractometer curve for the specimen. While the data are relative with respect to the assumed amorphous curve, they are in reasonable agreement with absolute values reported in the literature [2, 3c], if it is assumed that the 50% stretch saponified acetate is similar in crystallinity to textile viscose rayon.

Fiber birefringence was examined by both the Berek Compensator and Becke line methods. The former was more satisfactory, but the results reported are only approximate because of the difficulty in measuring fiber thickness at the point of retardation measurement.

Experimental Data

The fine-structure data for both the acetate and saponified acetate fibers examined are given in Table I. The tensile data for the same fibers are given in Table II.

The effect of varying degrees of steam stretching on the stress–strain behavior of cellulose acetate is shown in Figure 1. Note that tenacity, modulus, and yield stress increase regularly while elongation remains fairly constant at about 5%, above 100% stretch. The corresponding saponified acetates are shown in Figure 2. The regular progression of strength, modulus, and yield stress with increasing stretch is maintained, but the levels reached are somewhat changed from those of the acetates. This will be more fully explored below.

The fact that the acetates are essentially noncrystalline as compared to their saponified counterparts

[2] The calculation of "percent crystallinity" is not meant to imply the existence of a two-phase crystalline–amorphous structure. Rather, a distribution of orders exists, from completely random to 3-dimensional or crystalline [5a]. Percent crystallinity is a convenient method of establishing quantitatively the amount of ordered material, that is, material showing structurally regular regions above certain minimum dimensions.

TABLE I. Fine-Structure Data for Stretched, Saponified Acetates

Stretch, %	Orientation angle, deg. 101 Plane	Orientation angle, deg. 10$\bar{1}$ Plane	Relative crystallinity, %	Birefringence
0	37.7	35.7	39.8	—
50	26.4	21.0	41.7	0.033
100	23.1	17.5	44.8	0.041
150	21.7	16.1	46.8	0.046
200	21.7	15.9	47.2	0.046
300	19.9	15.0	48.4	0.045
500	19.9	14.8	52.0	0.053
1000	19.9	14.9	53.3*	0.046
2000	19.3	14.4	54.0	0.050

* Interpolated from other data on a similar series.

TABLE II. Mechanical Properties of Stretched and Stretched, Saponified Acetates

Fiber type	Stretch, %	23° C., 65% RH Yield stress, g./den.	Tenacity, g./den.	Elongation, %	Modulus, g./den.	23° C. wet Tenacity, g./den.	Modulus, g./den.
Acetate	50	1.1	1.8	7.1	60	1.2	37
	100	1.7	2.3	5.0	100	1.3	51
	150	2.1	2.8	4.5	110	1.8	61
	200	2.3	2.6	4.1	120	2.1	67
	300	2.5	3.5	4.6	130	2.1	70
	500	2.6	3.7	4.5	140	2.5	71
	1000	2.5	4.7	5.0	150	2.7	84
	2000	2.8	5.2	4.9	190	—	85
Saponified acetate	50	0.8	2.3	7.7	110	1.3	11
	100	1.0	3.2	5.5	160	1.7	26
	150	1.3	4.0	5.2	190	2.4	32
	200	1.4	4.7	5.1	220	2.8	46
	300	1.4	5.5	5.4	250	3.7	53
	500	1.5	6.1	5.3	260	4.2	66
	1000	1.6	6.7	5.3	280	5.3	88
	2000	1.7	8.2	5.6	310	—	92

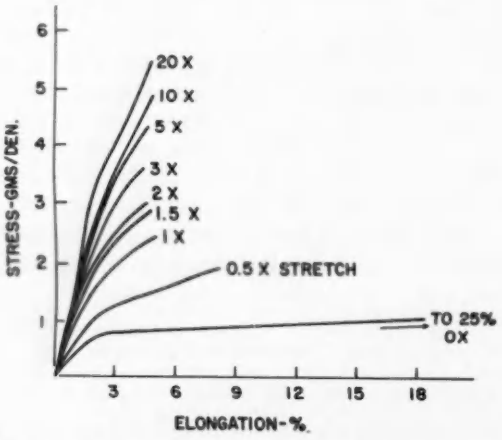

Fig. 1. Effect of stretching in moist steam on stress–strain properties of acetate.

is demonstrated by the X-ray diffraction pattern of Figure 3. Even at 100% stretch the saponified acetate is seen to be highly oriented, and the acetate also displays a higher diffraction intensity along the equator, suggesting considerable orientation of non-crystalline material.

The effect of stretch on crystalline orientation is given more fully in Figure 4. Here all orientation is seen to be essentially complete by 300% stretch, even though tenacity and modulus increase considerably at higher degrees of stretch. The orientation of the acetates can only be inferred because of the lack of crystallinity and inherently low birefringence of cellulose acetate of about 2.5 degree of substitution. However, it is quite reasonable to assume, because of the method of preparation and saponification, that the orientation of the crystallites in the saponified acetates also represents the minimum average molecu-

lar orientation for the acetates. Accordingly, the orientation of the acetates probably also reaches a constant level at about 300% stretch.

The over-all orientation of both the crystalline and noncrystalline regions as indicated by the birefringence data of the saponified acetates (Table I) reveals roughly the same picture, a constant level being reached at about 200% stretch. Scatter of the data is quite large because of the noncircular cross sections of the fibers.

The effect of stretch on crystallinity of the saponified acetates is shown in Figure 5. The increase in crystallinity is not large and has essentially reached a constant level by 500% stretch.

Figure 6 shows the effect of stretch on the initial modulus of the acetate and saponified acetate yarns. The difference in modulus between the two types of yarn is actually not as large as it appears at first glance. Saponification of the acetate reduces its molecular weight considerably. Accordingly, since modulus here is measured on a yarn weight basis (denier = weight per unit length) rather than on an area basis, a reduction in weight of the yarn due to saponification would raise the modulus proportionately, all other structural factors remaining constant. The theoretical rise in modulus due to reduction in molecular weight is shown by the dotted line in Figure 6. The major increase for saponified acetate occurs in the first 300% stretch. In the parent acetate the major increase in modulus also takes place

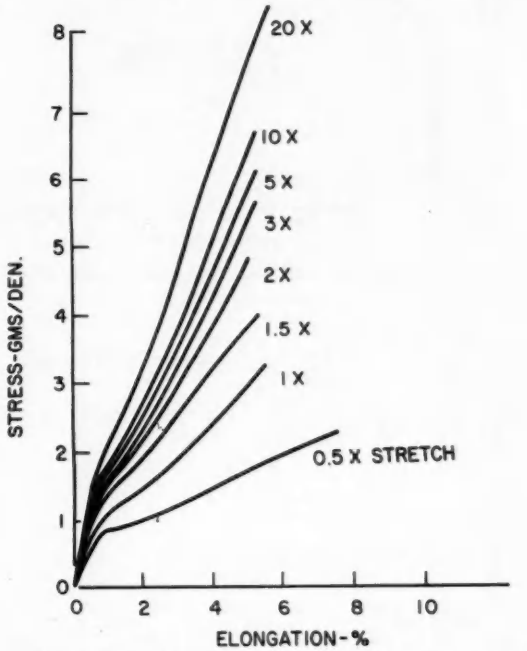

Fig. 2. Stress–strain properties of saponified steam-stretched acetates.

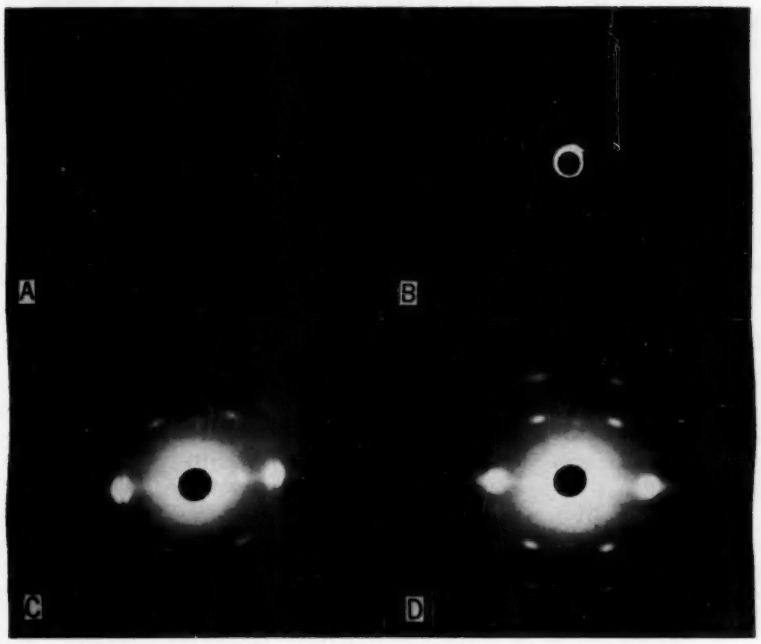

Fig. 3. X-ray diffraction patterns of stream-stretched acetate and saponified stretched acetate. A, Acetate 100% stretch; B, acetate 1000% stretch; C, saponified acetate 100% stretch; D, saponified acetate 1000% stretch.

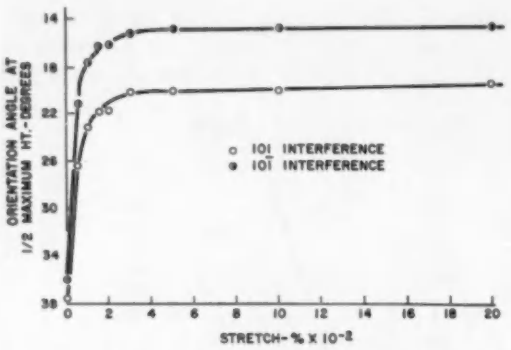

Fig. 4. Effect of stretch on crystallite orientation of saponified acetate.

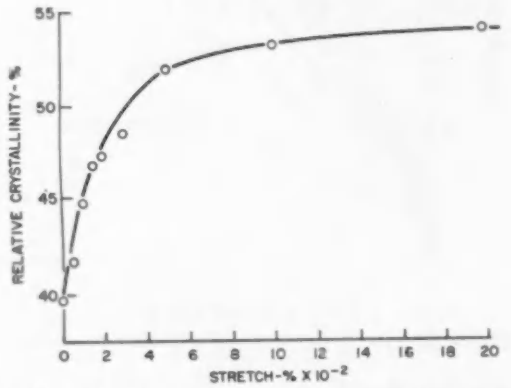

Fig. 5. Effect of stretch on crystallinity of saponified acetate.

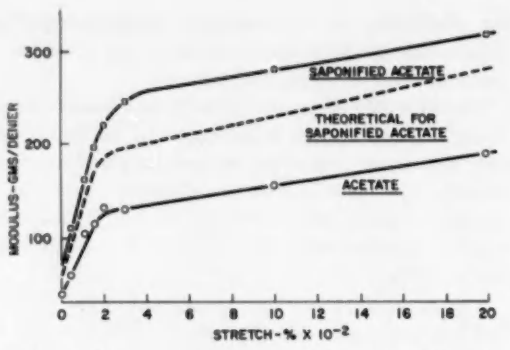

Fig. 6. Effect of stretch on modulus of acetate and saponified acetate.

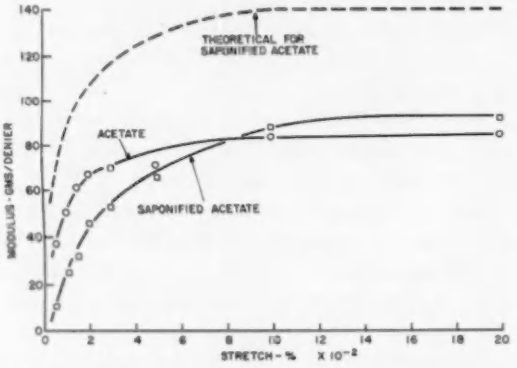

Fig. 7. Effect of stretch on wet modulus of acetate and saponified acetate.

in the first 300% stretch, with a relatively small further increase between 300% and 2000% stretch.

As is seen in Figure 7, in wetting out the fibers, the modulus is considerably reduced, although orientation is maintained, i.e., no fiber shrinkage occurs. The loss of modulus on wetting is much more severe with the saponified acetates and indicates clearly that the high dry modulus is not associated with crystallinity, since water does not appreciably swell the cellulose crystal [3d]. Accordingly, the modulus must be associated primarily with the straining of intermolecular secondary bonds which, in these cases, may be solvated with water, thus reducing their energy [5b]. In the case of cellulose, these secondary bonds appear to be hydrogen bonds associated with the numerous hydroxyl groups [3d].

Some further insight into the nature of the structure may be obtained by considering the relationship of tenacity to modulus under dry and wet conditions, as shown in Figure 8. The relatively continuous correlation for the dry and wet data for acetate, as compared to the separate correlations for the corresponding saponified acetates, suggests that strength and modulus in the acetates are controlled by the same type of intermolecular secondary bonds, in contrast to the case in the saponified acetates.

The considerably larger change in modulus for saponified acetates in the wet state suggests that water has lowered the glass transition temperature below room temperature, as a consequence of which the saponified acetates exhibit considerably higher segmental mobility.

Consideration of the dry and wet tenacity vs. stretch data shown in Figures 9 and 10 gives additional information. Under dry conditions, the strength of the saponified acetates is actually slightly less than would be predicted from the strength of the acetates, considering only the change in weight due to saponification. Accordingly, the crystallinity of the saponified acetate does not appear to con-

tribute to the dry strength. Under wet conditions, however, the strength of the saponified acetates is higher than the value predicted by saponification weight loss, suggesting that structure other than that present in the acetates is responsible for the strength. This structural factor may be the crystallites, which are essentially unaffected by water [3d].

The nature of the intermolecular secondary bonds in the cellulose acetate is less apparent. As was indicated above, the fact that strength and modulus of the acetates have approximately the same ratio in water and air, together with the large reduction in both properties in the presence of water, suggests that polar bonds capable of solvation with water are primarily responsible for preventing chain slippage. However, a wide distribution of energy for such bonds must be present, since even at elevated temperature in water, an appreciable fiber strength is obtained, and only at temperatures of the order of 145° C. (steam at a gauge pressure of 50 lb./in.²) is sufficient energy imparted to allow free chain slippage or draw.

This view is further reinforced by the results of relaxation and annealing experiments on acetate of 500% stretch. Figure 11 indicates that a minimum of 85% methylene chloride is required to produce sufficient solvation for appreciable shrinkage, suggesting the presence of relatively strong intermolecular bonds.

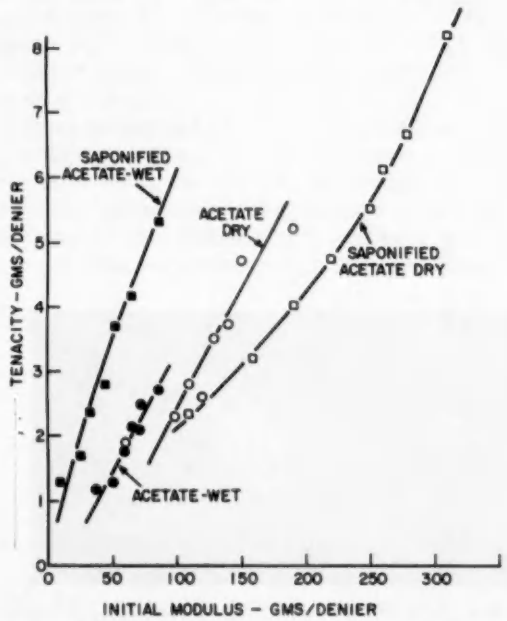

Fig. 8. Relationship of tenacity to initial modulus for acetate and saponified acetate, dry and wet.

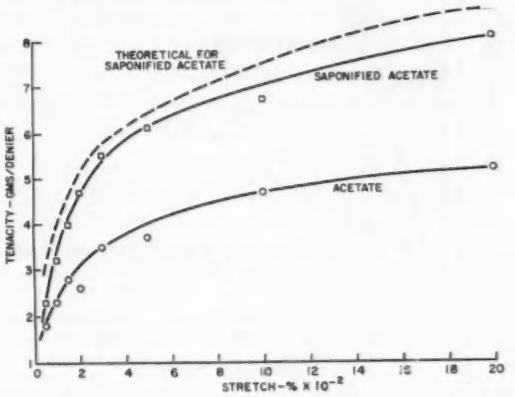

Fig. 9. Effect of stretch on the dry strength of acetate and saponified acetate.

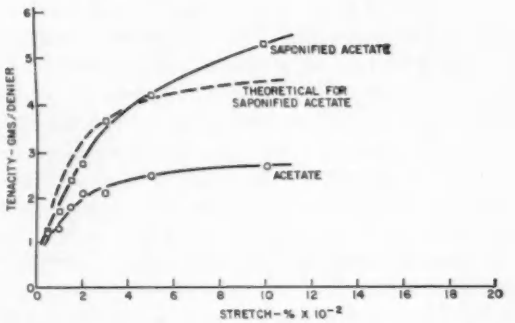

Fig. 10. Effect of stretch on the wet strength of acetate and saponified acetate.

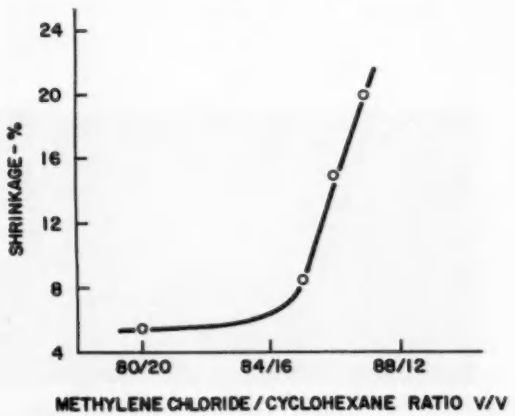

Fig. 11. Effect of methylene chloride concentration on shrinkage of steam-stretched acetate.

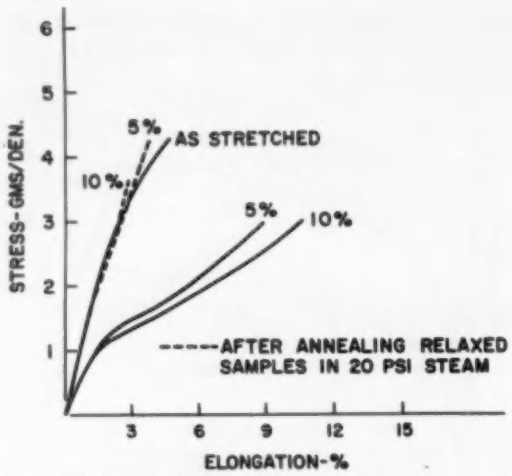

Fig. 12. Stress–strain properties of steam-stretched acetate relaxed in 86/14 methylene chloride/cyclohexane.

The curve of Figure 11 was obtained by immersing acetate fibers stretched 500% in various methylene chloride–cyclohexane mixtures and allowing them to shrink freely. The stress–strain behavior of the acetate, stretched 500% and allowed to shrink only 5% or 10% in 86/14 methylene chloride/cyclohexane, is shown in Figure 12. The shrunk fibers are, however, in a metastable state since they expand spontaneously and recover their original length and stress–strain behavior (see Figure 12) when given increased freedom of segmental motion by exposure to steam at a gauge pressure of 20 lb./in.^{2} This behavior is strongly reminiscent of crystallization, and in fact examination of X-ray diffraction photographs suggests that the swollen and steam annealed fiber has developed a very imperfect cellulose triacetate crystal pattern (Figure 13). That ordinary cellulose acetate is capable of developing a triacetate crystal pattern under sufficiently drastic conditions is shown by the steam annealed acetate film of Figure 13. Accordingly, it appears that the chains in discrete areas of the stretched acetate fibers are packed in a configuration closely resembling the triacetate lattice, and as such are much less susceptible to the solvating action of water than other portions of the fiber.

Proposed Structural Mechanism

Consideration of the data presented allows the following speculative general explanation of the observed effects. Moist steam at elevated temperatures hydrates the polar attractive forces in cellulose acetate sufficiently to allow chain slippage. Since the molecules are very stiff, orientation in the fiber direction occurs readily and is complete, in the gross sense, at a stretch of 300%. As further stretch is applied, local irregularities are "combed out" by additional chain slippage, giving a group of highly parallel chains. Deswelling then allows the structure to densify, with attendant formation of intermolecular secondary bonds. Where the spatial arrangement of the chains is favorable, packing approaching that associated with crystalline triacetate occurs, providing points of strong lateral attraction. At other points, the dipoles associated with the acetate side groups provide more easily hydratable lateral attractive forces. The increase in strength with stretch above 300% (where gross orientation has reached its maximum) is associated with the narrower distribution of chain segment lengths between points of strong lateral attraction (due to the "combing out" process), so that under strain all molecules tend to cooperate to nearly the same degree, rather than becoming taut

Fig. 13. Effect of steam treatment on the crystallization of acetate. A, acetate stretched 500%, relaxed 10%; B, acetate streached 500%, relaxed 10%, annealed in 20 lb./in.^{2} steam; C, acetate film, annealed in 30 lb./in.^{2} steam.

in a stepwise fashion. The higher modulus obtained at high stretch is also due to good molecular tautness brought about by the increased number of dipole interactions possible with a more highly parallelized structure. The concept of molecular tautness distribution has been discussed in more detail elsewhere [6, 8, 9].

The same reasoning applies to the saponified acetates, with the strong lateral attractive forces now being provided by well perfected crystallites, and the hydratable lateral attractive forces being associated with the hydrogen bonding potential of the hydroxyl groups. In this case also, the high dry strength and modulus are associated with the narrow molecular tautness distribution carried over from the steam stretched acetates. In the wet environment, the hydration of secondary bonds in the noncrystalline regions increases chain segment mobility between crystallites, resulting in considerable reduction of modulus. However, the cellulose crystallites maintain the overall tautness distribution and the strength in the wet state.

Summary

Series of acetate and cellulose yarns prepared by steam stretching and saponifying a parent cellulose acetate yarn have been examined for mechanical properties and fiber fine structure. Gross fine structure is shown to change with degree of stretch up to 300%, with resulting increase in tenacity and modulus and decrease in elongation. Further stretch up to 2000% continues to improve tenacity and modulus without significantly changing gross fine structure. The nature of the lateral interchain forces in acetate and saponified acetate and the dependence of the saponified acetate properties on those of the acetate precursor are discussed. A mechanism, based on the distribution of molecular segmental lengths between points of strong lateral interchain attraction, is suggested to explain the observed behavior.

Literature Cited

1. Hermans, P. H., "Physics and Chemistry of Cellulose Fibers," New York, Elsevier, 1949, p. 397–425, 481–494.
2. Hermans, P. H., and Weidinger, A., *J. Polymer Sci.* **5**, 565 (1950).
3. Howsmon, J. A., "Cellulose and Cellulose Derivatives" ("High Polymers," Vol. V), New York, Interscience, 1954. (a) p. 290; (b) p. 313; (c) p. 273; (d) p. 397–400.
4. Ingersoll, H. G., *J. Applied Phys.* **11**, 924 (1946).
5. Peters, L. and Woods, H. J., "Mechanical Properties of Textile Fibers," Amsterdam, North Holland Publishing Co., 1956. (a) p. 6; (b) p. 12–13.
6. Riley, J. L. and Carolan, K. T., American Chemical Society Meeting-in-Miniature, Newark, N. J., 1957.
7. Sisson, W. A., Textile Research Journal **30**, 153–170 (1960).
8. Sprague, B. S., Gordon Research Conference on Textiles, New London, N. H., 1959.
9. Sprague, B. S., Textile Research Journal **30**, 698 (1960).
10. Sprague, B. S., Riley, J. L., and Noether, H. D., Textile Research Journal **28**, 227 (1958).
11. Work, R. W., Textile Research Journal **19**, 381–393 (1949).

Manuscript received March 14, 1961.

The Effect of the Short Fibers in a Cotton on Its Processing Efficiency and Product Quality

Part III: Pilot-Scale Processing of Yarns

John D. Tallant and Louis A. Fiori

Southern Regional Research Laboratory,[1] New Orleans, Louisiana

David M. Alberson and Walter E. Chapman

USDA Ginning Laboratory,[2] Mesilla Park, New Mexico

Abstract

By differentially ginning a single lot of Acala 44 cotton, various short fiber content levels were obtained. Yarns produced from these cottons showed the effects of increases in short fiber content; namely, reduced strength, elongation, and appearance grade. The twist required for maximum strength was found to be largely unaffected by changes in short fiber content, except for a medium yarn number for which a relationship was demonstrated. A graph showing the close relationship between the percentage of fibers less than 3/8 in. and those less than 1/2 in., calculated for a wide number of cottons, is included. Spinning efficiency is shown to be adversely affected by changes in short fiber content.

Introduction

The first two reports of this series [7, 8] discussed the apparent effect of short fibers when cut fibers were added to a cotton and when differentially ginned [2] cotton was processed on a miniature scale. This report will discuss the effects of short fibers on yarn properties when a pilot-plant scale of spinning with conventional equipment and processing techniques was used. The indications of the importance of short fibers in cotton, reported in the previous papers of this series, were such that confirmation on the pilot scale was felt necessary. Also, on the scale of processing previously used there was no opportunity to obtain data on the important matter of the relative spinning efficiency of the various cottons with differing short fiber content.

All of the Acala 44 cotton used for spinning was produced from one lot of seed cotton obtained from the same farm. The differences in short fiber content were produced by a differential ginning technique and by blending together various proportions of normally and differentially ginned lots. The range in short fiber content (percent weight less than $\frac{3}{8}$ in.) available was from about 4% to 19%.

It is recognized that many of those working with short fibers are using different cut-off points below which the fibers are called "short." For this series, $\frac{3}{8}$ in. is taken as the upper limit, i.e., the sum of the first three $\frac{1}{8}$-in. length groups of the Suter–Webb array. Another common value in use for the upper limit is $\frac{1}{2}$ in., for which the first four length groups are added. Figure 1 shows the empirical relationship found between these two limits. As would be expected, the relationship is very good and, moreover, very simply expressed. The short fiber content for the $\frac{1}{2}$-in. limit is 50% more than for the $\frac{3}{8}$-in. limit. Conversely, the short fiber content for the $\frac{3}{8}$-in. limit is but $\frac{2}{3}$ of the content for the $\frac{1}{2}$-in. limit.

Studies are underway to determine whether one limit has any advantage over the other, since standardization would be desirable. Preliminary evaluations [6] indicate that the $\frac{3}{8}$-in. limit is somewhat superior, for, as longer fibers are included in the index, the probability of these fibers having sufficient length to be twisted into the yarn structure tightly enough to rupture rather than slip increases. This is in substantial agreement with early work by Köhler [3], who showed that at the higher twists the apparent length of slippage decreases to about

[1] One of the laboratories of the Southern Utilization Research and Development Division, Agricultural Research Service, U. S. Department of Agriculture.

[2] One of the laboratories of the Agricultural Engineering Division, Agricultural Research Service, U. S. Department of Agriculture.

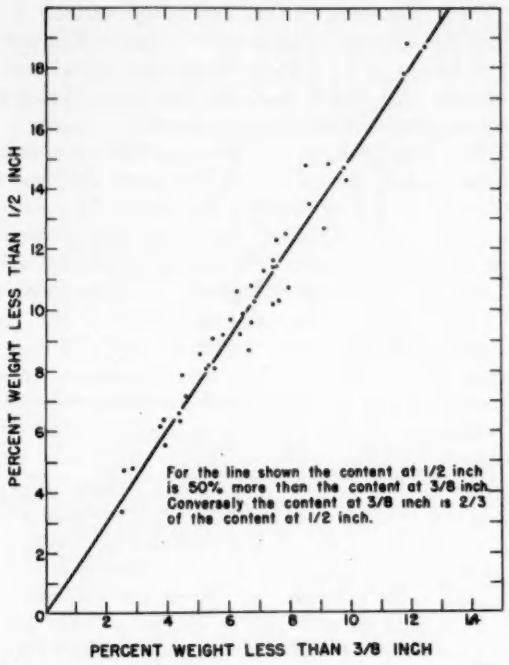
PERCENT WEIGHT LESS THAN 1/2 INCH
PERCENT WEIGHT LESS THAN 3/8 INCH
For the line shown the content at 1/2 inch is 50% more than the content at 3/8 inch. Conversely the content at 3/8 inch is 2/3 of the content at 1/2 inch.

Fig. 1. The relationship between short fiber contents of 42 cottons with $\frac{1}{2}$-in. and $\frac{3}{8}$-in. upper limits.

8 mm. or very nearly $\frac{3}{8}$ in., and this would seem to make the longer limit undesirable. The $\frac{3}{8}$-in. limit is used throughout this paper.

One factor which does seem to stand out in the consideration of methods of characterizing short fibers is the necessity for having a fixed upper limit. Underwood [11] and, more recently, Navkal [4], used "flexible" measures for the upper limit such as "percentage of weight . . . shorter than $\frac{3}{4}$ the mode." Both studies reported little, if any, importance in considering short fibers. It is felt that by having different upper limits for each cotton they masked the real effects of short fibers, since, for a given yarn size and twist, the length of slippage should be essentially the same for any cotton, as long as there were no large differences in the coefficient of friction.

Experimental Methods

The cotton used, Acala 44, was hand-picked and specially ginned in two stages by the differential ginning technique and also normally ginned for purposes of comparison. This resulted in three lots of cotton, from the same parent lot of seed cotton, each with a different level of short fiber content. In addition to these three cottons, three blends were made of the normally ginned and the second-pass differentially ginned cotton to give varying levels of short fiber content. Fiber data for second drawing sliver are given in Table I. The shapes of length–frequency distributions were normal although necessarily different as short fiber content increased. In order to have sufficient yarn for weaving into print cloth, about 150 to 250 lb. of each of three of the lots was produced. These large lots were: the first-pass differentially ginned cotton, which had the lowest short fiber content; the normally ginned cotton, with an intermediate short fiber content level; and a blend of 50% normal with 50% second-pass differentially ginned cotton, which gave a high short fiber content. The remaining lots of cotton were

TABLE I. Fiber, Carding, and Roving Data vs. Short Fiber Content for the Five Experimental Cottons

Short fiber content, % wt. < $\frac{3}{4}$ in.	Source of cotton*	Upper quartile length, in.	Micronaire reading	Pressley zero gauge, g./tex	Weight processed, lb.	Total waste, %	Nep count, neps/gr.	Roving twist,† turns/in.
5	100% A	1.26	4.42	41.8	258	5.42	2.84‡	1.28
8	100% B	1.25	4.72	42.0	230	6.91	4.22‡	1.39
10	75% B 25% C	1.24	4.72	41.0	16	7.04	3.52**	1.52
13	50% B 50% C	1.20	4.80	42.0	164	8.22	4.96‡	1.52
15	25% B 75% C	1.20	4.82	40.0	15	9.13	5.79**	1.62
19	100% C	1.13	4.98	41.0	12	11.93	8.40**	1.79

* A, 1st pass differentially ginned—$1\frac{1}{8}$ LM plus; B, normally ginned—$1\frac{3}{32}$ LM plus; C, 2nd pass differentially ginned—$1\frac{5}{16}$ SLM sp.
† Constant hardness as measured by Belger Roving Tester for 1.5 hank roving.
‡ After 18 lb.
** After 12 lb.

about 15 lb. in weight and permitted limited twist–strength curve determinations at three yarn sizes.

The fiber properties of each of the experimental cottons are shown in Table I. These properties follow the general pattern shown in previous papers [2, 7, 9] for differentially ginned cotton; namely, the upper quartile length shows progressive and significant decrease of about $\frac{1}{16}$ in. as short fiber content increases, with the exception of the highest level of short fiber content, which shows greater increases; the Micronaire reading [3] shows progressive increases; and the Pressley [3] strength shows little if any discernible pattern.

Carding and roving data, also shown in Table I, indicate a strong trend for waste and nep count to increase with increases in short fiber content. While the detailed breakdown is not presented, waste increased approximately proportionally in all categories —flat strips, cylinder and doffer strips, and motes and fly. To maintain approximately uniform "hardness" of roving as tested by the Belger Roving Tester,[3] roving twist had to be increased nearly 40% when the short fiber content increased from 5% to 19%. Of course, in this case, besides the increase in short fiber content there was a reduction of about $\frac{1}{8}$ in. in upper quartile and an increase in Micronaire reading which must be taken into account. However, using the roving twist nomograph developed by Corley et al. [1], it would appear that only about one half of this roving twist increase can be accounted for by changes in upper quartile and Micronaire reading; hence, it may be reasonably inferred that short fibers themselves are causing an increase in the roving twist required for constant "hardness."

Spinning Characteristics and Yarn Properties

All cottons were spun into 14/1 (42 tex), 22/1 (27 tex), and 36/1 (16 tex) yarns and where feasible over a range of twist multipliers from 3.50 to 5.75. The 14/1 (42 tex) yarn was spun from 1.0 (600 tex) hank roving and the other yarns were spun from 1.5 (390 tex) hank roving. In addition, for the cottons of 5%, 8%, and 13% short fiber content larger amounts were spun into 30/1 (20 tex) 4.3 twist multiplier and 40/1 (15 tex) 3.75 twist multiplier yarns for subsequent weaving into standard 80 × 80 print cloth. These fabrics will be reported on in a subsequent paper [10].

[3] It is not the policy of the Department to recommend the products of one company over those of any others engaged in the same business.

These pilot-scale results essentially verified the twist–strength curve characteristics reported in previous papers [7, 8]. Table II shows the actual twist multiplier for which the maximum skein tenacity was observed. Also shown is the skein tenacity of the 5% short fiber content cotton and the percentage of that tenacity for the cottons with other short fiber contents. It will be observed that for the 14/1 (42) and 22/1 (27) yarns the twist multiplier yielding maximum skein tenacity is substantially constant until the cotton of the very highest short fiber content is reached, the cotton for which there is also an appreciable change in upper quartile length. For the finest yarn spun, 36/1 (16), there appears to be a progressive increase in the twist multiplier required. Thus an interaction, with respect to twist multiplier, between short fiber content and yarn size is indicated for the finer yarn sizes. This must be qualified by observing that this is in contradiction to findings previously reported [8]. In the previous experiment, it will be recalled, cut short fibers were added in varying amounts to the parent cotton. A careful examination of those data showed that no change in twist was required for maximum skein tenacity for 36/1 (16) yarns as the short fiber content was increased from about 3% to 20%. A possible resolution of the contradiction may lie in the observation that in the earlier study [8] the upper quartile length changed only about $\frac{1}{32}$ in. while in the present study Table I shows a range in upper quartile length of about $\frac{1}{8}$ in. Thus, it is somewhat problematical whether the changes in twist for the 36/1 (16) yarn observed in Table II are due to short fibers per se or, rather, to the variation in upper quartile length, which is more critical at the finer yarn numbers.

No contradiction with the other report of this series [7] is involved, since the yarn size spun was 22/1 (27), for which all data indicate no relationship between short fiber content and twist for maximum skein strength.

If the interaction between short fiber content and twist for fine yarn sizes is real, it indicates that the utilization of cotton with moderately high short fiber content in fine yarn sizes may be aided by increasing the twist. It also must be borne in mind that increased twist has little effect on coarse and medium yarn skein tenacity.

Skein tenacity, at the twist for maximum strength, is seen to decrease progressively as short fiber content increases. The rate of decrease is about 2% to 3% tenacity loss for each 1% increase in short fiber

TABLE II. Twist Multiplier Yielding Maximum Skein Tenacity for Three Yarn Sizes Over a Range of Short Fiber Contents

Short fiber content, % wt. less than ¾ in.	14/1 (42 tex)		22/1 (27 tex)		36/1 (16 tex)	
	Twist multiplier	Maximum skein tenacity, g./tex, *or* % thereof	Twist multiplier	Maximum skein tenacity, g./tex, *or* % thereof	Twist multiplier	Maximum skein tenacity, g./tex, *or* % thereof
5	3.75	14.0	3.75 4.00*	12.5	3.75	11.1
8	4.00	91.4%	4.00	93.3%	4.00	89.8%
10	3.75	89.5%	4.00	90.4%	4.25	84.4%
13	4.00	81.8%	4.00	82.4%	4.50	74.4%
15	4.00	78.6%	4.00	78.6%	4.75	71.7%
19	4.75	66.1%	4.50†	67.0%	—‡	—‡

* Identical values.
† Highest twist multiplier spun.
‡ Impossible to spin.

content. The rate of decrease may be slightly higher for the 36/1 (16) yarn although this is not certain. It is significant that it was impossible to spin 36/1 (16) yarn from the cotton with 19% short fibers.

Of course, concommitant with changes in short fiber content there were minor changes in Micronaire reading and length (except that for the 19% cotton there were substantial decreases in upper quartile length) which undoubtedly have some effect on yarn properties and spinning efficiency. Unfortunately, the state of the art does not permit a precise determination of the relative importance of these properties; however, past experience and findings [8] in which these variables were held to an even smaller range indicate that by far the major portion of any effect found may be attributed to the short fibers.

Consistent and significant trends in the single-strand elastic properties of 4.50 twist multiplier yarns are shown in Table III. Increases in short fiber content are seen to cause significant decreases in breaking elongation as well as tenacity. These simultaneous losses seem serious when the product of tenacity and elongation is considered. This product is proportional to toughness or energy required for rupture. Thus, the yarns with the higher short fiber contents show a marked decrease in toughness. This decrease amounts to almost 50% between yarns with the lowest and the highest short fiber contents. It may be speculated that this effect would be important in the utilization of such yarns in fabrics to be treated with resin, since such finishing usually entails further strength and elongation losses. Data on fabric properties will be reported in a subsequent paper [10].

While strength and elongation are very important from the engineering aspect, the appearance of the yarn may be of the major importance in many end-uses where esthetics play a large role. Table IV shows the yarn appearance grade over a range of twists and yarn numbers. Increases in the short fiber content seriously degrade yarn appearance and have less effect on coarse than on fine yarns. For example, the 15% short fibered cotton produced a C grade yarn in the coarsest size and at the highest

TABLE III. Single Strand Tenacity and Elongation of 14/1, 22/1, and 36/1—4.50 T.M. Yarn

Short fiber content, % wt. less than ¾ in.	14/1 yarn		22/1 yarn		36/1 yarn	
	Tenacity, g./tex	Elongation, %	Tenacity, g./tex	Elongation, %	Tenacity, g./tex	Elongation, %
5	17.3	8.05	15.9	6.65	14.5	6.45
8	15.8	7.35	14.5	6.65	13.4	6.00
10	15.6	7.35	14.7	6.65	12.4	5.75
13	14.1	7.15	13.1	6.30	11.5	5.70
15	13.6	6.95	12.4	6.00	10.9	5.65
19	11.9	6.40	10.8	5.25	—*	—*

* Impractical to spin.

TABLE IV. Yarn Appearance Grade as Affected by Short Fiber Content Over a Range of Twists and Yarn Numbers

Nominal short fiber content, % wt. less than $\frac{3}{4}$ in.	14/1 yarn			21/1 yarn*		36/1 yarn		
	T.M.			T.M.		T.M.		
	3.50	4.50	5.75	3.50	4.50	3.50	4.50	5.75
5	B	B+	B+	B	B+	C+	B	B
8	B	B	B	C	B−	C−	C	C+
10	B	B−	B−	C+	C−	D+	C	C+
13	C−	C−	C	D	D	†	D−	D
15	D+	D+	C	D	D	†	D	D
19	D	D	D	†	D	†	†	†

* 5.75 twist multiplier not spun due to insufficient material.
† Impractical to spin due to excessive ends down rate.

twist, while the 5% cotton produced the same grade for the finest yarn at the lowest twist.

To illustrate the effect of short fibers on yarn appearance, Figure 2 shows photographs of 22/1 (27) yarn at 4.50 twist multiplier for three levels of short fiber content. The degradation in appearance is thus very drastic and may well be the controlling factor in utilization of cottons with high short fiber content, since for many purposes the strength losses, while troublesome, may not be prohibitive.

A factor, not hitherto considered in this series of papers but reported elsewhere [9], is the relationship of short fiber content to spinning efficiency. Table V indicates that fine, low twist yarn was impractical to spin because of the large number of ends down, which corroborates the findings already reported [9]. Sufficient amounts of 30/1 (20) and 40/1 (15) yarns were spun for weaving into print cloth using only the 5%, 8%, and 13% short fiber content cottons. These cottons were spun on a 240-spindle Whitin Piedmont Frame[3]; Table V shows the ends down rate and processing conditions. The ends down rate needs little comment except that it was impractical to spin the 13% cotton into 40/1 (15) filling yarn. Additional columns show the average ends down rate per 15 minutes per 120 spindle side of the frame, or, in other words, the ends down rate per 30 spindle hours.

Some of the standard deviations given in Table V are greater than the average ends down rates they describe. The handicap this extreme variability imposed in reaching meaningful conclusions prompted the development of a more sophisticated sequence of statistical techniques for evaluating ends down rates. The method is described by Schultz et al. [5] and the results obtained by use of the procedure are reported by Tallant et al. [9].

The findings on the interrelation between short fiber content and spinning efficiency show an extremely complex pattern due to the strong inter-

Fig. 2. Appearance boards of 22/1 (27 tex) 4.50 T.M. yarn with varying short fiber content. A, 5%; B, 13%; C, 19%.

TABLE V. Spinning Efficiency and Processing Conditions for Three Cottons of Different Short Fiber Content

Short fiber content, % wt. less than ½ in.	Yarn No.	Ends down/ 1000 sp. hr.	Total spindle hours	Ends down/15 min./side (30 sp. hours) Average	Standard deviation
5	30/1	20	3800	0.57	0.98
	40/1	95	4700	2.93	2.44
8	30/1	26	4000	0.81	1.04
	40/1	136	4500	3.95	3.20
13	30/1	70	3000	2.12	1.77
	40/1	over 1000	—	—	—

Processing conditions	30/1	40/1
Spindle speed	10500	8750
Twist multiplier	4.3	3.75
Ring diameter	2¼	2¼
Traveler	6/0	14/0

action of processing variables such as spinning tension, spindle speed, and yarn size [9]. Further, examples of such behavior are seen in Table V, which shows that the response to increases in short fiber content is much more severe in the 40/1 yarns with low twist than in the coarser 30/1 yarns with moderate twist. These and other studies indicate that processing variables may play a role of greater significance than do normal differences among cottons. For example, while it is to be concluded that short fibers are detrimental, their effects on product quality, as in the case of yarn appearance, may be minimized by utilizing the cottons of higher short fiber content in the coarser, higher twist yarns.

While spinning efficiency is conventionally reported in terms of "Ends Down/1000 Spindle Hours," it may be questioned whether this is the most meaningful base when technological change is constantly bringing about increased spindle speeds. Perhaps a better index might be "Ends Down/Pound of Yarn." When different spindle speeds are compared, this latter index would be the fairer criterion. Figure 3 shows the relationship between these two indices for various speeds at selected yarn sizes and twists. For example, a cotton spinning with 30 ends down per 1000 spindle hours at 9,000 r.p.m. could increase to 46.5 ends down at 14,000 r.p.m. and still have the same number of ends down per pound of yarn produced. It is thought that the apparent deterioration in the spinning efficiency of American cotton in recent years may be put into proper perspective if these considerations are taken into account.

Summary and Conclusions

Pilot-scale spinning on standard equipment corroborated and reinforced the findings of earlier work of this series [7, 8, 9]; namely, that increases in short fiber content result in (1) decreased yarn strength, with decreases in excess of 1% in tenacity for each 1% increase in short fibers; (2) decreased yarn elongation; (3) decreased yarn appearance grade and evenness; (4) increased difficulty in spinning at medium yarn numbers and low twists; and

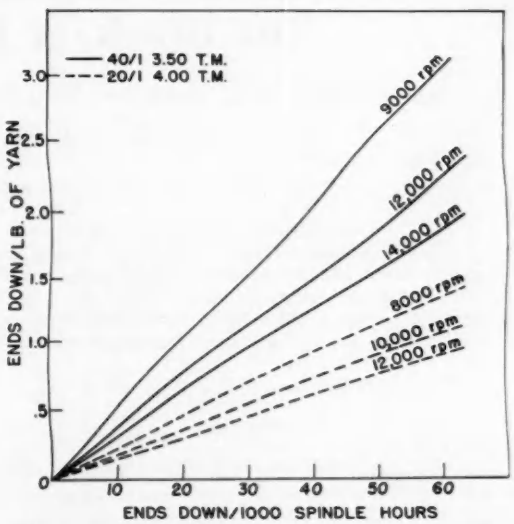

Fig. 3. Ends Down/Pound of Yarn Produced vs. Ends Down/1000 Spindle Hours for various speeds at selected yarn sizes and twists.

(5) increased twist in the roving for constant hardness.

The present study threw further light on the interplay of short fiber content and the twist required for maximum strength. In the cottons studied it was found that the short fiber content appeared to have no influence on the twist required for maximum skein tenacity in coarse and medium size yarns. This conclusion has been reported before [7, 8]. However, there were indications that short fiber content may affect the twist necessary for maximum strength in the finer yarn sizes, and further investigation is needed. This latter conclusion is at some variance with an earlier report [8], although because of small variations in the upper quartile lengths of the various cottons this must be taken with qualifications.

The deleterious effect of short fibers on end breakage can be minimized by allocating cottons of high short fiber content to coarser and higher twist yarns.

Literature Cited

1. Corley, J. R., Simpson, J., Fiori, L. A., and Brown, J. J., TEXTILE RESEARCH JOURNAL **23**, 750–754 (1953).
2. Griffin, A. C., Jr., McCaskill, O. L., Tallant, J. D., and Fiori, L. A., *The Cotton Gin and Oil Mill Press*, 19–20 (June 11, 1960).
3. Köhler, S., *J. Textile Inst.* **25**, T141–149 (1934).
4. Navkal, H., *Indian Cotton Growing Rev.* **11**, 469–481 (1957).
5. Schultz, E. F., Jr., Little, H. W., Tallant, J. D., and Fiori, L. A., TEXTILE RESEARCH JOURNAL, this issue, pp. 872–875.
6. Tallant, J. D., Fiori, L. A., and Cheatham, R. J., "Effect of Short Fibers in Cotton on Yarn and Fabric Properties and Spinning Performance," in process, intended for *Textile Bulletin*.
7. Tallant, J. D., Fiori, L. A., and Landstreet, C. B., TEXTILE RESEARCH JOURNAL **30**, 792–795 (1960).
8. Tallant, J. D., Fiori, L. A., and Legendre, D. C., TEXTILE RESEARCH JOURNAL **29**, 687–695 (1959).
9. Tallant, J. D., Fiori, L. A., Little, H. W., and Leitz, L. A., *Textile Inds.* **124**, 1929–1933 (1960).
10. Tallant, J. D., Fiori, L. A., and Sands, J. E., "The Effect of the Short Fibers in a Cotton on its Processing Efficiency and Product Quality. Part IV: Grey and Finished Fabrics," in process, intended for TEXTILE RESEARCH JOURNAL.
11. Underwood, C., *J. Textile Inst.* **26**, T309–335 (1935).

Manuscript received February 13, 1961.

A Statistical Procedure for Determining End Breakage Rate in Spinning

E. Fred Schultz, Jr.,[1] Herschel W. Little, John D. Tallant, and Louis A. Fiori

Southern Regional Research Laboratory,[2] New Orleans, Louisiana

Abstract

Standard deviations of yarn break data, taken by uniform increments of spindle hours, increased linearly with average rate of breakage and were larger than expected for a Poisson distribution. Transforming the numbers of breaks to $\log_{10}$ (1 + number of breaks) stabilized the variance. In a specific case, analysis of data for 720 spindle hours per yarn taken by 12 increments of 60 hours yielded 95% confidence limits describing the average number of breaks per yarn as within 30% of the observed number of breaks.

Introduction

Rate of yarn breakage, often called spinning efficiency, is a characteristic of great importance to spinners. Stewart et al. [5] indicated that approximately 5,000 spindle hours would be required for an accurate and significant spinning test on 30/1 warp yarn.

[1] Biometrical Services, Agricultural Research Service, U. S. Department of Agriculture, in cooperation with the Southern Regional Research Laboratory.

[2] One of the laboratories of the Southern Utilization Research and Development Division, Agricultural Research Service, U. S. Department of Agriculture.

Woo [8] argues from the nature of yarn breaks that they follow the Poisson distribution and calculates "critical values" of end breakage to be used in translating end breakage values for a limited number of spindle hours (less than 200) to those expected for a larger number. Barnes, Elting, and Byatt [1] generalize the idea of the Poisson distribution of ends down, showing curves for determining, with three choices of confidence percentages, the average number of ends down for any observed number (up to 14). Both of these discussions ignore the possibility of other components of variability in addition to the basic Poisson variability. Tallant et al. [7] observed ends down by 15-min. periods (30 spindle hours). They report standard deviations, based on 100 or more periods per yarn, roughly equal to (sometimes greater than) the mean number of ends down. Since the standard deviation of a Poisson variate is the square root of the mean, this indicates that ends down data are afflicted with variability in excess of that due to the Poisson distribution.

The Procedure

The data of Tallant's Table V [7], when plotted, indicated that the standard deviation increased linearly as the average ends down rate increased. This was borne out by examination of ten other lots with varying ends down rates observed on sides of 120 spindles at hourly intervals (120 spindle hours) for 20 to 30 hr. To stabilize the variance, thus enabling the use of analysis-of-variance techniques, the data were transformed to logarithms [2]. In this case, to avoid the difficulty occasioned by observational periods with zero down ends, the transformation actually used was $\log_{10}$ (1 + number of ends down).

Analysis of variance [3, 4] of several sets of transformed data indicated that differences involving yarns with smaller than average ends down rates, which by analysis of actual counts had seemed nonsignificant, would in some cases be judged significant. This is reasonable, since variances computed on the untransformed observations are "average" variances which are too small for applying to large means and too large for small ones.

In developing the statistical procedure and in planning the work reported by Tallant et al. [6], the variances obtained from the earliest of the analyses of transformed data (the three 30/1 cottons of Table V in [7] furnishing a total of 165 degrees of freedom) were used as an estimate of the variance of the procedure in future work. These were averaged (and rounded somewhat) to obtain an average estimate yielding the easily manipulated standard deviation of 0.25; thus variance was estimated as 0.0625.

Assuming that it would be desirable to differentiate between the ends down rate, y, of some yarn and a standard, X, which is 20% higher, then

$$X = 1.20\ y$$

and

$$\log X = \log y + \log 1.20$$

so that it would be important to differentiate between the logarithm of an experimental value and some arbitrarily chosen log value differing by not more than log 1.20 or 0.07918. The problem of recognizing such a difference is basically that of a two-tailed significance test or confidence limits on logarithmic values. This is properly done with the t-distribution if the situation is as described here, one priorly selected treatment to be compared with an arbitrary standard.

Since the true log ends down rate, μ, may be defined by the observed average logarithm and the confidence interval as:

$$\mu = \bar{y} \pm (t_{\alpha,d.f.})(\hat{\sigma}_{\bar{y}})$$

it is apparent that in log measure the one-half confidence interval may be identified with log 1.20 or 0.07918. In further definition $\bar{y}$ is the average logarithm of (1 plus ends per 60 spindle hours); t_α is Student's t at the α probability of chance occurrence (usually chosen as 0.05); $d.f.$ is the number of degrees of freedom with which the estimate of error (variance) was originally estimated; and $\hat{\sigma}_{\bar{y}}$ is the standard error of the mean log value, $\bar{y}$,

$$\hat{\sigma}_{\bar{y}} = \frac{\sqrt{\text{variance of logarithms}}}{\sqrt{\text{No. of 60-sp.-hr. periods in the mean}}}$$

Equating the one-half confidence interval with log 1.20 as noted above

$$(t_{\alpha,d.f.})(\hat{\sigma}_{\bar{y}}) = 0.07918$$

Substituting for $\hat{\sigma}_{\bar{y}}$, choosing $t_\alpha = t_{.05}$, and noting that variance was estimated with 165 degrees of freedom

$$(t_{.05,165})\left(\frac{\sqrt{\text{variance}}}{\sqrt{\text{No. of 60-hr. periods}}}\right) = 0.07918$$

or

$$\text{No. of 60-hr. periods} = \frac{(t_{.05,165})^2(\text{variance})}{(0.07918)^2}$$

Substituting the available numerical information:

$$\text{No. of 60-hr. periods} = \frac{(1.97)^2(0.0625)}{(0.07918)^2} = 38.7$$

This is about 40 periods of 60 spindle hours each, or 2400 spindle hours, required to differentiate an ends down rate from a standard which is 20% higher.

Whether this is excessive spinning time, or whether a mean ends down rate must be known this precisely, may be debated. However, in the particular study being planned there was not enough cotton to spin this long for each of the approximately 12 combinations of yarn number, twist multiplier, and spindle speed for which it seemed desirable to evaluate the experimental cottons. In consequence a different approach was taken, and the available cotton of each experimental lot was prorated among the proposed treatments; it was then seen that there would be sufficient to spin 12 periods of 15 min. each (60 spindle hours) for each of the 12 combinations of number, twist, and speed. The precision of averages of 12 periods could be estimated as

$$\hat{\sigma}_{\bar{y}} = \frac{\sqrt{\text{variance}}}{\sqrt{\text{No. of periods}}} = \frac{\sqrt{0.0625}}{\sqrt{12}} = 0.07217$$

Using this estimate of $\hat{\sigma}_{\bar{y}}$ to establish a 95% confidence interval

$$\mu = \bar{y} \pm (t_{.05,165})(\hat{\sigma}_{\bar{y}})$$

$$\mu = \bar{y} \pm (1.97)(0.07217) = \bar{y} \pm 0.1422.$$

The antilog of 0.1422 = 1.387, hence a value more than 0.387 larger than the mean would be significantly different. Thus 720 spindle hours were judged to be sufficient to define an ends down rate within about 40% of its average value. Note: The value of 20% reported in [6] as an estimate of the precision was due to a misunderstanding of the length of the tally period as 30 spindle hours rather than 60 (i.e., as one side of the frame for 15 min. rather than both sides).

All the foregoing discussion assumes that there is no additional error involved if the time periods are not successive or if the roving is recreeled and additional periods run at a later date. As noted in [6] there is an effect on ends down rate associated with the amount of cotton in the roving bobbins. This was obviated in that study by having equal numbers of roving bobbins that were approximately full, $\frac{2}{3}$ full, and $\frac{1}{3}$ full at all times. Further, a pilot study done before the experimental study, and a second replication run with one of the experimental cottons, gave no hint of increased variability from work at later times, hence the variability among successive 15-min. periods (240 spindles or 60 spindle hours) was accepted as the estimate of error in this process. When the variance estimates of the foregoing work are combined with those from data reported in [6], the result is a pooled estimate of variance = 0.0471 with 527 degrees of freedom.

The precision of averages of 12 periods is estimated as before but now using 0.0471 rather than 0.0625 as the estimate of variance. The result is

$$\hat{\sigma}_{\bar{y}} = \frac{\sqrt{.0471}}{\sqrt{12}} = 0.06265$$

$$\mu = \bar{y} \pm (1.96)(0.06265) = \bar{y} \pm 0.1228$$

Antilog 0.1228 = 1.328. Thus 720 spindle hours were judged sufficient to establish a mean within 1/1.33 times and 1.33 times its average value or within approximately ±30% of its average value. It should not be necessary to remark that the variance another worker might obtain using this same technique could be considerably different from that reported here, hence it is not to be taken for granted that a mean ends down rate can always be defined within ±30% in 720 spindle hours.

Literature Cited

1. Barnes, J. C., Elting, J. P., and Byatt, W. J., TEXTILE RESEARCH JOURNAL **29**, 844–845 (1959).
2. Bartlett, M. S., *Biometrics* **3**, 39–52 (1947).
3. Li, Jerome, C. R., "Introduction to Statistical Inference," Ann. Arbor, Mich., Edwards Bros., Inc., 1957.
4. Snedecor, G. W., "Statistical Methods," 5th ed., Ames, Iowa, Iowa State College Press, 1956.
5. Stewart, Ruby E., and Parsons, L. E., TEXTILE RESEARCH JOURNAL **19**, 283–287 (1949).
6. Tallant, J. D., Fiori, L. A., Little, H. W., and Leitz, L. A., *Textile Inds.* **124**, 1929–1933 (1960).
7. Tallant, John D. and Fiori, Louis A., TEXTILE RESEARCH JOURNAL this issue, pp. 866–872.
8. Woo, H. K. C., TEXTILE RESEARCH JOURNAL **28**, 612 (1958).

Manuscript received February 13, 1961.

Quantitative Investigation of the X-Ray Diffraction Picture of Some Typical Rayon Specimens Part II

P. H. Hermans and A. Weidinger

Institute for Cellulose Research of the AKU and Affiliated Companies, Utrecht, Netherlands[1]

IN this paper we wish to report the results obtained from the investigation of five more rayon specimens whose X-ray diffractograms were analyzed in exactly the same way as described in Part I [1].

This time, experimental yarns spun on small-scale equipment were investigated exclusively. They were all spun as heavy denier yarns corresponding to the titer and number of filaments usual for tire cord singles.

Brief specifications are given here:

710 Ordinary high alkali viscose spun in a zinc-free bath, 80% stretch.

711 Viscose as for common textile yarn; spinning bath with low zinc content; two-bath spinning with stretching in second hot bath; 80% stretch.

711A Same as 711 but with 55% stretch.

712 Low alkali viscose, low acid bath with high zinc content; no modifiers; two-bath spinning as above; 85% stretch.

713 Tire cord yarn conditions; 85% stretch.

We shall not dwell here on a description of the evaluation procedure but confine ourselves to giving the results in the form of tables corresponding to the tables given in Part I, to which the reader is referred for any further explication desired. It is again seen that the crystallinities estimated from two sets of data do not differ very much, neither do the crystallinities of the various specimens among each other, though the tire cord type (No. 713) yields the lowest figure. In accordance with previous results, no effect of a difference in percentage of stretch (Specimens 711 and 711A) is detectable.

It is emphasized that all intensities are based on those including the Lorentz and polarization factors

[1] Communication No. 114.

TABLE I. Values of $I_n(hkl)$ from Observations

hkl	2θ	710 A I 80	711 A II 80	711A B II 55	712 A III 85	713 B V 85
Paratropic						
101 (A_0)	12.1°	0.336	0.29	0.295	0.316	0.338
10$\bar{1}$ (A_1)	14.0°	0.132	0.130	0.131	0.113	0.064
10$\bar{1}$ (A_2)	20.2°	1.27	1.25	1.20	1.29	1.12
200 (A_4)	21.4°	1.38	1.40	1.35	1.51	1.26
Diatropic						
020	17°	0.102	0.088	0.100	0.108	0.085
040	34.8°	0.131	0.138	0.123	0.141	0.128
2nd layer line						
021	20.2°	0.36	0.34	0.415	0.42	0.33
Sum		3.711	3.636	3.614	3.898	3.325

In the table head A I 80, A II 80, etc. are reference numbers of our laboratory.

TABLE IA. Intensity Ratios of Some *hkl* Reflections Calculated from Table I

	710	711	711A	712	713
A_0/A_2	0.26	0.23	0.24	0.24	0.30
$021/A_2$	0.28	0.27	0.34	0.32	0.29
$020/A_2$	0.08	0.07	0.08	0.085	0.075
$040/A_2$	0.10	0.11	0.10	0.11	0.11
A_2/A_4	0.92	0.89	0.89	0.86	0.89

TABLE II. Crystalline Fraction as Derived from the Present Measurements if that of 705 of Part I is Set Equal to 0.40

	Specimen No.				
	710	711	711A	712	713
From sum of all lines listed in Table I	44.5	43.8	43.5	47	40
From $A_0+A_1+A_2+A_4$ only	47	46	44.5	48	41.2

TABLE III. Comparison of the Observed Relative Line Intensities with Those Calculated for the Andress Model ($A_3 + A_4$ set equal to 100)

	A_0	A_2A_4	II_0	IV_0	II_1
710	12.5	100	3.8	4.95	13.6
711	10.9	100	3.3	5.2	12.8
711A	11.6	100	3.9	4.8	16.2
712	11.3	100	3.9	5.0	15
713	14	100	3.5	5.4	13.8
Andress	10.4	100	3.9	15.7	12.8

associated with the experimental setup employed. They can therefore not be compared directly with the intensity figures derived from the same material and published in a recent letter [2] which represent figures corrected for the angle-dependent factors referred to.

TABLE IV. Integral Line Widths $b(2\theta)_i$ in Degrees

	710	711	711A	712	713
A_0	2.72	2.73	2.92	2.72	3.12
A_2A_4	2.48	2.75	2.82	2.70	2.75
020	1.15	1.18	1.33	1.13	1.24
040	1.19	1.30	1.25	1.05	1.27

TABLE V. Lowest Limit of Particle Size in Angstroms Calculated from Table IV after Scherrer's Equation

	710	711	711A	712	713
A_0	29	29	27	29	31
A_2A_4	33	29	29	30	29
020	69	68	60	70	64
040	70	64	66	79	65

Again the tire cord type is the one showing the widest equatorial lines (*cf.* Part I).

We may conclude that the results reported here are well in line with those of Part I and may serve as support for the previous work. The X-ray work has been carried out in the Laboratory for Technical Physics of the Technical University, Delft.

Summary

In addition to Part I the results of the evaluation of five more rayons, spun experimentally according to widely different procedures, are given. They are well in line with the ones previously reported.

Literature Cited

1. Hermans, P. H. and Weidinger, A., TEXTILE RESEARCH JOURNAL **31**, 558 (1961).
2. Hermans, P. H. and Weidinger, A., *J. Polymer Sci.*, **50**, S10 (1961).

Manuscript received February 1, 1961.

Cross-Linking Etherified Cottons with Dimethylol Ethyleneurea

Russell M. H. Kullman, John G. Frick, Jr., Robert M. Reinhardt, and J. David Reid

Southern Regional Research Laboratory,[1] New Orleans, Louisiana

Abstract

The effects of cross-linking with dimethylol ethyleneurea on several etherified cotton fabrics—carboxymethylated, hydroxyethylated, methylated, and cyanoethylated cottons—were studied and compared with its effects on unmodified cotton. The effect of replacing cellulosic hydroxyl groups on the reactivity toward dimethylol ethyleneurea is dependent on the nature of the substituent and the swellability of the etherified fiber. Hydroxyethylated and methylated cottons exhibit greater cross-linking efficiency with dimethylol ethyleneurea than does unmodified cotton. High moisture regain in conjunction with high wet and conditioned wrinkle recovery is possible with hydroxyethylated cotton. Increased extensibility observed in etherified cottons is directly related to the alkali concentration used in the etherifying reaction. The rate of strength loss on cross-linking, with unit improvement in crease recovery, is greater for etherified cottons, except hydroxyethylated, than for unmodified cotton.

Introduction

The treatment of cotton or other cellulosic textiles with cross-linking agents to produce wrinkle resistance and "wash-and-wear" properties has been a common finishing operation in recent years. Numerous articles in the literature describe the effect of such treatments on the practical properties of the textiles and also on the chemical and physical properties of the fibers. Similar treatments applied to chemically modified cottons, however, are reported in only a few instances. The application of cross-linking agents to carboxymethylated cotton was studied rather extensively [4, 5, 12]. Cross-linking of fabrics of other etherified cottons has been investigated to a lesser extent [3, 7, 8, 14]. The purpose of this paper is to present the results obtained by cross-linking etherified cotton fabrics with a relatively low degree of substitution, as compared with the results obtained on unmodified cotton, and to show the effect of the chemical nature of the substituent on the results.

In this work, cottons etherified with four different groups—methyl, hydroxyethyl, cyanoethyl, and carboxymethyl—were used. In no case did the degree of substitution exceed 0.5 groups per anhydroglucose unit. The etherified cottons and an unmodified cotton were treated with a common cross-linking agent, dimethylol ethyleneurea, to obtain the results described. Since the preparation of all the etherified cottons required an alkali treatment, which varied in each instance, a series of alkali-treated cottons was also included in the work. This gave information concerning the effect of alkali-swelling on the results of such cross-linking treatments.

The etherified cottons were chosen from those that could be easily prepared. They vary in reactivity from those with substituents completely inert to the cross-linking agent, to others which should show greater reactivity than cellulose itself. With one substituent, hydroxyethyl, it was possible to obtain etherification with radically different alkali treatments, thereby allowing some differentiation of the effects of etherification and alkali treatment.

Materials and Methods

Fabric Description

The cotton material used was a desized, scoured, and bleached 80 × 80 print cloth weighing 3.1 oz./yd.[2] To facilitate comparison of the effects of

[1] One of the laboratories of the Southern Utilization Research and Development Division, Agricultural Research Service, U. S. Department of Agriculture.

alkali treatment and the different alkalies used, all modified cottons were prepared from the same batch of fabric.

Preparation and Treatment of Etherified Fabrics

Cyanoethylated cotton (CN). Fabric was impregnated with 2% sodium hydroxide to an 80% wet pickup using two dips and two nips on a laboratory padder. The sample was loosely rolled with glass cloth and inserted in a reaction tube through which acrylonitrile was cycled at a temperature of 55–60° C. After 40 min., the sample was placed in 5% acetic acid to halt the reaction, then rinsed in water, and dried.

Another fabric was impregnated with 2% sodium hydroxide, immersed in 5% acetic acid, then rinsed and dried. This sample was designated as the "alkali control" for the cyanoethylated fabric.

Hydroxyethylated cotton (HE). Fabric was treated with 7% sodium hydroxide, rolled with glass cloth and inserted in a reaction tube. At room temperature a 10% solution of ethylene oxide in perchloroethylene was cycled through the sample. One sample was treated for 1 hr., and a second for 2 hr. The fabrics were acidified with 5% acetic acid and rinsed 10–20 min. in running tap water. A third sample was prepared similarly, using 15% sodium hydroxide treatment and 1-hr. reaction time.

"Alkali controls" were prepared by treatment with 7% and 15% sodium hydroxide, followed by acidifying with 5% acetic acid and rinsing.

Methylated cotton (ME). Methylation of cotton fabric was accomplished by padding the fabric to 180–200% wet pickup of 45% sodium hydroxide, rolling it with glass cloth, and cycling through it in the reaction tube a toluene solution containing

TABLE I. Properties of Untreated and Etherified Cotton Before and After Cross-Linking

Ether	(DS)	Nitrogen, %	Crease recovery angles (W+F), degrees		Breaking strength (W), lb.	Elongation at break, %	Moisture regain, %	Density dry, g./cm.³
			Conditioned	Wet				
Before cross-linking								
Cotton			191	193	48.0	10.0	6.7	1.545
—CH_2CH_2CN, 2% NaOH	(0.00)		196	187	49.0	11.7	6.5	1.541
	(0.36)	2.81	188	216	55.9	12.8	4.8	1.470
—CH_2CH_2OH, 7% NaOH	(0.00)		175	225	47.0	14.4	7.0	1.541
	(0.16)		155	228	47.3	14.1	8.0	1.522
	(0.25)		113	219	43.9	15.0	7.4	1.510
—CH_2CH_2OH, 15% NaOH	(0.00)		172	226	49.0	25.9	8.1	1.536
	(0.25)		151	257	52.8	31.7	10.8	1.497
—CH_3, 45% NaOH	(0.00)		208	198	49.6	33.7	8.9	1.526
	(0.50)		196	184	52.4	32.0	8.8	1.454
—CH_2COOH, 50% NaOH	(0.00)		216	220	46.7	30.0	8.5	1.523
	(0.09)		184	254	38.7	30.0	10.0	1.523
After cross-linking								
Cotton		1.08	290	266	26.3	6.0	5.4	1.541
—CH_2CH_2CN, 2% NaOH	(0.00)	1.13	297	276	23.4	6.2	5.1	1.536
	(0.36)	0.90*	267	270	32.7	7.9	4.3	1.466
—CH_2CH_2OH, 7% NaOH	(0.00)	1.09	280	266	26.1	7.5	5.6	1.537
	(0.16)	1.10	308	271	22.6	6.9	6.1	1.523
	(0.25)	1.02	300	276	23.5	7.9	6.3	1.509
—CH_2CH_2OH, 15% NaOH	(0.00)	1.10	268	271	23.6	11.3	6.9	1.529
	(0.25)	1.32	292	290	20.9	14.7	9.7	1.494
—CH_3, 45% NaOH	(0.00)	1.06	286	263	29.0	14.4	7.8	1.519
	(0.50)	1.12	241	273	29.5	14.1	8.4	1.453
—CH_2COOH, 50% NaOH	(0.00)	1.16	289	263	23.6	15.6	7.2	1.518
	(0.09)	0.90	232	292	19.4	11.5	10.6	1.523

* % Nitrogen (after cross-linking) minus % nitrogen (before cross-linking).

0.5 mole dimethyl sulfate for each mole of sodium hydroxide in the fabric. The methylating solution had been preheated to 84–87° C. and was maintained at this temperature during the reaction time of 20 min. The sample was next immersed in a boiling solution of 5% sodium carbonate for 10 min., rinsed thoroughly in running tap water, and dried.

The "alkali control" fabric was treated with 45% sodium hydroxide, boiled in sodium carbonate solution, soured in dilute acetic acid, then rinsed in running tap water and dried.

Carboxymethylated cotton (CM). Carboxymethylated cotton was prepared by impregnating fabric with a 20% aqueous solution of chloroacetic acid and then soaking it in 50% sodium hydroxide for 30 min. without tension. The fabric was obtained as the sodium salt of carboxymethylated cotton after washing, acidifying with dilute acetic acid, and rinsing. Prior to cross-linking, conversion was made to the free carboxyl form by soaking in 5% hydrochloric acid solution and then rinsing in distilled water and drying.

Determination of degree of substitution. All the etherified cotton fabrics were analyzed for functional groups and the results expressed as degree of substitution (DS) with the assumption that each group makes a separate substituent. This assumption probably gives a high DS for hydroxyethylated cotton, as it is likely that some polyoxyethylene chains are formed by reaction of ethylene oxide with hydroxyethyl groups. Hydroxyethyl content was determined by the method of Morgan [6]; cyanoethyl content by the Kjeldahl nitrogen procedure; methoxyl by the Zeisel procedure [1]; and carboxymethyl by back titration with 0.1 *N* hydrochloric acid to determine amount of 0.1 *N* sodium hydroxide neutralized by carboxymethyl groups [11].

Cross-linking with dimethylol ethyleneurea. The cross-linking treatment was applied to fabrics in every case by the usual techniques, namely, application of the treating solution by padding, followed by drying, curing, and an afterwash.

The treating solution was composed of 8% dimethylol ethyleneurea, 0.5% zinc nitrate hexahydrate, and 0.05% acetic acid. The dimethylol ethyleneurea was a commercial product obtained as a 50% solution. The solution was applied using the same pad pressure for every fabric. This pressure gave about 80% wet pickup with unmodified cotton, but generally higher pickups with the etherified cottons.

After padding, the fabric samples were mounted on pin frames, dried 7 min. at 60° C., and cured 4 min. at 160° C. Both operations were conducted in forced-draft ovens. Following the cure, the fabric samples were washed in a home-type automatic washing machine, using a slightly alkaline solution of a nonionic detergent, and tumble dried.

It was assumed that the concentration of the nitrile group in the cyanoethylated cotton remained unchanged during this treatment.

Test Methods

Conditioned crease recovery angles were determined by the Monsanto method, ASTM designation D 1295-53T [2a], wet crease recovery angles were determined by soaking the specimen 5 min. at 150° F. in water containing 0.1% wetting agent, removing excess moisture by touching the edge of the specimen to a blotter, and then following the procedure of the Monsanto method. Tearing strength was tested by the Elmendorf method, ASTM designation D 1424-56T [2b]; breaking strength and elongation were measured on the Instron Tensile Tester by the strip method [2c], except that a count of 80 threads was used instead of 1-in. width.

Dry density was determined by the method of Orr et al. [9].

Results and Discussion

The properties of the fabrics before and after cross-linking are presented in Table I.

Add-on of Cross-Linking Agent

The add-on of cross-linking agent is determined by the wet pickup of the treating solution and the extent of reaction of dimethylol ethyleneurea with cotton. This was judged by the increase in the nitrogen content of the fabrics. The data in Table I show that of all the etherified cottons and alkali controls, only hydroxyethylated cotton with a 15% alkali treatment had a significantly higher nitrogen content than the unmodified cotton after treatment.

It is considered that the amount of dimethylol ethyleneurea add-on should be a function of the swellability of the cotton. The alkali treatments swell the cotton, but it is believed that after rinsing and drying the fiber returns nearly to its original condition. Therefore, little increase in swellability or add-on would be expected with alkali treatments

below mercerizing strength. When mercerizing strength alkali is used, the fiber would be expected to recover less because of the strong disrupting effect on the regions of high lateral order within the fiber. No noticeable increase in add-on, however, was caused by alkali treatments of 15% and higher. Probably even at these high alkali concentrations, this is due to the lack of complete mercerization when the cotton fiber is bound in the yarn and fabric structure [13].

In the preparation of the modified cottons, the etherification takes places when the cotton is swollen by the alkali. The ether substituents then can prevent the return of the swollen cotton to its original, unswollen condition. The now modified cotton should have increased swellability and should absorb more of the treating solution. If the ether substituent is inert to the cross-linking agent, reactivity will be reduced. This effect will counter, to a greater or lesser extent, the effect of increased swellability, as unreacted agent will be washed off the fabric. The data show that the cottons modified with methyl, cyanoethyl, and carboxymethyl substituents, all of which are less reactive to dimethylol ethyleneurea than the hydroxyl group replaced, do not have higher nitrogen contents then unmodified cotton. The hydroxyethyl substituents, however, should be at least as reactive as the replaced cellulosic hydroxyl groups. Therefore, increased swellability of the hydroxyethylated cotton should result in increased nitrogen content. This is observed with hydroxyethylated cotton fabric prepared with 15% sodium hydroxide. It is not observed, however, with the hydroxyethylated cotton prepared with 7% sodium hydroxide. In the latter case the swelling at the time of etherification would be expected to be less and, from the results, is apparently not sufficient to cause a noticeable increase in add-on.

Conditioned Crease Recovery Angle

Etherification without cross-linking reduces in all cases the conditioned crease recovery angles of the fabrics below those of the alkali control fabrics. The increased swellability of the etherified fabrics, discussed previously, is due to disrupted interchain bonds or forces between molecular chains of cellulose or between elements composed of groups of cellulose chains in the cotton fiber. The presence of the ether group prevents re-formation of these bonds or forces on drying, which can occur to some extent with alkali-treated, nonetherified samples. Since these forces also contribute to resiliency, the ability of the fiber to recover from creasing is reduced.

With an 8% dimethylol ethyleneurea treatment, the maximum crease recovery was obtained with unmodified cotton. In fact, the treatment described supplies more dimethylol ethyleneurea than the amount required for maximum crease recovery in the unmodified fabric. The etherified cottons, except the hydroxyethylated cotton, give lower conditioned crease recovery angles, although the nitrogen content is relatively high. To compensate for the bonds disrupted by etherification, it would be expected that more cross-linking, and thus higher dimethylol ethyleneurea add-on would be required to obtain maximum crease recovery angles. On the etherified cottons, which have lower initial crease recovery angles, sufficient cross-linking is not obtained from an 8% solution to give the crease recovery angles obtained on unmodified cotton. Indeed, such high crease recovery angles may be unobtainable with etherified cottons. It would be expected that such a high degree of substitution could be obtained on cotton etherified with inert groups that the cross-link formation necessary to reach the high crease recovery angle obtained on unmodified cotton would be prevented.

With hydroxyethylated cotton, however, conditioned crease recovery angles of the cross-linked fabric are even higher than those obtained on cross-linked unetherified cotton with comparable nitrogen content. This can be explained if more efficient cross-linking occurs with hydroxyethylated cotton, that is, if more and shorter cross-links are formed for the same amount of bound dimethylol ethylene-

TABLE II. Formaldehyde/Ethyleneurea Ratio of Cross-Linked Fabrics

Ether	(DS)	Formaldehyde, %	CH_2O/EU Ratio*
Cotton		1.65	1.4
$-CH_2CH_2CN$	(0.36)	1.30	1.3
$-CH_2CH_2OH$	(0.25)†	1.73	1.6
$-CH_2CH_2OH$	(0.25)‡	2.14	1.5
$-CH_3$	(0.5)	1.80	1.5
$-CH_2CO_2H$	(0.09)	1.25	1.3

* $\frac{\%\ CH_2O}{30} \div \frac{\%\ N}{28}$.

† 7% NaOH pretreatment.
‡ 15% NaOH pretreatment.

urea. The increased number of cross-linkages, then, compensates for the natural bonds disrupted by etherification. Such an increase in cross-linking efficiency is indeed indicated by other data.

An alternate explanation is that the replacement of natural forces contributing to resiliency by the force of covalent cross-links, which are more stable under stress, results in improved resiliency and crease recovery. Therefore, crease recovery angles are obtained that are higher than any believed to be obtainable on unmodified cotton fabric no matter how much dimethylol ethyleneurea is applied under the treating conditions described.

Cross-Linking Efficiency

In general, it would be expected that with the cellulose ethers used in this study, except in the case of the hydroxyethylated cottons, the number of cross-links per unit of nitrogen content would be reduced. Replacement of cellulosic hydroxyl groups by groups inert or less reactive to dimethylol ethyleneurea will reduce the number of reactive sites. This should lead not only to less bound nitrogen, but also to fewer cross-links from the bound nitrogen, because the methylol compound, after initial reaction, will have fewer possibilities of completing the cross-link. Therefore, a higher proportion of bound but not cross-linking material, or longer, polymeric cross-links between more distant cellulosic hydroxyl groups, will result. Hydroxyethylation, of course, substitutes another hydroxyl group for the cellulosic hydroxyl group replaced.

The efficiency of cross-linking is shown by the ratio of formaldehyde residues to ethyleneurea residues, Table II, calculated from formaldehyde and nitrogen analyses. The higher the ratio, the greater is the efficiency of cross-linking, or the greater the number of cross-links for the amount of applied material. A ratio of 2 is the maximum and would indicate that each dimethylol ethyleneurea molecule forms a single cross-link. A ratio lower than 2 indicates either that some proportion of the applied dimethylol ethyleneurea forms cross-links containing more than one dimethylol ethyleneurea residue, or that there is some proportion of bound, but not cross-linking residues. The minimum possible value of 1 for the ratio would indicate no cross-linking.

The higher ratio for hydroxyethylated cotton than for unmodified cotton, in Table II, indicates increased cross-linking. This may be due to a more reactive hydroxyl group in the substituent group than the replaced cellulosic hydroxyl group. This would tend to confirm the hypothesis presented earlier as to why high conditioned crease recovery angles are obtained with this etherified cotton at nitrogen contents equivalent to those of cross-linked, unmodified cotton, although the hydroxyethylated cotton is in a more swollen condition.

A higher ratio, and hence greater cross-linking efficiency, also seems to occur with methylated cotton. This is surprising because of the high substitution of a substituent inert to dimethylol ethyleneurea. The highly swollen structure expected in this product, and confirmed by density measurements, results, however, in poor conditioned crease recovery angles. In this instance the increased cross-linking is apparently not sufficient to overcome the effects of swelling.

The other two ethers show lower cross-linking efficiency, which contributes to lower conditioned crease recovery angles. Even the small degree of substitution in carboxymethylation causes a noticeable drop in ratio.

Wet Crease Recovery

Wet crease recovery results from different causes in the cross-linked and noncross-linked cotton. Increases in conditioned crease recovery are due to the presence of cross-links which prevent permanent dislocation of the elements of the cotton fiber. Improved wet crease recovery is due partly to the above effect, but is, in addition, also due to swelling by water, which makes a more resilient fiber by means of a tensioning effect, as in the inflation of a balloon. In cotton that is not cross-linked, the swelling effect is added to the natural resiliency of the fiber, and wet crease recovery will depend a great deal on the swellability of the fiber. In cross-linked cotton with high conditioned crease recovery, the swelling effect is usually small, and the wet crease recovery is due to the same cause as the conditioned recovery—cross-linking—with the effects modified by the lubricating or other effects of water.

Etherification of cotton without cross-linking increases the wet crease recovery angle because of increased swellability, except for the unexplained results with methylated cotton. With hydroxyethylated samples, fabric prepared with 15% sodium hydroxide, and therefore more swollen than that prepared with 7% sodium hydroxide, has higher wet

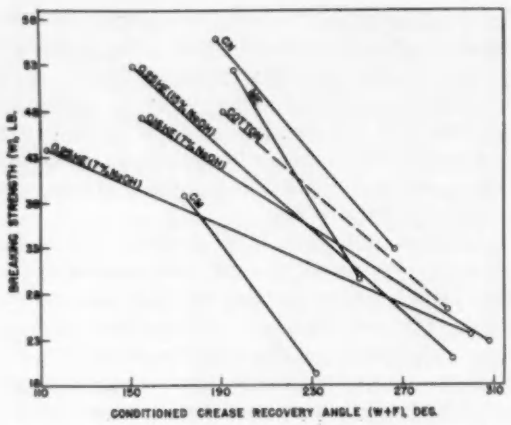

Fig. 1. Changes in breaking strength with change in conditioned crease recovery angle.

crease recovery at the same degree of substitution. Even a low substitution of the highly polar carboxyl group, which causes a relatively large increase in swellability, gives high wet crease recovery.

Cross-linked etherified cottons, except cyanoethylated cotton, have consistently higher wet crease recovery than the corresponding alkali controls, although the difference is small in some instances. The contribution of swelling to wet crease recovery apparently still exists in these fabrics even though they are cross-linked. This is true not only with the fabrics with low conditioned crease recovery angles, where the degree of cross-linking relative to the disordered regions present is relatively low, but also with hydroxyethylated cottons that have high conditioned crease recovery angles. In cyanoethylated cotton, apparently the low degree of cross-linking adds little to wet crease recovery, but does reduce the effect of swelling.

Moisture Regain

Moisture regain is another property related to the degree of swellability and degree of lateral order in the cotton fiber. Treatment with increasing concentrations of sodium hydroxide gives increasing values of moisture regain. Following the previous line of reasoning regarding the swellability of the cellulose ethers, etherification would be expected in all cases to give a product with higher moisture regain than the corresponding alkali control. The nature of an ether substituent, however, has an important effect in modifying this relationship. Cyanoethyl and methyl groups do not bring about the expected increased moisture regain. This is true even with the relatively high degree of substitution, 0.5, in the methylated cotton. On the other hand, the highly polar and hydrophilic carboxymethyl group causes a large increase in moisture regain with a degree of substitution of only 0.09 and, as judged from the density, little actual increase in swelling when dry.

Except for the carboxymethylated cotton, the dimethylol ethyleneurea treatment reduced the moisture regain of all fabrics from that of the fabric before cross-linking. In the cross-linked alkali controls and etherified cottons with more hydrophilic substituents, it appears that moisture regains are higher at a given crease recovery angle than in cross-linked, unmodified cotton. This is obviously true in the hydroxyethylated cottons. The cross-linked hydroxyethylated cotton prepared with 15% sodium hydroxide has a 9.7% moisture regain with a high conditioned crease recovery angle. These results indicate that replacement of those natural bonding forces of cotton lost in etherification by covalent cross-links to produce the same resiliency or recovery properties in an etherified cotton as in an unmodified cotton, gives a product with increased accessibility.

Breaking Strength of Cross-Linked, Etherified Cotton

Breaking strengths were determined on samples stripped to 80 threads to eliminate the effect of shrinkage.

No readily observed differences can be noted in the relation of final crease recovery angle to breaking strength in any of the cross-linked fabrics except the carboxymethylated cotton. The lower breaking strength of cross-linked carboxymethylated cotton at the relatively low conditioned crease recovery angle is undoubtedly due to the strength lost on etherification.

The average loss in breaking strength for unit gain in crease recovery angle, however, does vary among the different fabrics. These differences are shown graphically in Figure 1 by lines connecting the points determined by the initial and final relations of breaking strength and conditioned crease recovery angle. The variance is apparently due to the changes in the relation caused by etherification before cross-linking. The increased strength of methylated and cyanoethylated cotton results in a greater loss as crease recovery angle increases on cross-linking and the strength–recovery relation ap-

proaches that of unetherified cotton. On the other hand, the low recovery angles of hydroxyethylated cottons allow a greater increase in crease recovery angle on cross-linking for the same strength loss as occurs in unetherified cotton.

The data include only initial and final values of crease recovery angles and strength, hence only limited conclusions can be drawn. From the data available, however, it seems that in general the effect of etherification on the breaking strength–crease recovery relationship of cross-linked cotton fabrics is adverse except for any increase in strength that may be caused by the etherification itself.

Extensibility

Examination of load–elongation curves, Figures 2A and 2B, shows that elongation at break increases with the use of higher alkali concentrations. This increased elongation is due to a decreased initial modulus, that is, at low loads. The etherified cottons have curves almost identical to their alkali controls, with the exception of hydroxyethylated cotton prepared with 15% sodium hydroxide. In this exception, the ether has a curve exhibiting a lower initial modulus than its alkali control.

Cross-linking decreases elongation in all cases, as seen in Figures 2C and 2D. The etherified cottons

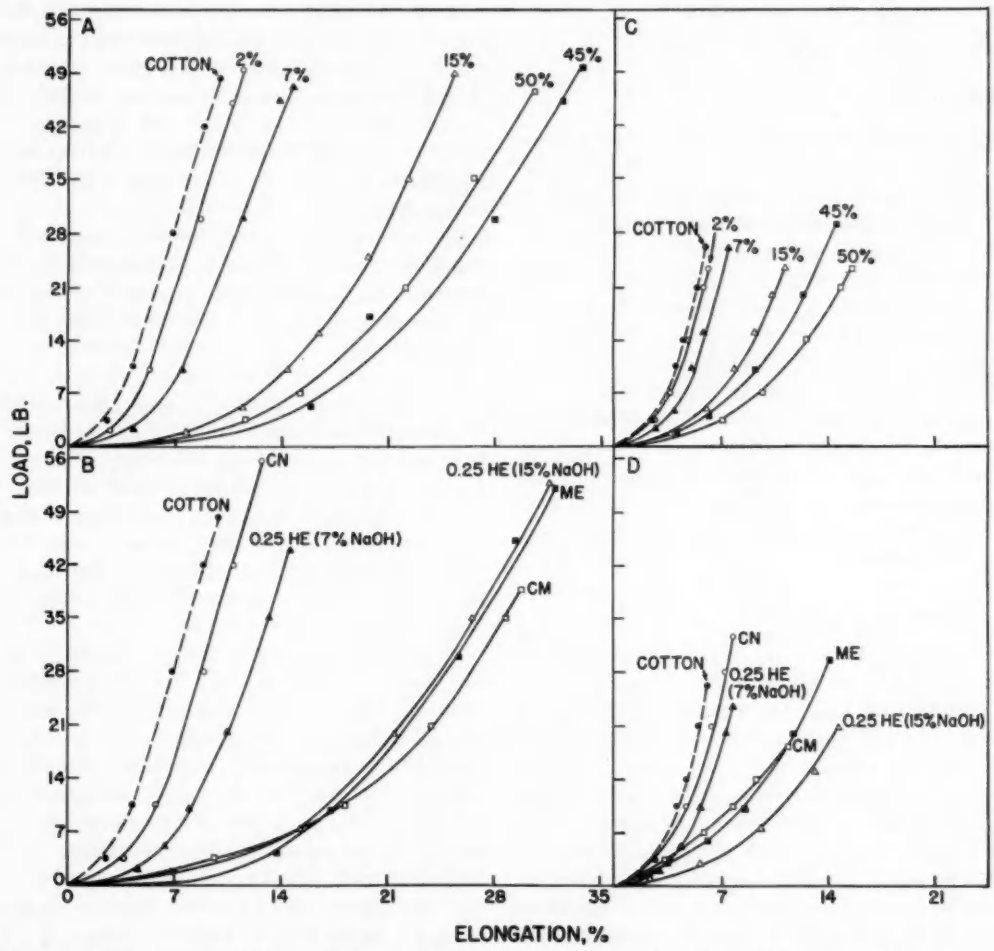

Fig. 2. Load–elongation curves before and after cross-linking. A, alkali controls; B, etherified cottons; C, alkali controls, cross-linked; D, etherified cottons, cross-linked.

and their alkali controls still show greater elongation and less steep load–elongation curves than the unmodified cotton, but the difference has been reduced.

Much of the reduction in initial modulus is probably due to yarn pucker from shrinkage in the alkali treatment and not directly to decreased lateral order in the fiber. Presumably, most of this initial elongation is irreversible and could have been removed if the samples had been mechanically conditioned before testing. In the case of the cross-linked samples, the initial extension is apparently reversible, which is shown by the high conditioned crease recovery and high elongation of the 45% and 50% alkali controls and by one etherified cotton at least—the hydroxyethylated cotton prepared with 15% sodium hydroxide

Relative Toughness

One factor that affects the service life of a fabric is the relative toughness, an index of which is one-half the product of breaking strength and elongation at rupture [15]. Cross-linked hydroxyethylated cotton, prepared with 15% sodium hydroxide, and cross-linked nonetherified cotton, both of which have comparably high conditioned crease recovery angles, have relative toughness values of 154 and 79 respectively. On this basis a longer service life would be predicted for the cross-linked hydroxyethylated fabric. The relative toughness values are based on total elongation and do not separate recoverable and nonrecoverable fractions. For this reason, the comparison may be of questionable value, as relative toughness based on recoverable elongation only may be a better indication of service life.

Dry Density

As explained previously, it is believed that the alkali treatment swells the cotton fiber and that etherification in this swollen state prevents collapsing on drying. However, on drying after alkali treatment without etherification, the cotton collapses nearly to its original condition. This theory is supported by the dry density values; the density of the alkali controls is not as much below that of unmodified cotton as are the corresponding etherified samples. The density of etherified cottons, in the range of substitution investigated, depends on the strength of the alkali used, which determines the extent of swelling in the treatment, and on the degree of substitution, which limits the return of the fiber to its original form.

The data show decreasing density with increasing degree of substitution. The effect of alkali is shown by the decreased density of the hydroxyethylated cotton prepared with 15% alkali as compared with hydroxyethylated cotton with the same degree of substitution prepared with 7% alkali.

The change in density due to cross-linking with dimethylol ethyleneurea was small in all the fabrics.

Summary

Treatment of cotton with solutions of from 2% to 50% sodium hydroxide has little effect on the reactivity of the fabric to dimethylol ethyleneurea. Partial replacement of cellulosic hydroxyl groups with ether substituents inert to dimethylol ethyleneurea decreases reactivity even though swellability would normally be expected to increase reactivity. The effect of swelling is noticed when a group reactive to dimethylol ethyleneurea, such as a hydroxyethyl group, is used.

Some interchain bonds or forces between molecular cellulose chains are disrupted permanently by etherification, and a reduction in resiliency of the fabric, as shown by decreased conditioned crease recovery angle, results. As a consequence, these etherified fabrics require more cross-linking than unmodified cotton to reach the same level of wrinkle resistance. Hydroxyethylated and methylated cotton fabrics exhibit greater cross-linking efficiency with a given amount of applied dimethylol ethyleneurea than does unmodified cotton. The high swellability of methylated cotton results, however, in lower conditioned crease recovery, but hydroxyethylated cotton, on the other hand, acquires crease recoveries as high as or higher than unmodified cotton.

Wet crease recovery is generally higher in etherified cottons than in cotton. This is probably due to increased swellability introduced in the fiber during etherification. As a result of this increased swellability, cross-linked etherified cottons have higher wet crease recovery than cross-linked cotton.

Moisture regain is also influenced by swellability and by the nature of the ether substituent. In some instances, cross-linked hydroxyethylated cotton with high conditioned crease recovery actually has greater moisture regain than unmodified cotton.

Cross-linking of etherified cotton in general causes a greater loss in breaking strength per unit gain in

crease recovery angle than cross-linking of unmodified cotton fabric. Hydroxyethylated cotton is an exception because of its low crease recovery before cross-linking. The rate of strength loss is magnified by increasing the strength of alkali used in the etherification reaction.

Increased elongation of etherified cotton fabrics as compared with unmodified cotton is directly related to the concentration of alkali used in etherification. This increase is attributed to a decreased initial modulus caused mainly by yarn pucker from alkali treatments. Cross-linking with dimethylol ethyleneurea lowers elongation at break, but the same general order of extensibility among fabrics is retained as prior to cross-linking.

Dry density decreases with increasing degrees of substitution of the groups studied, and little change was noted on treatment with dimethylol ethyleneurea.

Acknowledgments

The authors wish to thank Edna M. Ellerbusch, Annie B. Cooper, and Wilbur F. McSherry for textile evaluation tests; Alva F. Cucullu and Julian F. Jurgens for chemical analyses; Frank W. Snowden for his help in the laboratory; and George I. Pittman for the drawings.

Literature Cited

1. Assoc. Offic. Agr. Chemists, "Official Methods of Analysis," 8th edition, Washington, D. C., 1955, pp. 810–811.
2. ASTM Designation (a) D 1295–53T; (b) D 1424–56T; (c) D 1682–59T, American Society for Testing Materials, Philadelphia, Pa.
3. Cooke, T. F., Eastes, J. W., and Fluck, L. A. (to American Cyanamid Co.), U. S. Patent 2,923,597 (February 2, 1960).
4. Daul, G. C., and Reid, J. D. (to U. S. A. as rep. by Secy. of Agr.), U. S. Patent 2,584,114 (February 5, 1952).
5. Daul, G. C., Reinhardt, R. M., and Reid, J. D., Textile Research Journal **22**, 792–797 (1952).
6. Morgan, P. W., *Ind. Eng. Chem. Anal. Ed.* **18**, 500–504 (1946).
7. Negishi, M. and Aida, N., Textile Research Journal **29**, 982–989 (1959).
8. Negishi, M., Itō, H., and Aida, N., Textile Research Journal **29**, 990–995 (1959).
9. Orr, R. S., Weiss, L. C., Moore, H. B., and Grant, J. N., Textile Research Journal **25**, 592–600 (1955).
10. Reeves, W. A., Guthrie, J. D., and Drake, G. L., Jr. (to U. S. A. as rep. by Secy. of Agr.), U. S. Patent 2,906,592 (September 29, 1959).
11. Reinhardt, R. M., Fenner, T. W., and Reid, J. D., Textile Research Journal **27**, 873–878 (1957).
12. Reinhardt, R. M., Reid, J. D., Fenner, T. W., and Mayne, R. Y., Textile Research Journal **29**, 802–810 (1959).
13. Segal, L. and Conrad, C. M., *Am. Dyestuff Reptr.* **46**, 637–642 (1957).
14. Stoffel & Co. (by P.-A. Koch and G. Frey), German Patent 1,017,131 (October 10, 1957).
15. Tripp, V. W., Orr, R. S., Ziifle, H. M., and Conrad, C. M., Textile Research Journal **28**, 404–417 1958).

Manuscript received February 27, 1961.

A Quantitative Study of Differential Dyeing of Cotton as a Means of Elucidating Fiber Structure

L. Rebenfeld and Hong Wu

Textile Research Institute, Princeton, New Jersey

Abstract

An analytical procedure is described for placing the differential dye test for cotton fiber maturity on a quantitative and objective basis. The procedure involves the extraction of the two dyes from a differentially dyed sample and spectrophotometrically analyzing the red and green dye uptake. The G/R value, defined as the ratio of green and red dye uptake, is shown to be a sensitive index of cotton fiber maturity. The mechanism of the differential dye test is discussed in terms of dyeing rates and fiber structure. The effects of swelling treatments on the differential dyeing test are also discussed.

Introduction

The differential dye test as developed by Goldthwait and his co-workers [8, 9] has proved to be extremely useful in visually identifying immature cotton. The maturity or secondary wall thickness of cotton is important in terms of both processing characteristics and end-product quality [5, 10]. Since other methods are available for measuring cotton fiber maturity and because of the subjective nature of this technique, the potentialities of the differential dye test have not been fully exploited.

In the Goldthwait differential dye test, a sample of cotton is dyed in a single bath composed of two direct dyes. While several combinations of dyes may be employed successfully, the most commonly used dyes are Chlorantine Fast Green BLL (mol. wt. 1350, C.I. No. Pr. 425) and Diphenyl Fast Red 5BL (mol. wt. 675, C.I. No. 278). Cotton is dyed with a mixture of these dyes under normal direct dyeing conditions and subsequently subjected to a rapid stripping operation in boiling water. Thin-walled or immature fibers are preferentially dyed green, while the mature thick-walled fibers are found to be red. Thus, depending upon the over-all shade which a bulk sample of cotton attains, the proportion of mature and immature fibers is deduced by visual comparison with previously prepared color standards.

In this differential dye test, the shade differences which are attained by cotton fibers of varying maturity result from a combination of the following factors: (a) differences in the equilibrium dye uptake of the red and green dye; (b) differences in the extent of dye stripping which occurs during the boiling water treatment; and (c) differential optical effects during visual examination of fibers of varying cross-sectional area [6].

The first two factors, extents of dye uptake and stripping, are influenced by structural characteristics of the fiber, such as crystallinity and orientation. It would therefore be desirable to isolate these factors and eliminate the complications arising from the varying optics of coarse and fine fibers. In order to accomplish this, it is necessary to determine analytically the amount of dye absorbed by the fibers, and not rely upon a visual comparison of sample colors with previously prepared standards. An analytical determination of dye uptake would also allow a more quantitative estimate of fiber structure than is possible by simple visual examination.

Pal and Esteve [11] studied the relationship between cotton fiber properties and equilibrium dye absorption for several cotton samples and found significant relationships between dye absorption and maturity. While these workers used the two direct dyes commonly employed in the differential dye test, the dyeings were performed separately for each dye. Furvik [7] observed that the equilibrium dye uptake for mature and immature cotton fibers is equal, but that the rate of dye absorption or desorption is greater for the immature cotton fibers. Armfield and Boulton [1] applied the differential dye test to 1.5 and 50.0 denier viscose fibers and ascribed the shade

differences to a net effect of the relative dyeing rates of the two component dyes, the differential optical effect of visually examining coarse and fine fibers, and the influence of fiber surface on the rate of dyeing and ease of stripping. Boulton [3] reported half-dyeing times for the two dyes commonly used in the differential dye test and found these to be 0.88 min. for the red dye, and 55.2 min. for the green dye. Similar observations, for these two dyes, were made by Crespo [4], who found equilibrium to be attained in about 80 min. for the green dye and about 10 min. for the red dye.

It may be concluded therefore that, in the differential dye test, true equilibrium is not attained and that, in view of the stripping treatment in boiling water, the rate of dye desorption is of particular importance. The analytically determined dye content should therefore not be considered as the equilibrium dye uptake but merely as the amount of dye taken up by cotton under the carefully defined conditions of the differential dyeing procedure. In the differential dye test the important consideration is the relative amount of the two dyes which is absorbed rather than the actual uptake of either dye. Thus, if G is defined as the dye uptake in milligrams per gram of cotton of the high-molecular-weight green dye, and R as the dye uptake of the low-molecular-weight red dye, then the value G/R may be a sensitive estimate of the structural characteristics of cotton fiber. It is necessary that both G and R be determined on samples dyed in a multicomponent dye bath and not from separate dyeing experiments.

In this work an attempt has been made to place the differential dye test on a quantitatively objective basis rather than a subjective basis. The influence of cotton fiber structure on dyeing characteristics has been studied, and the effects of certain chemical swelling treatments which are known to alter cotton fiber structure have been examined.

Experimental

Dyeing Procedure

One-gram samples are introduced into dye baths composed of 25 ml. 0.1% solution of Diphenyl Fast Red 5BL, 50 ml. 0.1% solution of Chlorantine Fast Green BLL, 10 ml. 0.5% NaCl. Dyeing is allowed to proceed at boiling temperatures (under reflux) for 1 hr. The dyed samples are washed over a glass fritted funnel with cold distilled water until the wash water is colorless. The critical dye stripping is accomplished by placing the dyed samples in 100 ml. vigorously boiling distilled water for exactly 30 sec. with continual stirring. The samples are subsequently quenched in 100 ml. cold distilled water, washed on a funnel until wash water is colorless. Excess water is then removed by suction and the samples are air dried.

Dye Extraction

In order to achieve uniformity, the dyed samples are ground in a Wiley mill to pass through a 20-mesh sieve. For dye extraction, 150 mg. of the ground sample is placed in a test tube and 25 ml. of 25% aqueous pyridine solution is added. The test tube, covered with a funnel, is placed in a boiling water bath for 30 min. and subsequently cooled with running tap water for 5 min. The supernatant solution in the test tube is used directly for spectrophotometric analysis. Each dyed sample is extracted and analyzed in duplicate. Several analyses are run simultaneously.

Spectrophotometric Analyses

Optical densities of the extract at two wavelengths are measured on a Beckmann DU spectrophotometer. The bands of maximum optical densities for the green and red dyes were found to be 600 mμ and 510 mμ, respectively. This previously established fact [11] was confirmed in this investigation. Dye concentrations were determined from master calibration curves and calculated as milligrams of dyestuff absorbed per gram of standard conditioned cotton. Excellent reproducibility was attained for each dyed sample.

Samples

Nine experimental cottons in card sliver form were used in these studies. These nine cottons, listed in Table I, were chosen primarily on the basis of their maturity values as determined by the array method. No purification treatments were given to these cottons other than the removal of large particles of nonfibrous foreign matter.

Both cottons in the original raw cotton state and mercerized cottons were dyed. The mercerization consisted of treating 1-gram samples in 50 ml. 20% (weight) NaOH for 5 min. at room temperature. After being thoroughly washed with water, the samples were neutralized in 60 ml. 1% acetic acid for

TABLE I. Experimental Cottons

Cotton code no.	Description	Array method: Maturity, %	Array method: Fineness, μg./in.
39	NR-AHA-C	98	5.3
55	1954 Lengupa	92	6.4
5	Hopi Acala 46-124	90	4.0
37	Pima S-1	90	3.3
38	Amsak	90	3.1
45	Acala 1517C	84	4.0
49	Smooth Leaf 1000	84	4.8
41	Acala 4-42 (Shafter)	78	4.0
36	Paymaster 54	75	4.0

TABLE II. Dye Uptake and G/R Values for Standard, Raw and Mercerized Cottons

	Dye uptake, mg./g.			G/R values
	Red	Green	Total	
Nine cottons, raw	7.3	11.7	19.0	1.60
Nine cottons, mercer.	10.8	24.0	34.8	2.22
Crystalline std.	6.8	4.1	10.9	0.60
Amorphous std.	9.1	24.9	34.0	2.72

5 min. at room temperature, washed with distilled water to remove excess acid, and air dried.

Three of the nine cottons representing the extreme and medium values in maturity were subjected to other swelling treatments.

(a) Water treatment—30 min. at room temperature in distilled water and air dried.

(b) Urea treatment—30 min. at room temperature in 10 *M* aqueous urea, washed and air dried.

(c) Combination treatments—mercerized samples subsequently treated with 10 *M* urea; and 10 *M* urea-treated samples subsequently mercerized.

In order to establish the dyeing characteristics of samples which have a wide range in supermolecular order, a crystalline standard and an amorphous standard were also used. The crystalline standard was prepared by subjecting a purified cotton cellulose to hydrolysis in 1 *N* HCl for 24 hr. at 60° C. The residue from the hydrolysis was filtered, washed, and dried, and had been used previously as a crystalline standard in the development of an X-ray method for

TABLE III. Dye Uptake and G/R Values for Nine Raw Cottons

Cotton code no.	Maturity, %	Dye uptake, mg./g.: Red	Green	Total	G/R value
39	98	7.7	7.8	15.5	1.01
55	92	7.2	8.9	16.1	1.24
5	90	7.5	11.2	18.7	1.49
37	90	6.7	10.8	17.5	1.61
38	90	6.9	11.4	18.3	1.65
45	84	7.6	13.8	21.4	1.82
49	84	7.5	12.8	20.3	1.71
41	78	7.1	12.7	19.8	1.79
36	75	7.4	15.9	23.3	2.15

TABLE IV. Dye Uptake and G/R Values for Nine Mercerized Cottons

Cotton code no.	Maturity, %	Dye uptake, mg./g.: Red	Green	Total	G/R value
39	98	11.0	19.6	30.6	1.78
55	92	10.6	19.8	30.4	1.87
5	90	11.6	25.7	37.3	2.22
37	90	10.4	24.9	35.3	2.39
38	90	10.4	24.6	35.0	2.36
45	84	10.6	26.0	36.6	2.45
49	84	11.4	25.5	36.9	2.24
41	78	10.0	23.2	33.2	2.32
36	75	11.0	26.8	37.8	2.44

TABLE V. Comparison in Dye Uptake and G/R Values for Nine Cottons in the Raw and Mercerized Conditions

Cotton code no.	Maturity, %	G/R value: Raw	Mercer.	M/R	Total dye uptake, mg./g.: Raw	Mercer.	M/R
39	98	1.01	1.78	1.76	15.5	30.6	1.97
55	92	1.24	1.87	1.51	16.1	30.4	1.89
5	90	1.49	2.22	1.49	18.7	37.3	2.00
37	90	1.61	2.39	1.48	17.5	35.3	2.02
38	90	1.65	2.36	1.43	18.3	35.0	1.91
45	84	1.82	2.45	1.35	21.4	36.6	1.71
49	84	1.71	2.24	1.31	20.3	36.9	1.82
41	78	1.79	2.32	1.29	19.8	33.2	1.68
36	75	2.15	2.44	1.14	23.3	37.8	1.62

determining cotton cellulose crystallinity [2, 13]. The amorphous standard was prepared by the Southern Regional Research Laboratory, ARS, USDA, by treatment of cotton with anhydrous ethylamine for 4 hr. followed by chloroform extraction, which resulted in a crystallinity content by acid hydrolysis of 28% [12, 13].

Results

In Table II are shown dye uptake and G/R values for the crystalline and amorphous standards and average values for the nine experimental cottons in both raw and mercerized conditions. The high (2.72) G/R value for the amorphous standard and the low (0.60) G/R value for the crystalline standard demonstrate the expected result; a higher fraction of the large green dye is taken up by amorphous cellulose and a higher fraction of the small red dye is taken up by crystalline cellulose. The potentialities of this method for accessibility measurements are thus quite apparent. It is reasonable to expect G/R values for cotton to fall between 2.72 and 0.60, which are the values for amorphous and crystalline standards, respectively. The G/R value for raw cotton of 1.60 (average for nine cottons) is thus a reasonable one. Since mercerization without tension involves decrystallization, a G/R value of 2.22 (average for nine cottons) further indicates the potentialities of this technique.

It now becomes of interest to examine the dye uptake and the G/R values for the nine cottons individually in order to ascertain the effects of cotton fiber structure on dyeing characteristics. In Table III are shown dye uptake and G/R values for the nine cottons in the raw state, while in Table IV are listed data for the mercerized cottons. A comparison between the raw and mercerized cottons can be seen in Table V, where the total dye uptake and the G/R values are tabulated.

The uptake of the red dye is constant for the nine cottons in both the raw and mercerized conditions, as indicated in Figure 1 where red dye uptake is plotted against cotton fiber maturity. As shown in Figure 2, the green dye uptake is significantly and inversely dependent upon cotton fiber maturity. This dependence is also reflected in the relationship between the total dye uptake and cotton fiber maturity as graphically indicated in Figure 3. Since in the differential dyeing technique one is interested in the relative red and green dye uptake, the significant dependence of the G/R value on cotton fiber maturity

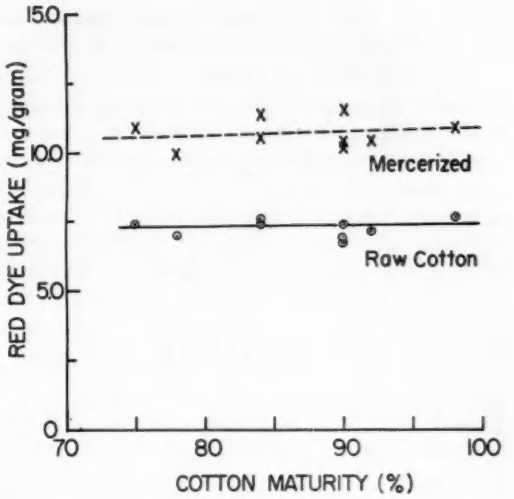

Fig. 1. Relationship between Diphenyl Fast Red 5BL dye uptake and cotton fiber maturity for mercerized and raw cottons.

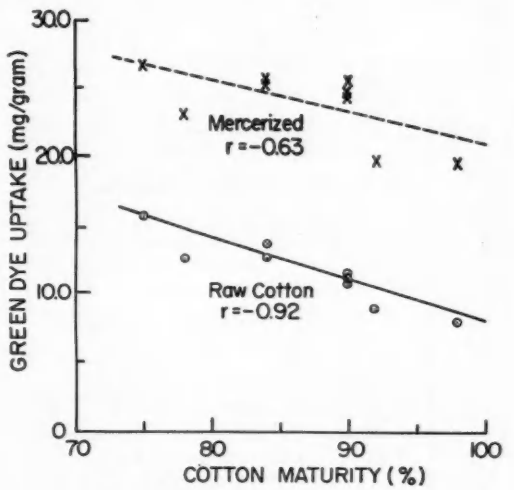

Fig. 2. Relationship between Chlorantine Fast Green BLL dye uptake and cotton fiber maturity for mercerized and raw cottons. (r = correlation coefficient)

is particularly important, as shown in Figure 4. The G/R value for more mature cottons is lower than for the less mature cottons in both the raw and mercerized conditions. In view of the data shown in Table II for the crystalline and amorphous standards, one may conclude that the more mature cottons are characteristic of higher supermolecular order than are the less mature ones. Since mercerization involves decrystallization, the G/R values for the mercerized

cottons are significantly higher than for the raw cottons. The change in the G/R value for each cotton as a result of mercerization is also significantly dependent upon cotton fiber maturity, as shown in Figure 5. The more mature cottons, which are presumably more crystalline, undergo a greater increase in the G/R value, which would indicate that they experience a greater decrystallization effect during mercerization. This leveling-out effect of mercerization on the G/R value may also be inferred from the slopes of the regression lines in Figure 4, where a greater dependency of the G/R value on cotton fiber maturity is indicated for the raw cotton than for the mercerized cotton.

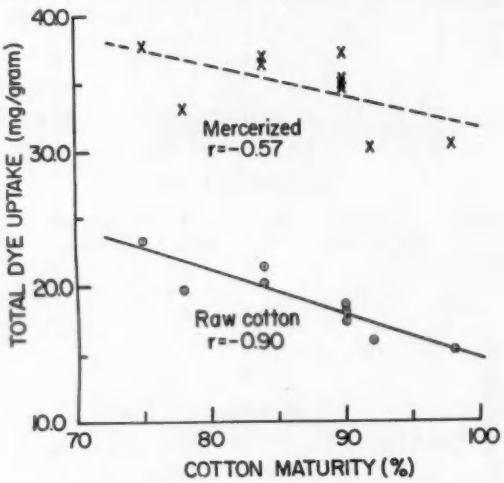

Fig. 3. Relationship between total dye uptake and cotton fiber maturity for mercerized and raw cottons. (r = correlation coefficient)

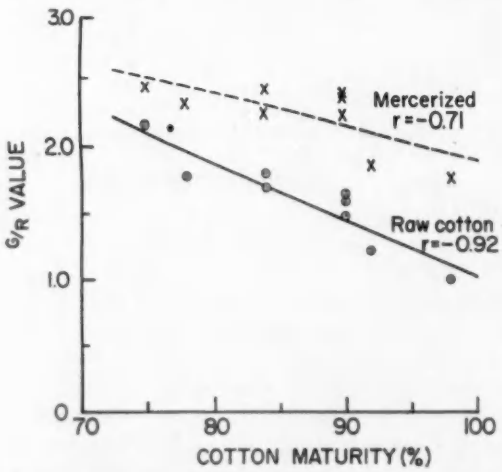

Fig. 4. Relationship between the G/R value and cotton fiber maturity for mercerized and raw cottons. (r = correlation coefficient)

In Tables VI, VII, and VIII are shown dye uptake and G/R values for three cottons of varying maturity after several swelling pretreatments. Values for raw cotton and mercerized cotton are included for comparison. The total dye uptakes for the raw cotton, water-treated cotton, and 10 *M* urea-treated cotton are approximately equal for each of the three cottons. For these three non-mercerizing treatments, the total uptake is least for the most mature cotton, intermediate for the intermediately mature cotton, and highest for the least mature cotton. These results parallel the data shown in Figure 3 and indicate that the effects of the water and the 10 *M* urea treatments on total dye uptake are not significant and that the three cottons of varying maturity respond in the same manner to these non-mercerizing treatments. The G/R values increase markedly, however, as a result of the water and the 10 *M* urea treatments. Thus, while the total dye uptake is not affected by a water treatment nor by a 10 *M* urea treatment, the distribution of the red and green dye is altered in such a manner as to indicate a decrystallization effect of these non-mercerizing treatments. As in the case of mercerization (Figure 5), greater effects of water and 10 *M* urea are noted for the more mature and presumably more crystalline cottons.

In the mercerizing treatments alone, followed by or preceded by a 10 *M* urea treatment, a significant

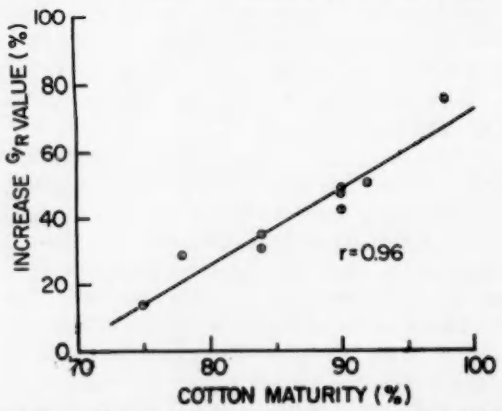

Fig. 5. Relationship between the increase in the G/R value as a result of mercerization and cotton fiber maturity. (r = correlation coefficient)

TABLE VI. Dye Uptake and G/R Values for Cotton #39 (Maturity = 98%) after Several Pretreatments

Treatment	Dye uptake, mg./g.			G/R value
	Red	Green	Total	
Control	7.9	7.5	15.4	0.95
Water	6.7	9.9	16.6	1.48
10 *M* urea	6.8	11.0	17.8	1.62
Mercerization	12.0	21.0	33.0	1.75
10 *M* urea & mercer.	11.5	18.9	30.4	1.64
Mercer. & 10 *M* urea	11.1	23.4	34.5	2.11

TABLE VII. Dye Uptake and G/R Values for Cotton #5 (Maturity = 90%) after Several Pretreatments

Treatment	Dye uptake, mg./g.			G/R value
	Red	Green	Total	
Control	7.1	10.3	17.4	1.45
Water	6.6	12.7	19.3	1.92
10 *M* urea	7.1	15.3	22.4	2.15
Mercerization	12.3	24.6	36.9	2.00
10 *M* urea & mercer.	11.2	24.4	35.6	2.18
Mercer. & 10 *M* urea	11.1	21.0	32.1	1.89

TABLE VIII. Dye Uptake and G/R Values for Cotton #36 (Maturity = 75%) after Several Pretreatments

Treatment	Dye uptake, mg./g.			G/R value
	Red	Green	Total	
Control	7.3	15.6	22.9	2.14
Water	6.2	16.1	22.3	2.60
10 *M* urea	7.2	16.9	24.1	2.35
Mercerization	10.1	23.8	33.9	2.36
10 *M* urea & mercer.	11.1	25.0	36.1	2.25
Mercer. & 10 *M* urea	9.8	22.4	32.2	2.28

increase in the total dye uptake is noted for the three cottons relative to those receiving the non-mercerizing treatments. The total dye uptake is approximately equal following the three mercerizing treatments, and only minor differences are noted among the three cottons. The G/R values for the cottons receiving the three mercerizing treatments are significantly higher than the values for the raw cotton, but not significantly higher than for the water- and 10 *M* urea-treated cottons.

Discussion

The results of this investigation of the differential dye test shed additional light on the dyeing characteristics of the two dyes commonly used in the test and on the manner in which these dyeing characteristics are influenced by cotton fiber structure. The results of this investigation also indicate the potentialities of the differential dye test as a quantitative and objective means of estimating cotton fiber maturity.

It is interesting to note that, under the conditions of the differential dye test, the red dye uptake is independent of cotton fiber maturity and that only green dye uptake is influenced by this fiber characteristic. This observation is valid only when the dyeing is allowed to proceed from a dye bath containing a mixture of the two dyes as is specified in the differential dye test. The results obtained by Pal and Esteve [11] indicate that both the red and green dye uptake values are functions of cotton fiber maturity when the dyeing is carried out from single-component dye baths. The dye uptake values reported by Pal and Esteve [11] cannot be strictly compared with the values reported in this paper since their dyeings were carried out from single-component dye baths and the dyed samples were not subjected to the crucial stripping operation in boiling distilled water. Since it is known that the half-dyeing times for the two dyes in question differ by a factor of approximately 60, it is reasonable to assume that different amounts of red and green dye will be stripped from a differentially dyed cotton sample. Thus, in the differential dye test the final total uptake of dyestuff and the ratio of red and green dye uptake values are dependent upon the relative dyeing rates of the two dyes in question and upon the structural characteristics of the fiber. The effects of the differential dye test are dependent upon a competition between the two dyes for active absorption sites and upon the relative rates of stripping of the two dyes during the stripping operation in boiling water. Either the competition for sites or the rate of stripping of the two dyes, or both of these factors, are influenced by cotton fiber maturity. Thus, the relative green and red dye uptake, as expressed by the G/R value, is a sensitive index of cotton fiber maturity.

Prior to this investigation the differential dye test for cotton maturity relied upon a visual examination of differentially dyed cotton samples and a comparison with previously prepared standards. While this procedure has found certain utility in cotton research, its usefulness has been curtailed by the subjective nature of the classification. In view of the established importance of cotton fiber maturity in terms of processing efficiency and end-product quality [5,

10], it would be desirable to have available a rapid, quantitative, and objective means of evaluating cotton fiber maturity. The highly significant correlation between the G/R value and cotton fiber maturity clearly indicates the applicability of the differential dye test for this purpose. The nine cottons used in this investigation were chosen to cover the range of maturity values which are of particular interest to the cotton industry. Even within this rather narrow range the G/R value provides a sensitive means of classification.

The influence of swelling treatments on the G/R value is also of interest since changes in the G/R value may be used to characterize the efficiency of such pretreatments. Particularly, those treatments which exert a decrystallizing effect may be quantitatively evaluated by this analytical modification of the differential dye test.

Literature Cited

1. Armfield, W. and Boulton, J., TEXTILE RESEARCH JOURNAL **19**, 212 (1949).
2. Bauer, F. W. and Pacsu, E., TEXTILE RESEARCH JOURNAL **22**, 385 (1952).
3. Boulton, J., *J. Soc. Dyers Colourists* **60**, 5 (1944).
4. Crespo, R., TEXTILE RESEARCH JOURNAL **31**, 80 (1961).
5. Fiori, L. A., Louis, G. L., and Sands, J. E., TEXTILE RESEARCH JOURNAL **29**, 706 (1959).
6. Fothergill, F., *J. Soc. Dyers Colourists* **60**, 93 (1944).
7. Furvik, Nils-Bertil, *J. Soc. Dyers Colourists* **74**, 299 (1958).
8. Goldthwait, C. F. and Sloan, W. G., *Am. Dyestuff Reptr.* **45**, 813 (1956).
9. Goldthwait, C. F., Smith, H. O., and Barnett, M. P., *Textile World* **97**, 105 (1947).
10. Leitgeb, D. J. and Wakeham, H., TEXTILE RESEARCH JOURNAL **26**, 543 (1956).
11. Pal, P. N. and Esteve, R. M., Jr., TEXTILE RESEARCH JOURNAL **29**, 811 (1959).
12. Segal, L., Nelson, M. L., and Conrad, C. M., TEXTILE RESEARCH JOURNAL **23**, 428 (1953).
13. Wakelin, J. H., Virgin, H. S., and Crystal, E., *J. Appl. Phys.* **30**, 1654 (1959).

Manuscript received March 23, 1961.

Adsorption of Calcium and Polyphosphates on Cotton Cellulose and Its Effect on Soil Deposition[1]

Beverly J. Rutkowski and Albert R. Martin

Whirlpool Corporation Research Laboratories, St. Joseph, Michigan

Abstract

This study was undertaken to define the role of polyphosphate builders in detergent systems. Radiochemical methods were employed to trace polyphosphate and calcium reactions with cotton at various calcium to polyphosphate ratios. Cotton does not adsorb polyphosphate in the absence of polyvalent metal ions. The amount of calcium and polyphosphate adsorbed by, or deposited on, cotton during a 10-min. wash in hard water is dependent on the calcium–polyphosphate phase present. A heterogeneous (precipitate) phase results in considerable deposition of a calcium-polyphosphate salt, while little deposition or adsorption occurs in a homogeneous (solution) phase. Deposition of clay soil onto cotton is not influenced by the presence of insoluble calcium-polyphosphate salts. However, there appears to be a direct relationship between soil deposition and number of unsequestered or unprecipitated calcium ions remaining in the wash solution. Tetrasodium pyrophosphate is relatively more efficient in achieving minimum soil deposition than sodium tripolyphosphate.

Introduction

Detergent chemists and applicance manufacturers have realized for years that soil removal, soil redeposition, and other parameters of washing are greatly affected by water hardness. Historically, numerous methods for overcoming water hardness in

[1] Presented at the 138th National Meeting of the American Chemical Society, New York, New York, September 1960.

washing have been devised. Examples of these methods are the use of rain water for washing, the use of soda ash or potash, and excessive use of soaps. More recently, the ion exchange water softener for home use has been introduced.

During the 1930's, synthetic detergents began to replace soap in the home washer. Hard water was the major cause of this replacement. Early experience with synthetic detergents showed the necessity of adding builders to the formulation to achieve detergency equal to that of soap. Polyphosphates were among the first builders employed.

Several studies [1, 4, 6] have been made in the past on the role of polyphosphate builders in detergency. These investigations outlined the extent to which polyphosphates affect adsorption of surface active agents on cotton and on soil, but failed to establish a definite relationship between this adsorption and detergency. Other investigations [3] have shown that addition of polyphosphates to anionic detergents reduces surface and interfacial tensions and increases wetting speed. Both are important factors in detergency. Addition of polyphosphates to nonionic detergents does not show these specific effects. Detergency is improved in spite of this. Therefore, the importance of polyphosphates as detergent builders seems to lie in their abilities as sequestrants and in their influence on electrokinetic phenomena occurring in the washing process. The present study was initiated to study these properties of polyphosphate builders.

The method employed for this work was the simultaneous tracing by radiochemical means of two of the more widely used polyphosphates, sodium tripolyphosphate and tetrasodium pyrophosphate, and the divalent calcium cation in various washing systems. Cotton fabric and a particulate soil were included in the systems studied. The dynamic nature of the wash systems investigated made the concurrent use of two isotopes necessary. If the path of the polyphosphates and calcium had been individually traced, only descriptive results would have been obtained under such nonequilibrated conditions.

Materials and Reagents

Preparations of Labeled Sodium Tripolyphosphate

Sodium tripolyphosphate hexahydrate, tagged with radioactive P^{32}, was synthesized in the following manner. Approximately 10 ml. of an aqueous solution containing 0.0025 moles of sodium dihydrogen phosphate and 2.5 mC of P^{32} as $[P^{32}O_4]^{=}$ was mixed for 30 min. The resulting tagged monosodium salt was recrystallized with ethanol, filtered, and dried at 105° C. to a constant weight. Disodium hydrogen phosphate, sufficient to make a 1:2 mole ratio with the tagged monosodium salt, was weighed out. The two salts were then ground until an intimate mixture was obtained. This mixture was transferred to a platinum dish and fired at 540° to 580° C. for 2 hr. After cooling, the product was dissolved in de-ionized water, filtered, recrystallized with ethanol, and air dried.

Chemical and radiochemical yields were 88% and 80.7%, respectively. Infrared analysis showed the product to be sodium tripolyphosphate hexahydrate of high purity. The specific activity of the pure radioactive product was 2 mC/g.

Preparation of Labeled Tetrasodium Pyrophosphate

Anhydrous tetrasodium pyrophosphate, also tagged with radioactive P^{32}, was synthesized using the following procedure. Approximately 10 ml. of an aqueous solution containing 0.01 moles of disodium hydrogen phosphate and 2.5 mC of P^{32} in the form of $[P^{32}O_4]^{=}$ was mixed for 30 min. The tagged disodium salt was recrystallized with ethanol, filtered, and dried to a constant weight. The salt was then fired in a platinum dish for 2 hr. at 625° C. The product was dissolved in de-ionized water, filtered, recrystallized with ethanol, and dried at 105° C. Chemical and radiochemical yields were 87% and 79%, respectively. Infrared analysis established the high purity of the product. The specific activity of the pure radioactive tetrasodium pyrophosphate was 2 mC/g.

Preparation of Labeled Hard Water

The naturally occurring hardness ions of tap water were tagged by the addition of 0.05 mC of radioactive Ca^{45} per liter of water. The total hardness of the water thus obtained was 157.7 parts per million calculated as $CaCO_3$.

Cotton Fabric

Bleached, desized, white cotton fabric, 92 × 80 thread count, 3 oz./yd.^{2} (obtained from the North Carolina Finishing Company, Salisbury, North Carolina) was cut into 4 × 4-in. swatches. Unless otherwise indicated, the cotton was used as received.

TABLE I. Adsorption of Calcium Ions of Hard Water on Cotton

Wash No.	Calcium adsorbed/g. cotton, millimoles × 10^3	
	Acid-treated cotton	Normal cotton
1	7.07	5.75
2	7.00	5.73
3	6.83	5.80
4	6.94	5.75
5	6.85	5.82

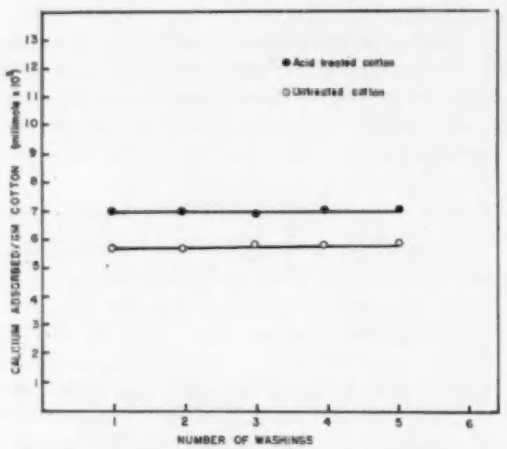

Fig. 1. Comparison of the adsorption of calcium on untreated and acid-treated cotton fabric during repeated washings in hard water.

Soil

A kaolinite type clay (Spink's Bandy Black, obtained from Spinks Clay Company, Paris, Tennessee) was used as a "soil." The choice of a clay soil for this work was based on the investigation of Powe [7], who showed by electron micrographs that the major component of redeposited soil is clay. Spink's Bandy Black is a representative clay and is dark enough to be measurable on cotton by optical means.

Procedures

In order to obtain data of a practical nature, the adsorption characteristics of cotton fabric for polyphosphates and polyvalent metal ions were determined using a Terg-O-Tometer [2] under conditions simulating home laundering. The procedure followed for each adsorption test was as follows. The wash solution was prepared and sampled for radiometric analysis. Ten swatches, weighing together *ca.* 10 g., were then added to 250 ml. of the wash solution and agitated for 10 min. at a rate of 68 strokes/min. The temperature was maintained at 125° F. After the wash period, the swatches were passed through a wringer between white blotting paper, reweighed in a tared, glass-stoppered weighing bottle, and dried at 140° F. for 30 min. The spent wash solution was sampled for radiometric analysis. The radioactivity of the swatches and solutions was determined using proportional counting equipment with a gas-flow detector tube.

For those adsorption procedures which utilized both P^{32}-tagged polyphosphate and Ca^{45}-tagged hard water, it was necessary to apply a radiometric adsorption counting technique. The different maximum energies of the beta particles emitted by P^{32} (1.7 mev.) and Ca^{45} (0.25 mev.) permitted the separation and quantitative determination of the two isotopes when they occurred in the same sample. By interposing an absorber of a density of approximately 68 mg./cm.^{3} between the sample to be counted and the window of the gas-flow counter tube, all the Ca^{45} radiations were blocked out. A definite percent of the more energetic P^{32} radiations penetrated this absorber and were counted. By subtracting the count due to P^{32} from the count obtained with no absorber present, the count due to Ca^{45} was obtained. Calculation of the total amount of polyphosphate and/or calcium retained on the cotton swatches was based on the counting rate of the original wash solution and the average count obtained from the ten dried swatches. The polyphosphate and/or calcium retained in the form of dried residual wash solution was calculated from the counting rate of the spent wash solution and the volume of this solution retained by the swatches. This material present as dried residual wash solution was then subtracted from the total material retained and the difference reported as the amount actually adsorbed on the swatches. When this method was used to calculate test results, the precision of the figure reported was not affected when the difference in counting rates between original and spent wash solutions was small.

In those procedures which included soil in the wash solution, the amount of soil deposited on the fabric was reported in terms of reflectance. Reflectance readings were made on a Gardner Color Difference Meter and reported as the Rd. From these values

[2] Manufactured by United States Testing Company, Hoboken, New Jersey.

the more useful "K/S function" was calculated by the Kubelka–Munk equation [5].

Results and Discussion

The adsorption of calcium from hard water was determined. Untreated cotton swatches and cotton swatches that had been treated in 0.1 *N* HCl and thoroughly rinsed were washed five times in Ca^{45}-tagged hard water. The amount of calcium adsorbed on the cotton during each wash is shown in Table I and Figure 1. Acid-treated cotton, because it is free of naturally occurring cations, has a higher adsorption capacity for calcium than has untreated cotton. It is apparent that in the absence of soil or detergent, maximum calcium adsorption occurred during the cotton's first exposure to hard water. Repeated washings in hard water showed no build-up of calcium on the fabric. These results are typical for an ion-exchange reaction rather than for some other type of adsorption process.

The results of introducing various concentrations of sodium tripolyphosphate, the most widely used detergent builder, to a hard-water system of constant calcium content, are shown in Table II and Figure 2. The data presented in Table II show that the retention on cotton of calcium and tripolyphosphate from hard water containing various tripolyphosphate concentrations is dependent on the calcium–tripolyphosphate phase present. Quimby [8] has shown that in the range 20:1 to 1:1 calcium to tripolyphosphate mole ratios an insoluble calcium-tripolyphosphate salt is formed. The hard water used in these tests contained 1.58 millimoles of calcium per liter; therefore, at tripolyphosphate concentrations of 0.08 to at least 1.58 millimoles/liter, deposition of an insoluble calcium-tripolyphosphate salt occurred as well as the adsorption of calcium by ion exchange. Figure 2 shows that maximum deposition of calcium and tripolyphosphate occurred at a tripolyphosphate concentration of 0.68 millimoles/liter. When the tripolyphosphate content exceeded this concentration, sequestration of calcium began; thus, deposition of the insoluble salt decreased. This point of maximum retention was at a calcium to tripolyphosphate mole ratio of 2.3:1. A trial experiment showed that cotton does not adsorb tripolyphosphate in the absence of polyvalent metal ions. Therefore, the tripolyphosphate picked up by the cotton from hard water must be in the form of an insoluble calcium salt. From this, and the knowledge of the calcium–tripolyphosphate mole ratio at which maximum retention occurs, it can be deduced that the probable composi-

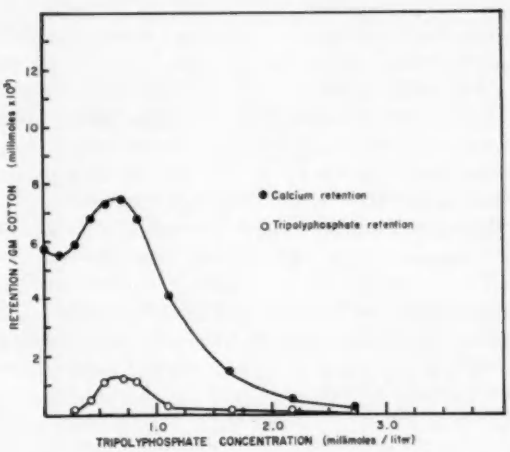

Fig. 2. Effect of increasing tripolyphosphate concentration in hard water on the retention of calcium and tripolyphosphate on cotton fabric.

TABLE II. Retention of Tripolyphosphate (TPP) and Calcium on Cotton

TPP concentration		TPP retained/g. cotton, millimoles × 10^3	Ca retained/g. cotton, millimoles × 10^3
Millimoles/l.	Percent		
0	0	0	5.78
0.136	0.005	0.060	5.50
0.272	0.01	0.146	5.95
0.408	0.015	0.437	6.8
0.54	0.02	1.07	7.37
0.68	0.025	1.19	7.50
0.82	0.03	1.08	6.84
1.09	0.04	0.209	4.12
1.63	0.06	0.087	1.50
2.17	0.08	0.106	0.52
2.72	0.1	0	0.20

TABLE III. Retention of Tripolyphosphate, Calcium, and Soil on Cotton

TPP concentration		TPP retained/g. cotton, millimoles × 10^3	Ca retained/g. cotton, millimoles × 10^3	Soil retained	
Millimoles/l.	Percent			Rd	K/S
0	0	0	6.60	76.8	0.035
0.136	0.005	0.125	6.30	76.7	0.035
0.272	0.01	0.252	6.70	76.5	0.036
0.408	0.015	0.674	6.95	78.5	0.029
0.54	0.02	1.09	8.41	78.4	0.030
0.68	0.025	1.11	8.45	79.5	0.027
0.82	0.03	1.07	7.80	80.7	0.023
1.09	0.04	0.258	5.55	82.8	0.018
1.63	0.06	0	3.28	84.1	0.015
2.17	0.08	0	1.37	83.0	0.017
2.72	0.10	0	0.83	83.8	0.016

tion of the calcium-tripolyphosphate salt deposited on the cotton was $Ca_5(P_3O_{10})_2$.

Table III and Figure 3, illustrate the effect of calcium–tripolyphosphate systems on deposition of a clay soil onto cotton. Increased tripolyphosphate concentration resulted in decreased clay deposition even at concentrations where retention of an insoluble calcium-tripolyphosphate salt was appreciable. Minimum soil deposition was reached at that tripolyphosphate concentration (a 1:1 calcium to tripolyphosphate mole ratio) which completely sequestered the calcium of the hard water. Therefore, clay deposition appears to be directly related to the calcium ion concentration of hard water. This theory was substantiated by showing that clay deposition is directly related to calcium adsorption on cotton, which, in turn, is dependent on the calcium ion concentration of hard water. The amount of calcium adsorbed on the cotton, as differentiated from that deposited as an insoluble salt, was calculated by assuming all tripolyphosphate detected on the fabric to be in the form of $Ca_5(P_3O_{10})_2$. Thus, adsorbed calcium equals total calcium less 2.5 times the amount of tripolyphosphate on the cotton. Figure 4, based on the results of this calculation, illustrates the direct relationship between calcium adsorption and clay deposition. It may be noted that at increasing tripolyphosphate concentrations calcium adsorption decreases at a slower rate than clay deposition. Since clay, as well as cotton, exhibits ion exchange properties, this apparent excess of calcium is probably due to the presence of calcium-bearing clay.

Tetrasodium pyrophosphate is the second most widely used polyphosphate builder in detergent formulations. For this reason a study, analogous to that with sodium tripolyphosphate, was carried out using this builder.

Table IV and Figure 5 show the reactions of

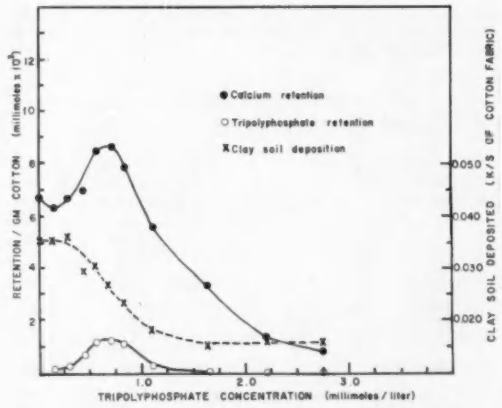
Calcium retention
Tripolyphosphate retention
Clay soil deposition
RETENTION / GM COTTON (millimoles x 10³)
CLAY SOIL DEPOSITED (K/S OF COTTON FABRIC)
TRIPOLYPHOSPHATE CONCENTRATION (millimoles / liter)

Fig. 3. Relation between soil deposition and the retention of calcium and tripolyphosphate on cotton.

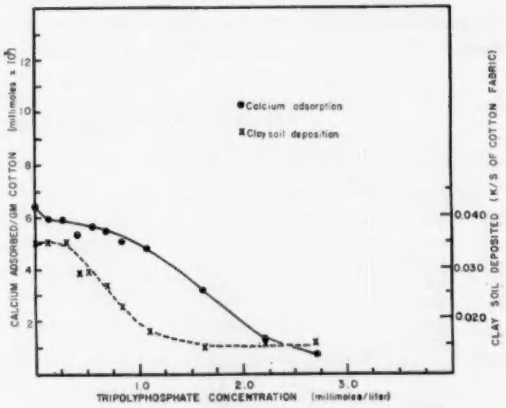
Calcium adsorption
Clay soil deposition
CALCIUM ADSORBED/GM COTTON (millimoles x 10³)
CLAY SOIL DEPOSITED (K/S OF COTTON FABRIC)
TRIPOLYPHOSPHATE CONCENTRATION (millimoles/liter)

Fig. 4. Relation between calcium adsorption and soil deposition on cotton.

pyrophosphate in hard water. As was the case with tripolyphosphate, a heterogeneous phase resulted in considerable deposition of an insoluble calcium salt on the fabric. According to Diamond [2], the phase boundary of a calcium–pyrophosphate system at the temperature of this study should occur at a calcium to pyrophosphate mole ratio of 1:1.3. Figure 5 shows that there are two such boundaries. The first occurs at a pyrophosphate concentration of 1 millimole/liter, which is a calcium to pyrophosphate mole ratio of 1:0.63. The second boundary falls at a pyrophosphate concentration between 2 and 2.5 millimoles/liter. This latter region corresponds to calcium: pyrophosphate mole ratios of 1:1.26 to 1:1.58. The existence of two distinct boundaries indicates the formation of more than one species of insoluble calcium-pyrophosphate salt.

The effect of calcium–pyrophosphate reactions on clay deposition is shown in Table V and Figure 6. Here again, the results are similar to those of procedures using tripolyphosphate. Clay deposition was not influenced by the presence of considerable amounts of precipitated calcium-pyrophosphate salts. The formation of more than one calcium salt made it impossible to differentiate between adsorbed calcium and deposited calcium-pyrophosphate. Therefore, no definite relationship could be established between the amounts of calcium adsorbed and clay deposited on cotton fabric. However, it appears that the amount of unsequestered or unprecipitated calcium remaining in solution governed the amount of clay deposited.

The relative efficiencies of tripolyphosphate and pyrophosphate in preventing clay deposition are illustrated in Figure 7. Pyrophosphate attains minimum deposition at a concentration of approximately 0.025%. This is only one-half the amount of tripolyphosphate required to achieve the same results.

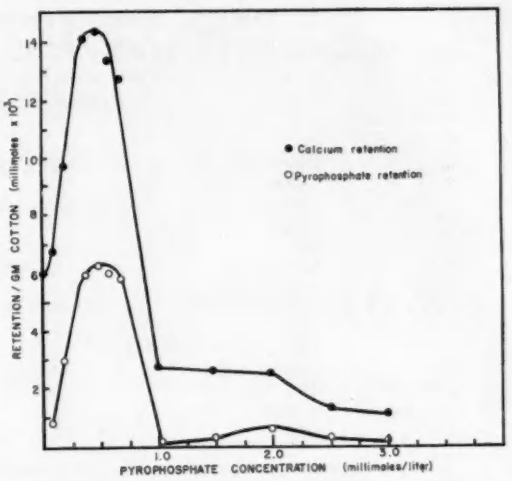

Fig. 5. Effect of increasing pyrophosphate concentration in hard water on the retention of calcium and pyrophosphate on cotton.

Conclusions

In the absence of detergent and soil, calcium adsorption on cotton from hard water results from an ion-exchange type of reaction.

The retention of the polyphosphates, sodium tripolyphosphate and tetrasodium pyrophosphate, on cotton is dependent on the presence of polyvalent metal ions. Within the limits of certain calcium to polyphosphate mole ratios, precipitation of insoluble calcium-polyphosphate salt occurs. This insoluble salt is readily deposited on cotton fabric from a wash solution.

The deposition of a clay soil onto cotton is not

TABLE IV. Retention of Tetrasodium Pyrophosphate (TSPP) and Calcium on Cotton

TSPP concentration		TSPP retained/g. cotton, millimoles × 10^3	Ca retained/g. cotton, millimoles × 10^3
Millimoles/l.	Percent		
0	0	0	5.78
0.1	0.0027	0.88	6.87
0.2	0.0053	3.04	9.83
0.4	0.011	6.03	14.20
0.5	0.0133	6.30	14.40
0.6	0.016	6.06	13.50
0.7	0.019	5.85	12.90
1.0	0.027	0.075	2.76
1.5	0.04	0.34	2.70
2.0	0.053	0.65	2.52
2.5	0.066	0.30	1.32
3.0	0.08	0.28	1.05

TABLE V. Retention of Pyrophosphate, Calcium, and Soil on Cotton

TSPP concentration		TSPP retained/g. cotton, millimoles × 10^3	Ca retained/g. cotton, millimoles × 10^3	Soil retained	
Millimoles/l.	Percent			Rd	K/S
0	0	0	6.6	76.8	0.035
0.1	0.0027	0.94	7.27	77.0	0.034
0.2	0.0053	2.78	10.3	77.1	0.034
0.4	0.011	4.47	12.5	79.2	0.027
0.5	0.013	5.69	13.6	79.6	0.026
0.6	0.016	5.26	12.1	80.7	0.023
0.7	0.019	4.28	10.5	81.8	0.020
0.8	0.021	3.32	9.53	83.2	0.017
1.0	0.027	0.109	3.33	84.3	0.015
1.5	0.04	0.450	3.13	83.8	0.016
1.75	0.047	0.792	3.52	83.2	0.017
2.0	0.053	0.544	2.64	83.8	0.016
2.25	0.06	0.062	1.64	83.6	0.016
2.5	0.066	0.262	1.43	83.0	0.017
3.0	0.08	0.182	1.05	83.0	0.017

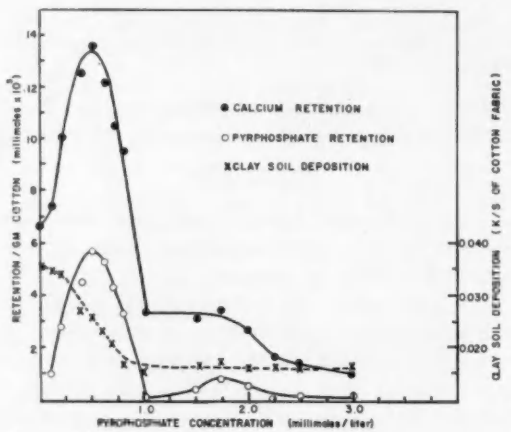
CALCIUM RETENTION
PYRPHOSPHATE RETENTION
CLAY SOIL DEPOSITION
RETENTION / GM COTTON (millimoles x 10³)
CLAY SOIL DEPOSITION (K/S OF COTTON FABRIC)
PYROPHOSPHATE CONCENTRATION (millimoles / liter)

Fig. 6. Relation between soil deposition and retention of calcium and pyrophosphate on cotton.

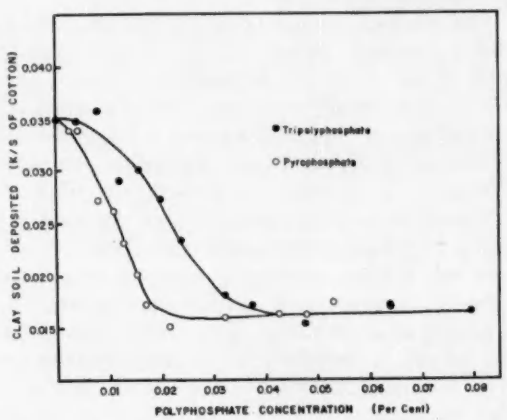

Fig. 7. Comparison of the relative efficiency of tripolyphosphate and pyrophosphate in prevention of soil deposition.

influenced by the presence of calcium-polyphosphate precipitates. The presence of unsequestered or unprecipitated polyvalent metal ions in a wash solution, or bound to the cotton, is of main concern in relation to clay deposition.

Tetrasodium pyrophosphate is more efficient than sodium tripolyphosphate in preventing clay deposition onto cotton fabric.

Literature Cited

1. Boyd, T. F. and Bernstein, R., *J. Am. Oil Chemists' Soc.* **33**, 614–619 (1956).
2. Diamond, W. J., *J. Phys. Chem.* **63**, 123–124 (1959).
3. Harris, J. C., *Am. Dyestuff Reptr.* **37**, 266–270 (1948).
4. Jason, G. G., *J. Appl. Chem.* **9**, 429–435 (1959).
5. Judd, D. B., "Color in Business, Science and Industry," New York, John Wiley and Sons, 1952, pp. 314–317.
6. Meader, A. L. and Fries, B. A., *Ind. Eng. Chem.* **44**, 1636–1648 (1952).
7. Powe, W. C., TEXTILE RESEARCH JOURNAL **29**, 879–884 (1959).
8. Quimby, O. T., *J. Phys. Chem.* **58**, 603 (1954).

Manuscript received March 20, 1961.

Physical Properties of Wool Fibers at Various Regains

Part III: Study of the State of Water in Wool by N.M.R. Techniques

G. W. West

Division of Tribophysics, C.S.I.R.O., University of Melbourne, Parkville, Victoria, Australia

A. R. Haly and M. Feughelman

Division of Textile Physics, C.S.I.R.O. Wool Research Laboratories, Ryde, N.S.W., Australia

Abstract

Both direct absorption curves and derivative curves due to proton magnetic resonance absorption in wool have been obtained. Peak heights and widths of the absorption lines were measured for wool samples equilibrated at a number of relative humidities in the range 0 to 90%. All water protons in wool appear to be less firmly bound than the keratin protons, but less mobile than liquid water. It seems clear that an increment of absorbed water changes the binding energies of previously absorbed water. No evidence was obtained of a subdivision of water in wool into two or three fractions with different binding energies which are *successively* bound as the equilibrium regain is increased.

Introduction

The effects of absorbed water on wool are so important and so general that in practically no department of wool science is it permissible to neglect the state of hydration of the material.

It has been shown that nuclear magnetic resonance (n.m.r.) techniques can be applied to the determination of the nature and amount of water in a wide range of materials [10, 11, 12]. A recent publication by Shaw, Elsken, and Lundin [13] deals with some aspects of the wool–water complex. Basically the method relies on the fact that the absorption line from protons of the absorbed water is narrower than that from protons of the wool keratin, and by suitable arrangement of the experimental conditions the lines can be effectively separated.

The techniques used to obtain information about the resonance absorption fall into two general classes. In the first case the magnetic field is varied linearly with time over a range greater than the line width, and the output from the detecting apparatus is proportional to the absorption. Figure 1a shows the shape of the line obtained from material such as wool. The narrow central line is due to the absorbed water, and this is superimposed on the very broad line due to the protein. The broad line is usually so small in amplitude that it becomes indistinguishable from the

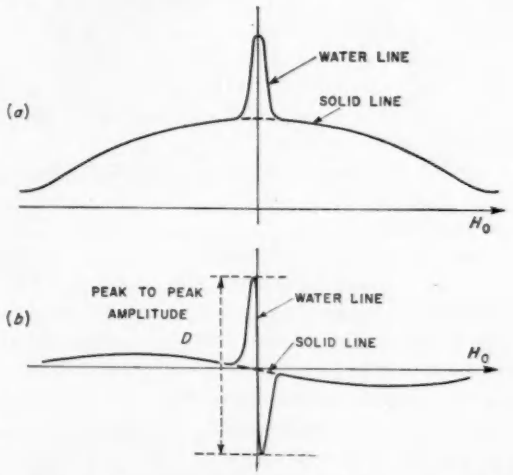

Fig. 1. (a) An example of the type of n.m.r. absorption line obtained from hydrated materials like wool by linearly changing the magnetic field (see Pople, Schneider, and Bernstein [9]). (b) The derivative curve obtained, using the same material, by sinusoidal modulation of the magnetic field.

general noise in the apparatus, and only the sharp, narrow line is obtained.

In the second method the magnetic field is varied sinusoidally over a range which is small compared with the line width, while the frequency (or magnetic field) is varied linearly to sweep through the absorption band. The output is then a close approximation to the first derivative of the absorption line (Figure 1b). To obtain an adequate signal from the broad line, the modulation must be so large that it causes distortion of the narrow line. Hence it is necessary to use different values of modulation depending on which line is being studied. When the modulation is reduced to a very low value (a small fraction of the width of the narrow line) no effective signal is obtained from the absorbent so that the curve obtained is essentially that from the absorbed water.

Experimental

Resonance Conditions

In the present work both methods of detection were used. To obtain the absorption signal directly, a radio-frequency bridge circuit (Anderson [1]) was used at 30.5 Mc./sec. and the absorption line displayed on a cathode ray oscilloscope. A permanent record was obtained by photographing the oscilloscope screen. The magnetic field was increased linearly over a range of 0.85 gauss at a rate of 2 gauss/sec., and the radio-frequency field within the specimen was approximately 0.01 gauss to minimize the effects of saturation. For each line, the peak height and the line width ($\delta H'$) at half the maximum amplitude were measured.

A Pound–Knight–Watkins Spectrometer operating at 17.1 Mc./sec. was used to obtain the derivative curves. The magnetic field was modulated sinusoidally at a frequency of either 50 c./sec. or 280 c./sec. For most of the water lines in wool, the modulation amplitude was 20 milligauss peak-to-peak, but for some specimens with low water content the value was increased to 200 milligauss; this was still low relative to the line width. To obtain the protein line in the case of dry wool the modulation was 1 gauss. The radio-frequency field was approximately 0.02 gauss. For each derivative curve the peak-to-peak height was measured, as was the line width (δH) between peaks on the derivative curve. The specimen coils for both types of test were approximately 7 mm. inside diameter and 6 mm. long.

TABLE I

Sample	Concentration of solution	RH, percent
1	—	~0
2	Sat. $ZnCl_2$ in H_2O	10
3	92% by wt. glycerol-water	25
4	84% by wt. glycerol-water	40
5	78.5% by wt. glycerol-water	50
6	72.3% by wt. glycerol-water	60
7	63% by wt. glycerol-water	70
8	52% by wt. glycerol-water	80
9	35% by wt. glycerol-water	90
10	Sat. K_2CO_3 in D_2O	~44

All the experiments were done in a magnetic field provided by a Varian 12-in. electromagnet. To measure the variation of magnetic field throughout the specimen volume, a similar volume of distilled water was placed in the specimen coil. The width of this proton resonance line is due almost entirely to the variation of magnetic field. In the present case the line width ($\delta H'$) at one-half the maximum height was 18 milligauss.

Preparation of Wool Samples

Ten wool samples were prepared. Each sample contained 0.13 g. of dry wool, and each was packed loosely in a glass tube of 4.7 mm. internal diameter. Each was then placed in a separate vessel in which the required relative humidity was maintained. The samples were allowed to condition for 6 weeks; then the wool was compressed into the bottom of the tubes so that it occupied a length of 15 mm. and the tubes replaced to condition for a further 5 weeks. At the end of this time the tubes were rapidly sealed off. Samples 3 to 9 were conditioned over aqueous glycerol solutions, the data for the RH over the solutions being obtained from the values published by Hermans [4]. Analytical reagent glycerol was used. Sample 1 was dried over silica gel in the same way. To obtain 10% RH, a saturated solution of zinc chloride was used [8]. Sample 10 was conditioned as above over a saturated solution of potassium carbonate (~44% RH) made up using anhydrous salt and deuterium oxide. Table I shows the concentrations and relative humidities employed.

The temperature of conditioning was 20° ± 1° C. and the wool used was from a pen-fed Corriedale sheep.

Since the average weight per unit length was constant for all specimens it was assumed that equal amounts of wool were within the specimen coils.

Results

Absorption by Protons of both Keratin and Water

Derivative lines were obtained from all specimens using 280 c./sec. modulation with an amplitude of 1 gauss peak-to-peak. The nominally dry specimen (No. 1) gave a curve which indicated the presence of a small amount of water. This is to be expected, for Watt (private communication) has shown that complete dehydration is not achieved by desiccation at room temperature and pressure. The line width (δH) for the protein alone was 8.8 gauss, and for the water approximately 1 gauss. The regain was probably in the vicinity of 1–2%. This result shows that the protons of even the very firmly bound water are more mobile than the protons of the keratin.

For Samples 4 to 9 the lines from the absorbed water were large enough to cause serious distortion of the protein line, and no separation of the two lines was attempted. However, Samples 2 and 3 gave water lines which were small enough to allow each composite derivative curve to be approximately separated into its two components. In order to obtain an estimate of the proportion of water contributing to each narrow line for Samples 2 and 3, the integrated intensity (i.e., the area under the absorption curve) of each component was determined by numerical integration. If we assume that saturation effects are negligible (or the same for both protein and absorbed water) these intensities should be proportional to the number of protons contributing to each component. For each of Samples 2 and 3 the ratio *keratin protons*:*water protons* was measured in this way. The values were 16 and 6 respectively. The same ratio was calculated using values of 4.5% and 7.5% for the regains of the samples, and 4×10^{24} for the number of protons in 100 g. of wool. The corresponding results were 13 and 8. Thus the indication is that a large proportion of the water in each case is contributing to the narrow line, and it seems reasonable to assume that all the water is so contributing. This is consistent with the observation that, in the curves under discussion, the line width in its broadest condition is approximately 1 gauss; as noted by Shaw et al. [13] it can be deduced that there must always be some sort of relative motion between the resonating water nuclei.

The integrated intensity of the proton line for Sample 10 was lower by 10–20% than that for the nominally dry Sample 1. If all normal D–H exchange had taken place the reduction would be approximately 20%. This value was calculated using the data of Burley et al. [2] and the above number of protons in 100 g. of wool. The line after exchange is somewhat narrowed, indicating that the protons which exchange were contributing to the outer edge of the keratin line.

Experiments in Which Only Water Protons Contribute to Absorption

In addition to reducing the modulation to a minimum of 20 milligauss peak-to-peak, the frequency was reduced to 50 c./sec. to minimize distortion of the narrow line.

Some derivative curves obtained at various RH's are shown in Figure 2, while Figure 3 presents a number of absorption curves obtained using the bridge technique. Line widths taken from these and the other curves are plotted against RH in Figure 4. The ratio of line width $\delta H'/\delta H$ changes from 1.7 at 90% RH to 1.4 at 50% RH. It can be shown that the ratio should be $\sqrt{3}$ for a Lorentzian line shape and approximately 1.2 for a Gaussian line shape, thus there is a gradual change from a Lorentz curve shape as the water content decreases. Figure 4 also shows how the peak-to-peak height of the derivative curves changes with RH. It will be seen that there is an abrupt change of slope of this plot in the range 60–70% RH; the peak heights obtained using the bridge technique showed a similar change of slope. When, however, the peak heights are plotted against regain as in Figure 5 the abrupt change is no longer apparent, though the maximum slope is reached in the same RH range. Regain–RH data published by Cassie [3] were used to obtain regains corresponding to the known RH's.

Discussion

We have seen that all water protons in wool appear to be more mobile than the keratin protons. At the same time it must be noted that line width (at half peak height on the absorption curve) at 90% RH was 93 milligauss, while the line width for a water specimen of dimensions similar to the wool specimen was only 18 milligauss. Hence, as found by Shaw et al. [13], all sorbed water is much less mobile than liquid water.

A third interesting deduction can be made from the shape of the resonance absorption curves at various relative humidities. Figure 3 gives an indication

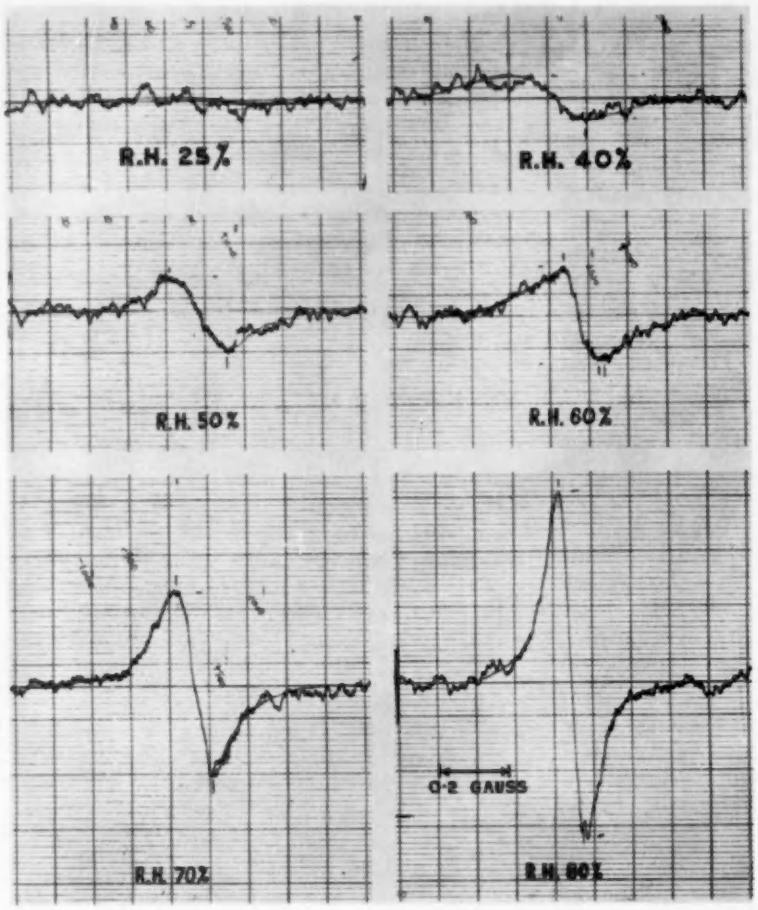

Fig. 2. Derivative curves due to the water in wool samples equilibrated at various relative humidities.

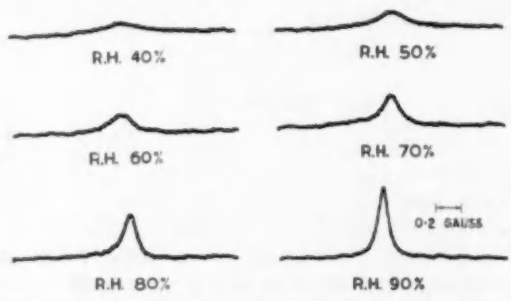

Fig. 3. Direct absorption curves due to the water in wool samples equilibrated at various relative humidities.

of a phenomenon frequently observed in this work, namely that the line width narrows with increasing water content of the samples: e.g., in Sample 9 none of the water is as firmly bound as at least some of the water in Sample 4. Hence, as would be expected, an increment of absorbed water leads to a change in binding of water already present. The change probably follows chiefly from interaction between water molecules, but there may be some effect due to the increasing freedom of polypeptide chains as the regain increases. It does not follow that we must abandon the idea that at any one regain there are various water fractions each with its own binding energy. It seems clear, however, that the ideal sorption postulated by both Cassie [3] and Windle [15] is an approximation. Here "ideal sorption" means that there is no interaction between the various water fractions.

Cassie's [3] analysis of the wool–water isotherm was based on the assumption that some of the absorbed water in wool is bound on localized sites, and

the remainder is analogous to liquid water. Windle [15] included a third water fraction to explain the dielectric behavior of the wool–water system [16, 17] and suggested that a greater number of fractions may exist. In the present work no evidence was found of a subdivision of water in wool into two or three fractions of different binding energies. However, the method would not detect such fractions unless they were successively absorbed. Morrison and Hanlan [7] have made such a proposal, concluding that in keratin the first molecular layer of absorbed water is completed at a molar regain (n) of 0.45–0.50, the second molecular layer at $n = 0.9$, and as n goes from 0.9 to saturation the absorbed water is mobile and with characteristics of a condensed film. If this view were rigorously true we should expect to see distinct regions in line width vs. regain curves and in peak height vs. regain curves.

Despite the evidence that Cassie's and Windle's analyses are simplified in some respects it appears that their results represent a reasonable approximation to the actual state of water in wool. In Figure 5 Cassie's quantities of "free" water are plotted against regain, and it will be seen that the curve shape, over a substantial regain range, is not very different from the shapes of the curves showing peak heights at various regains. A similar statement can be made about Windle's data if his values of mobile and intermediate water are summed ($W_s + W_m$) and plotted in the same way. Again, Haly and Feughelman [5] found a strong correlation between Cassie's "free" water data and the rates of recovery at various regains of cohesively set fibers. These rates are considered to be dependent on the breaking of hydrogen bonds and hence on the quantity of water and its mobility. Finally, King [6] explained the coefficients of diffusion of water in horn in terms of Cassie's model. There was evidence that the curve showing diffusion coefficients plotted against regain becomes concave to the regain axis at a regain of about 17%, and King suggested refinements to the theory to account for this. We must note, however, that both the curves showing the diffusion coefficients of wool obtained by Watt [14] become concave to the regain axis at approximately 10% regain and hence cannot be accounted for on the same simple theory.

Since peak heights are a function of both quantity and mobility of water, it may be worthwhile to define a mobility factor which is peak height per unit regain. The results are presented in this form in Table II.

These values show that at regains higher than 1.15 mole/100 g. wool (80% RH) the mobility

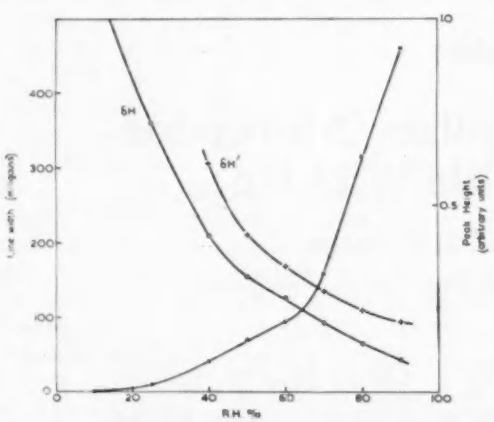

Fig. 4. Line widths of both derivative and absorption curves plotted against relative humidity. δH is width between peaks on derivative curve and $\delta H'$ is line width at half maximum height on absorption curve. Peak-to-peak heights of the derivative curves are also shown.

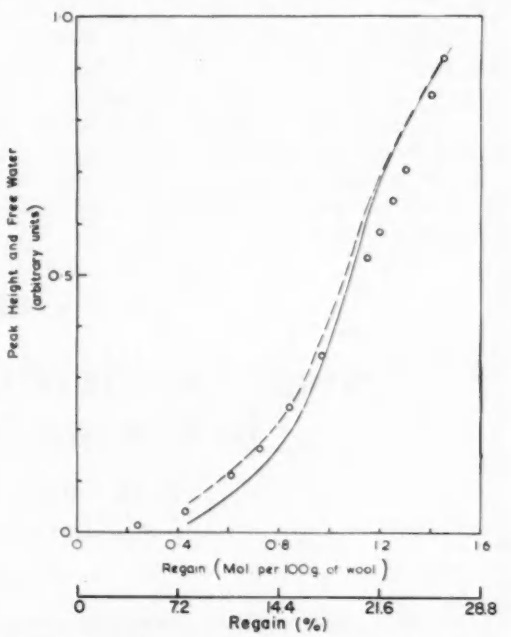

Fig. 5. Peak heights of both absorption and derivative curves plotted against wool regain. Also shown are the quantities of water analogous to liquid water given by Cassie's [3] analysis of the wool–water isotherm. All curves have been made to coincide at a regain of 1.45 mole per 100 g. of wool. ——— derivative; - - - absorption; o "free" water.

TABLE II. Mobility Factors (Peak Heights/Regain) for Both Absorption and Derivative Curves*

RH, %	Regain		Mobility factors	
	Mol./100 g.	Percent	Absorption curves	Derivative curves
90	1.45	26.1	63	63
80	1.15	20.7	56	55
70	0.97	17.5	38	33
60	0.84	15.1	28	23
50	0.72	13.0	26	19
40	0.61	11.0	18	13
25	0.43	7.7	—	4.7

* The regains at various RH's were deduced from data provided by Cassie [3]. Mobility factors are in arbitrary units.

factor increases very slowly with increase of regain and appears to be approaching a limit of about 66 (arbitrary units) at saturation regain.

Conclusions

1. At any regain above 1–2% all water protons in wool are more mobile than the keratin protons.

2. As found by Shaw et al. [13] all absorbed water is less mobile than liquid water.

3. Water fractions with a distinct difference in their binding energies (or their spectrum of binding energies) are not *successively* absorbed.

4. An increment of absorbed water changes the binding energies of previously absorbed water.

5. The mobility of water in wool increases only slowly with increase of equilibrium regain above a regain of 1.15 mole/100 g. (20.7%).

Literature Cited

1. Anderson, H. L., *Phys. Rev.* **76**, 1460 (1949).
2. Burley, R. W., Nicholls, C. K., and Speakman, J. B., *J. Textile Inst.* **46**, T427 (1955).
3. Cassie, A. B. D., *Trans. Faraday Soc.* **41**, 458 (1945).
4. Hermans, P. H., "Contribution to the Physics of Cellulose Fibres," New York, Elsevier Publishing Co., 1946, p. 27.
5. Haly, A. R. and Feughelman, M., TEXTILE RESEARCH JOURNAL **31**, 131–140 (1961).
6. King, G., *Trans. Faraday Soc.* **41**, 479 (1945).
7. Morrison, J. L., and Hanlan, J. F., "Proc. 2nd Int. Congress of Surface Activity: Solid/Gas Interface," London, Butterworth's, 1957, p. 322.
8. O'Brien, F. E. M., *J. Sci. Instr.* **25**, 73 (1948).
9. Pople, J. A., Schneider, W. G., and Bernstein, H. J., "High Resolution Nuclear Magnetic Resonance," New York, McGraw-Hill Book Co., 1959.
10. Shaw, T. M., and Elsken, R. H., *J. Chem. Phys.* **18**, 1113 (1950).
11. Shaw, T. M. and Elsken, R. H., *J. Appl. Phys.* **26**, 313 (1955).
12. Shaw, T. M., Elsken, R. H., and Kunsman, C. H., *J. Assoc. Offic. Agr. Chemists* **36**, 1070 (1953).
13. Shaw, T. M., Elsken, R. H., and Lundin, R. E., *J. Textile Inst.*, T562 (1960).
14. Watt, I. C., TEXTILE RESEARCH JOURNAL **30**, 644 (1960).
15. Windle, J. J., *J. Polymer. Sci.* **21**, 103 (1956).
16. Windle, J. J. and Shaw, T. M., *J. Chem. Phys.* **22**, 1752 (1954).
17. Windle, J. J. and Shaw, T. M., *J. Chem. Phys.* **25**, 435 (1956).

Manuscript received March 6, 1961.

Some Aspects of Capillary Absorption in Fibrous Textile Wicking

R. D. Laughlin and J. E. Davies

HRB-Singer Research Laboratories, State College, Pennsylvania

Abstract

An experimental study of the rate of capillary absorption in the porous media commonly called wicking has been made. Data are presented on rates of fluid rise in vertically suspended samples of cotton and felt wicking, along with mass absorption rates. Deviations from an assumed model of capillary flow are given. Techniques for finding the coefficients of an approximate flow equation and a method for calculating the amount of fluid absorbed as a function of wick length are presented.

Introduction

A number of earlier papers [3, 6, 8] have discussed the problems involved in measuring the rate of fluid absorption in capillary absorbing media. Some of these have considered absorption in textile assemblies such as yarn and cloth while others have considered single textile fibers.

In the study to be presented here, the fibrous material commonly designated as wicking (as used for the purpose of lubricating bearings, etc.) has been chosen. For purposes of comparison both felt (wool) and cotton wickings have been used, and the fluid used was a light grade of lubricating oil.

In general, two quantities that are related to flow in these materials were desired. These are the rate of rise or the rate of fluid advance along a dry wick, and the relative fluid–wick density as a function of wick height.

Single-Channel Capillary Flow

As a basis for calculation, the assumption was made that the mechanism for fluid flow into the porous medium was capillary in nature. If one further assumes that Poiseuille flow (i.e., isothermal streamline flow) dominates for these cases [1], the use of interfacial tension forces in the Poiseuille flow law yields for the rate of rise

$$dh/dt = 2R\gamma/8\eta h - R^2gd/8\eta \qquad (1)$$

The variable are: the fluid height h, the capillary radius R, the surface tension γ, the fluid density d, and g, the gravitation constant. This equation holds for the case of a vertical capillary tube where the displaced fluid is air (negligible viscosity), the displacing fluid has viscosity η, and the contact angle is zero.

It is clear that the complex of fibers that constitute wicking cannot be resolved into a simple model of straight capillaries of uniform cross section. A number of analyses using the concept of the hydraulic radius have been put forward [5], and good agreement with theory has resulted when the fiber arrangement is known to such an extent as to allow the calculation of such a parameter. In the cases quoted in this paper, one cannot calculate the hydraulic radius or the pore distribution function because of the nonuniformity of the fiber arrangement. It is of interest, however, to determine the deviation from "pure" capillary flow for several reasons. Such a deviation allows some basis for selecting, among wicking of the same structure, wicks of greater or lesser ability to transport fluid, and, second, it allows the calculation of the amount of fluid absorbed as a function of wicking length.

To determine the deviation from capillary flow (for the streamline flow case), the exact treatment for height as a function of time must be made. Let

$$\alpha = 2R\gamma/8\eta \text{ and } \beta = R^2gd/8\eta \qquad (2)$$

Using these definitions, Equation 1 becomes

$$dh/dt = \alpha/h - \beta \qquad (3)$$

Integration of this relation combined with the condition that h equals zero at time zero gives

$$\beta t = h_m \ln\left[\frac{h_m}{h_m - h}\right] - h \qquad (4)$$

In this equation h_m is the maximum height reached by the fluid in infinite time and is equal to α/β as shown by Washburn [7].

The curve in Figure 1 was calculated from Equation 4. All experimental data taken fitted this general form of curve.

In many reported experiments [4], the dominant term is of the form $h^2 = Ct$, where C is a constant. This relation should appear from the results of Equation 4. To show this, the term $\ln(1 - h/h_m)$ may be expanded in a series to give

$$\beta t = h^2/2h_m + h^3/3h_m^2 + h^4/4h_m^3 + \cdots \qquad (5)$$

Thus the leading term is of the form $h^2 = Ct$ where C is identified as $2h_m\beta$.

Analysis and Experiment

Since a number of experiments on textile materials and paper wicking have shown close adherence to a square law, it was hoped that the wicks to be tested would also follow this simple law. If this were so, some sort of "figure of merit" could be assigned since, if

$$h^2 = Ct \qquad (6)$$

then

$$dh/dt = \tfrac{1}{2}(C/t)^{\frac{1}{2}} \qquad (7)$$

Volume flow is related to rise rate by the relation

$$V = A(dh/dt) \approx C^{\frac{1}{2}} \qquad (8)$$

where A is the area available for flow. For a given wick structure, the greater the value of C, the greater

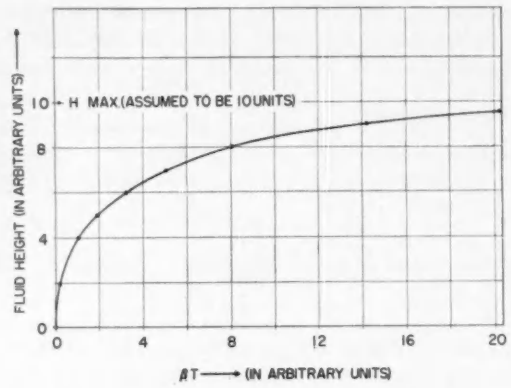

Fig. 1. Height vs. time curve for ideal capillary flow.

volume of fluid that will flow. This argument holds for the case of fluid flowing up a dry wick but not necessarily for an already saturated wick from whose surface fluid is being continually removed. A plot of h^2 vs. t for a wicking material that accurately follows Equation 6 will show a straight line whose slope is the constant C.

Experimental results using a radioisotope method [2] for tracing the moving wavefront are shown in Figure 2. The fluid used was a light lubricating oil (SAE 5 approx.) with the following physical properties: viscosity 100 SSU/100° F., surface tension 25–28 dynes/cm., and flash point 325° F. Examination of the h^2 vs. t curve for #5355 felt wicking shows an approximately straight line, but there is some curvature and therefore an accurate slope determination to obtain the value of C is not possible. Felt wicking #7546 also shows a curved line, so no value of C can be found. Conversely, cotton wick #147046 showed a quite good straight line agreement. These diverse results make it impossible to use this single simple constant as a "figure of merit" for a wick.

Since it was found that $h^2 = Ct$ does not hold in general, a modification of this law was made so that an approximate flow law could be formulated. The form chosen was

$$h = C't^k \tag{9}$$

Taking the logarithm of both sides of this equation gives

$$\ln(h) = k\ln(t) + \ln C' \tag{10}$$

This equation has the form of a straight line.

Experiments following the above analysis were carried out and such a power law was found to be valid for moderate values of time. These values varied from 30 min. to 5 hr. before another term in the series was necessary to correct for the curvature of the log-log plot. Because of the experimental uncertainty in the determination of the true position of the moving oil wavefront, a least-squares solution for the resulting straight line was made. A plot of $\ln(t)$ vs. $\ln(h)$ made prior to the computation of the least-squares solution shows in which region the solution is valid. A typical set of such curves is shown in Figure 3. These curves are seen to be substantially straight lines for times corresponding to 40 or 50 min. The rise-rate curves are easily obtained from the results obtained by the least-squares solution. As an example, the #16 bleached fluid wicking solution by least squares was

$$h = 1.8t^{0.44} \tag{11}$$

Differentiation of this yields

$$dh/dt = 0.79t^{-0.56} \tag{12}$$

A tabulation of the results obtained is given in Table I. The degree of deviation of the exponent from $\frac{1}{2}$ is an indication of the deviation from what may be termed "pure" capillary action.

It is easily shown that for a circular capillary tube, the fluid mass increase as a function of time should follow a power law having the same exponent as that found in the height vs. time relation. For the fibrous wicking tested, this relation has not been found valid and another approximate power law has been used. The form $m = Bt^l$ was tested and found satisfactory for this situation.

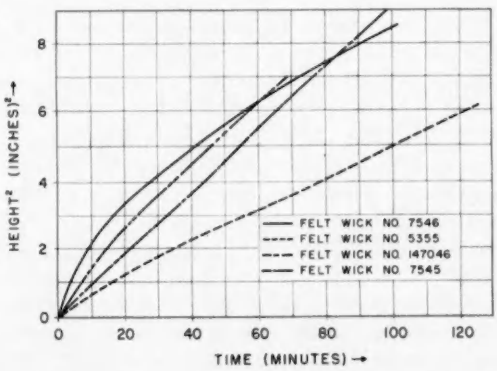

Fig. 2. Height squared vs. time for various wick samples.

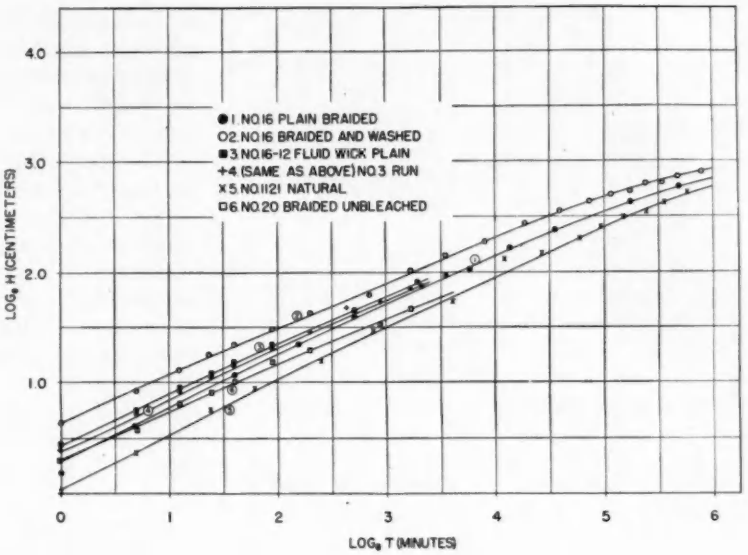

Fig. 3. ln(height) vs. ln(time) for various wick samples.

Distribution of Mass as a Function of Height

When a dry wick is suspended in a vertical position with its lower end immersed in fluid, the fluid rises in the wick. As was shown, the fluid reaches some ultimate height, h_m, which is determined by the balance between the upward forces of capillary action and the downward forces of gravity.

Visual observation of the surface of the wick shows that there is considerably more fluid located at the bottom of the wick near the source than at the top of the wick, which is almost dry. It is of interest to determine the distribution of fluid mass as a function of height of rise and to compare with experiment.

Consider two curves, one representing height as a function of time, and the other the mass of fluid absorbed as a function of time. From these curves one can get, for each value of dt, a differential increment in the mass absorbed in the time dt, and also the differential height increment. If it is assumed that there is no further net migration of oil out of the saturated (or partially saturated) volume with time after the moving wavefronts pass these differential volumes, a plot of height vs. mass using t parametrically can be made, or the approximate analytical expressions for h vs. t and m vs. t found previously may be used as follows. If

$$h = C't^k \quad \text{and} \quad m = Bt^l \tag{13}$$

and if the coefficients have been determined as described in the previous section, an analytical combination valid for a specific period of time can be made.

TABLE I. Approximate Power Law Followed by Various Wicks

Wick designation	Approximate power law, $h = C't^k$	Rise rate, cm./min.	Region (time) of validity, min.
#1121 Natural Pett	$1.07\ t^{0.47}$	$0.50\ t^{-0.53}$	40
#20 Unbleached cotton	$1.40\ t^{0.41}$	$0.57\ t^{-0.59}$	25*
#16 Bleached fluid	$1.78\ t^{0.44}$	$0.79\ t^{-0.56}$	31*
#20 Bleached	$1.8\ t^{0.42}$	$0.75\ t^{-0.58}$	19*
#7545 Felt wick	$1.48\ t^{0.44}$	$0.65\ t^{-0.56}$	23
#5355 Felt wick	$0.98\ t^{0.45}$	$0.44\ t^{-0.55}$	40
#1195 Wick	$0.99\ t^{0.45}$	$0.44\ t^{-0.55}$	19*
#147046 Cotton wick	$0.74\ t^{0.50}$	$0.37\ t^{-0.50}$	100

* Maximum test time; region of validity may be longer.

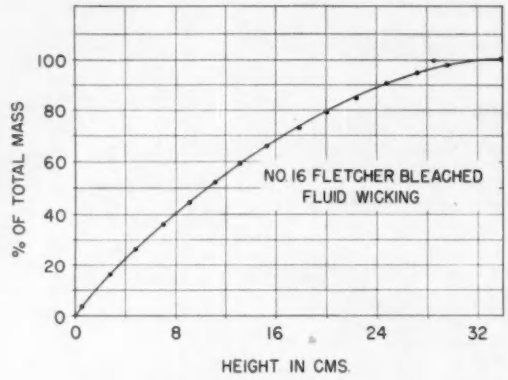

Fig. 4. Mass distribution vs. height for #16 Fletcher wicking.

Combining these two equations by eliminating the variable, time, yields

$$h = Dm^{k/l} \tag{14}$$

$$m = Eh^{l/k} \tag{15}$$

where E and D are constants.

In examining Equation 15 it is convenient to consider three cases, i.e., l/k less than, equal to, or greater than, unity. For the type of fluid imbibition considered in this paper, l/k can never be greater than unity since this gives a nonphysical case. It is expected from this that the values of the exponents in the approximate power law are such that $l/k \leqslant 1$. Experimentally, we find this to be true for all wicking tested.

In Equation 15, evaluation of the constant term E, from boundary conditions, shows that

$$m = m_m \left[\frac{h}{h_m} \right]^{l/k} \tag{16}$$

It is only a fair approximation to use the simplified equations to determine the mass distribution. The degree of approximation is dependent upon the material being tested, since some follow the simple power law for many hours and then deviate while others deviate after only a few hours of absorption. Experimentally, we have verified the relationship between m and h as shown in Equation 16 by the following method. A vertical wick was allowed to come to complete equilibrium over a period of several days and then 1-cm. lengths of the saturated wicking were carefully cut off in a sequential manner and weighed. The wicking was held during the imbibition phase by placing it on a brass rod of small diameter whose surface was covered with masking tape (sticky side out) and gently pressing the wicking against the tape. This provided a firm contact holding the wick in a vertical position and maintained a small contact area between wick and holder. Tension in the wick due to the extra weight of absorbed oil is also reduced.

The mass of oil per unit length was determined by weighing the samples on an analytical balance and subtracting the dry weight of the wicking. Figure 4 shows a plot of the data, obtained in the above manner, for a #16 Fletcher wicking. The abscissa is the height of the wicking, and the ordinate is the percentage of total mass of oil absorbed. The exponential dependence of this curve, predicted to be l/k from Equation 16, is found from the slope of the curve of $\ln(h)$ vs. $\ln(m)$. Experimentally, it was found that l/k was equal to 0.79; from theory, $l/k = 0.75$ (theory here meaning the particular analytical combination of experimental curves as previously determined). A second experiment on the same type of wick gave $l/k = 0.82$ by the segmentation method.

The exponent l in Equation 16 was measured by a weight-difference technique. In this method, oil

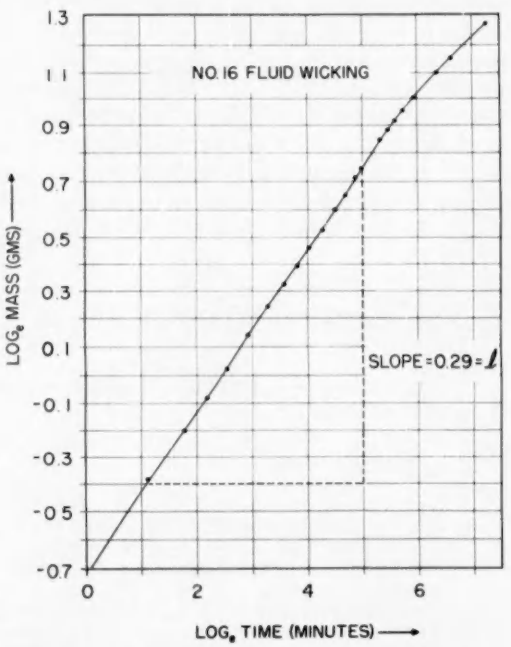

Fig. 5. Graphical determination of l for #16 Fluid wicking.

in a beaker was weighed prior to wick immersion and then, after a measured time of fluid imbibition by the wick, another weighing allowed the mass of fluid absorbed to be determined. Use of several containers of oil allowed uninterrupted measurements of mass as a function of time. The data were processed as described above and the slope of the $\ln(m)$ vs. $\ln(t)$ curve is the desired l value.

As pointed out before, it was assumed that there is no "filling in" of the fluid in the wick section after the moving oil front passes the particular height being investigated. Some redistribution of the oil in the wick has been noticed, and the moving front does not truly saturate the wick at the fluid–dry-wick interface. It is probably this effect that makes the ratio of l/k somewhat higher in the fully saturated wick than the value for this ratio as determined by the moving-wavefront method.

A second verification of this is given in Figure 5, which shows the determination of slope (i.e., the l value) from a $\ln(m)$ vs. $\ln(t)$ plot for a similar size wick of different material. A similar plot, Figure 6, shows the k value determination for the same wick. These two data yield an l/k value of 0.85. In this case, however, one must choose between the two slopes present in Figure 6. From time $t = 0$ to time $t = 26$ min. ($\ln(t) = 3.25$), the slope is such as to give an l/k ratio of 0.65, whereas from time $t = 26$ min. to time $t = 420$ min. the slope is such as to give a ratio of 0.85, as stated above. In such a situation, the slope that persists for the longer time has been chosen as the more important. One might wish to use an average of the two, and if this is done, the weighting should be in favor of the value leading to a greater l/k value.

Further verification was accomplished by making a vertical scan with an isotope wavefront-tracing device on a wick saturated with fluid in which a small amount of radioactive S^{35} was mixed. If the surface activity is taken as proportional to the oil density inside the wick, as seems reasonable, then a chart of activity vs. wick height is a measure of mass distribution. Such a chart was made for a #147046 wick, and the curve is in general agreement with the above theory.

Reproducibility of Results

It is known from the form of Equation 1 that the rise rate is in part determined by the ratio of γ/η, i.e., the ratio of interfacial tension to viscosity. Since

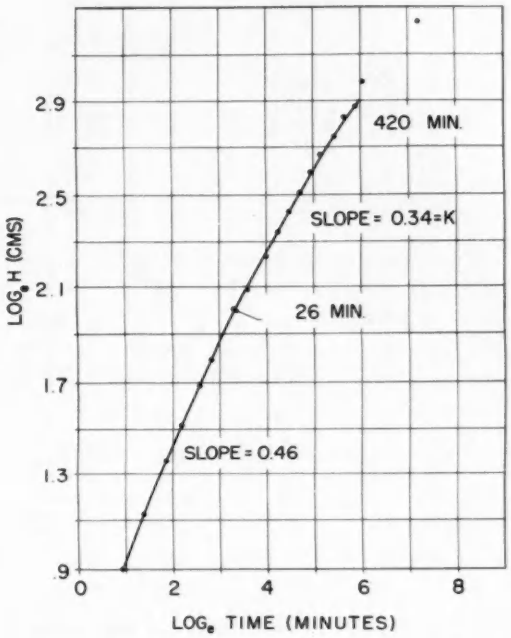

Fig. 6. Graphical determination of k for #16 Fluid wicking.

viscosity and interfacial tension are temperature dependent, rise rate is also. Other factors, such as variations in fiber spacing due to tension or twist in the wicking, can cause large variations in the parameters as measured. In the experiments reported, an attempt was made to control these factors as well as temperature and humidity.

To determine the variation in the results of h vs. t measurements among like samples, four separate wicks of $\frac{1}{2}$ m. length were tested simultaneously. For this test, a small amount of an oil-soluble red dye (Calco Chemical Co. N-1700) was dissolved in the oil. The moving wavefront was traced optically by means of a cathetometer and telescope arrangement. All four samples were of #16 bleached fluid wicking from the same roll. The samples were all immersed simultaneously to a depth of $\frac{1}{2}$ in., and the height and time readings were commenced immediately. The data were analyzed after a preliminary plotting of $\ln(h)$ vs. $\ln(t)$ according to the method of least squares for a straight line fit. The constants were found as in a previous section and allow a comparison of the parameters of interest. Figure 7 shows the results.

As can be seen in Table II, the four samples

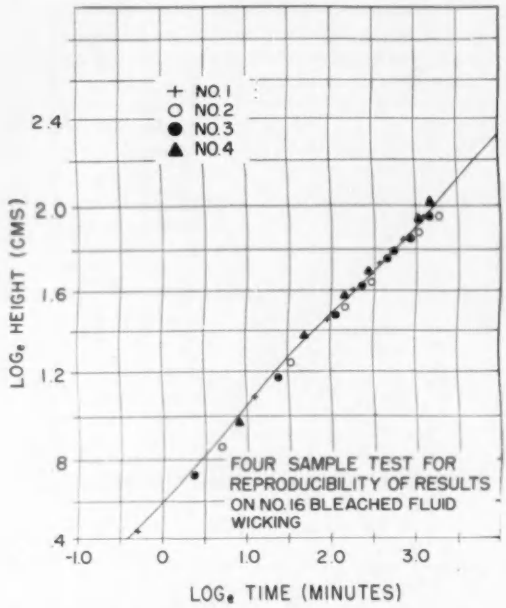

Fig. 7. ln(height) vs. ln(time) for #16 Fluid wicking.

TABLE II. Measured Parameters of Four Different Samples of No. 16 Bleached Fluid Wicking

Sample No.	Values of the coefficient, C'	Values of the exponent, k	dh/dt
1	1.78	0.45	$0.79\,t^{-0.55}$
2	1.77	0.44	$0.78\,t^{-0.56}$
3	1.76	0.45	$0.80\,t^{-0.55}$
4	1.81	0.44	$0.80\,t^{-0.56}$
Mean value	1.78	0.45	$0.79\,t^{-0.56}$

showed good agreement in the exponent and coefficient, and a corresponding good agreement in the calculated values of dh/dt. The least-squares solution for the coefficient of the rise-rate equation gave an average value of 0.79 for the four samples. The maximum deviation from this mean was about 1%; the other coefficients differed negligibly. The exponent, k, from the h vs. t data is seen to vary by about the same amount. These data indicate that accurately reproducible results can be obtained by an observer if precautions are taken to ensure the same physical condition of the wicking. Data taken on different days may vary due to environmental changes. For example, a sample of the same wicking tested in a similar manner a week prior to the tests described, yielded the following:

$$h = 1.90t^{0.43}$$

Calculation of the coefficient for dh/dt in this case gives 0.82, which may be compared to the mean coefficient of 0.79 above. The difference is about 4%. The exponent in the dh/dt calculation is seen to be equal to 0.57, and the corresponding figure from the four-sample experiment was 0.56, giving a difference of about 2% from the mean value.

These comparisons lead us to believe that measurements of dh/dt, which can be related to flow, can be made with a reproducibility of about 7% at the longest times measured, and somewhat less (~5%) at shorter times.

Literature Cited

1. Barrer, R. M., *Disc. Faraday Soc.*, No. 3 (1948).
2. Laughlin, R. D., HRB-Singer Report 504-BR-2 (1959).
3. Minor, F. W., Schwartz, A. M., Wulkow, E. A., and Buckles, L. C., TEXTILE RESEARCH JOURNAL **29**, 931 (1959).
4. Müller, R. H. and Clegg, D. L., *Anal. Chem.* **23**, 403 (1951).
5. Palmer, W. B., *J. Textile Inst.* **44**, T391 (1955).
6. Peek, R. L., Jr. and McLean, D. A., *Ind. Eng. Chem., Anal. Ed.* **6**, 85 (1934).
7. Washburn, E. W., *Phys. Rev.* **17**, 273 (1921).
8. Winch, A. R., TEXTILE RESEARCH JOURNAL **29**, 193 (1959).

Manuscript received December 19, 1960.

Letters to the Editor

The Molecular Configuration of Wool Keratin

The University of New South Wales
School of Wool Technology
Kensington, N. S. W.
June 23, 1961

To the Editor
Textile Research Journal

Dear Sir:

Recent theories concerning the macromolecular structure of wool keratin [1, 3] have centered on the high-molecular-weight, sulfur-deficient microfibrils and their association with the sulfur-rich matrix [2]. The existence of a series of low and high stability regions (X and Y zones) along the microfibril satisfies the conditions imposed by the interrelationships of set, transition temperature, supercontraction, and stress relaxation [2, 4].

Before this theory is acceptable, experimental data concerning load–extention and creep in the post-yield region must be shown to be compatible with this generalized structure; a drastic alteration in the stability of the zones must, therefore, be reflected in a predictable fashion by all the mechanical properties of the fiber.

Figures 1, 2, and 3 and Table I illustrate the results of load–extension, creep, supercontraction, and set experiments on fibers treated with Van Slyke's reagent [5]. The latter not only de-aminates but also confers great structural stability, increasing the transition temperature from *ca.* 60° C. to > 80° C.

The sample used has been previously studied [9] and exhibits an extremely slow rate of creep in the post-yield region. This causes complications when the region is further stabilized as in the present treatment. Creep experiments were necessarily con-

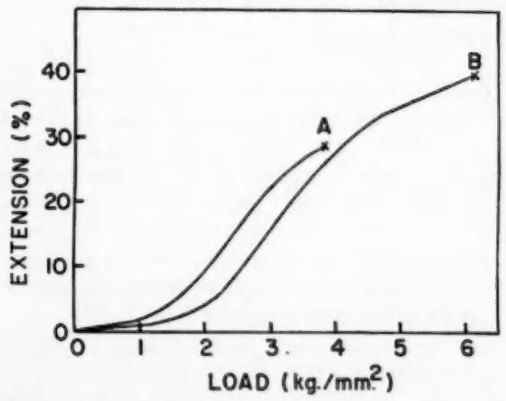

Fig. 1. Load–extension curve (A) treated, (B) untreated wool fibers in H_2O at 22° C.

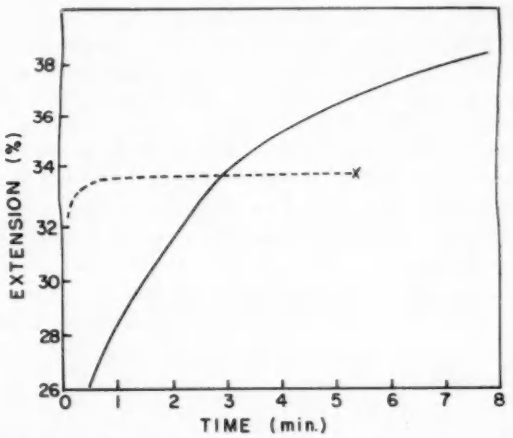

Fig. 2. Creep of (- - - -) treated, (———) untreated wool fibers in H_2O at 22° C. Load = 6.0 kg./mm.²

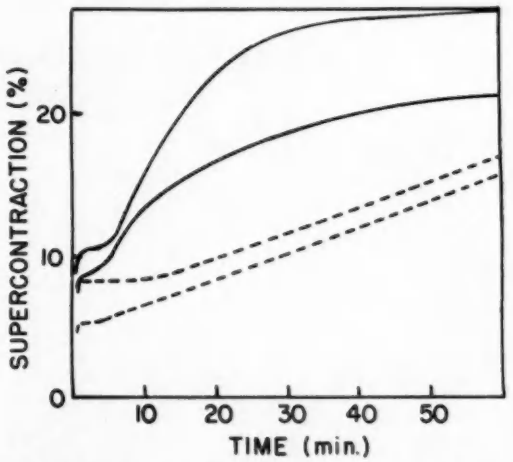

Fig. 3. Kinetic contraction curves of (- - - -) treated, (———) untreated wool fibers in 8.3 *M* NaI at 100° C.

TABLE I. Fibers Extended 40% in H_2O at 50° C., then Boiled 60 min., before Relaxing at Boil for Various Times

Time of relaxation, min.	Extension, %	
	Treated	Untreated
5	−2.7	13.5
10	−4.3	7.6
20	−5.5	4.0
40	−7.5	−0.5
60	−10.8	−2.5
	6 Fibers	8 Fibers

ducted over short periods and breakages were severe. This is not surprising as the load applied (6 kg./mm.^{2}) was greater than the mean breaking stress observed during the load–extension trials.

The work to extend treated fibers in the yield region was considerably lessened, but little extension in the post-yield region was possible and the turnover point into the post-yield region occurred at a significantly lower strain. The untreated fibers also exhibit an unusually low breaking strain and this appears to bear a direct relationship to their creep behavior. This relationship will be the subject of a later paper.

Supercontraction results are in agreement with an earlier paper [8], being closely related to the later stages of creep. The data on set can be similarly interpreted.

All the results offer support for the two-zone theory and further emphasize the significance of the post-yield region of wool fibers [10]. It must be remembered, however, that this treatment virtually immobilizes the post-yield region [6]. There is a variety of treatments which simply modify it, and under these conditions it becomes obvious that the theoretical treatment does not hold. The introduction of bis-thio-ether linkages or the weathering of fibers, for example, can alter the various mechanical properties in opposite directions. It would appear that the Y zone must be further subdivided into two zones on the basis of disulfide bond reactivity. These results will be the subject of forthcoming papers.

Literature Cited

1. Crewther, W. G. and Dowling, L. M., TEXTILE RESEARCH JOURNAL **29**, 541 (1959).
2. Earland, C. and Wiseman, A., *Biochim. et Biophys. Acta* **36**, 273 (1959).
3. Feughelman, M. and Haly, A. R., *Kolloid-Z.* **168**, 107 (1960).
4. Feughelman, M., Haly, A. R., and Mitchell, T. W., TEXTILE RESEARCH JOURNAL **28**, 655 (1958).
5. Rigby, B. J., TEXTILE RESEARCH JOURNAL **29**, 926 (1959).
6. Speakman, J. B., *Proc. Roy. Soc. (London)*, **103B**, 377 (1928).
7. Speakman, J. B. and Stott, G. L., *Trans. Faraday Soc.* **30**, 539 (1934).
8. Whiteley, K. J., *Nature* **186**, 473 (1960).
9. Whiteley, K. J., Ph.D. Thesis, Leeds, 38 (1959).
10. Whiteley, K. J. and Speakmen, J. B., TEXTILE RESEARCH JOURNAL **30**, 46 (1960).

K. J. WHITELEY

Non-Lint Content Measurement by the One-Pass Shirley Analyzer Procedure

Technological Laboratory
Indian Central Cotton Committee
Adenwala Road, Matunga, Bombay 19, India
May 29, 1961

To the Editor
TEXTILE RESEARCH JOURNAL

Dear Sir:

I have read with interest the letter with the above title by Mr. Jacob V. Shepherd [1] published in the January 1961 issue of your Journal. In this connection, I have to point out that a similar investigation was conducted at the Technological Laboratory of the Indian Central Cotton Committee, Bombay, and that the results were published in the March 1959 issue of the *Indian Cotton Growing Review* [2] and as *Technological Bulletin, Series B*, No. 66 of the Laboratory. Mr. Shepherd does not appear to have seen this article.[1] In that study, 20 samples of cotton were tested under controlled conditions, 84° F. and 65% RH. The method followed for the determination of the non-lint content of the cotton was a single-passage procedure very like that followed by the Stoneville Laboratory,

[1] Editor's note: Mr. Shepherd had indeed not seen this article and was glad to have it called to his attention.

except for some minor details. The results obtained showed that the single passage gave lower values than the double passage for the trash content actually measured, the total loss, and the invisible loss, the differences being, on the average, 0.48%, 1.05%, and 0.56%, for the three quantities.

Although the single-passage method gave lower values than the double-passage method, there was a very high degree of correlation between the values obtained by the two methods, the correlation coefficients being +0.997, +0.995, and +0.935, respectively. Because of this high correlation, the value according to the double-passage method could be derived from that according to the single-passage method with a high degree of accuracy, and regression equations have been derived for predicting these values. The accuracy of determinations by the two methods is also the same, since the corresponding standard errors are nearly equal. It has also been pointed out that the single-passage method is not only much easier, but saves considerable time as compared with the double-passage method.

It is pleasing to note that the results obtained by Mr. Shepherd are in close agreement with those obtained in the earlier study mentioned above. His suggestion for the addition of 0.36 g. to the weight of the clean lint would further enhance the accuracy of the results by allowing for the weight loss due to weighing the clean lint immediately after passing it through the machine without conditioning it.

Literature Cited

1. Shepherd, Jacob V., Textile Research Journal **31**, 75–78 (1961).
2. Gupte, V. V. and Iyengar, R. L. N., "A Comparison of Different Methods of Testing by the Shirley Analyser," *Indian Cotton Growing Review* **13**, 101–108 (1959); *Indian Central Cotton Comm., Technol. Lab. Technol. Bull., Ser. B*, No. 66.

R. L. N. Iyengar

Molecular Conformation in Oriented Fibers

Textile Research Institute
Princeton, New Jersey
June 22, 1961

To the Editor
Textile Research Journal

Dear Sir:

One of the most important advances in polymer science was the elucidation of the molecular conformations and the mean square end-to-end distance of the randomly coiled polymer chain. This knowledge was important in developing the equation of state for rubber elasticity, for deriving equations expressing intrinsic viscosity in terms of chain length, for interpreting light-scattering data from dilute solutions, and for promoting the growth of other important theoretical concepts. No similar study has heretofore been made of the molecular chains in an oriented fiber. This paper summarizes the results of such a theoretical analysis.

The molecular chains in a fiber are considered to trace out a path on a cubic crystal lattice. The chain passes through amorphous regions in which the link vectors of the chain successively point in the three-dimensional coordinate directions $\pm x$, $\pm y$, and $\pm z$. The chain also passes through crystalline regions in which successive x components all point in the $+x$ direction or the $-x$ direction. This model corresponds to a fiber whose crystallites are completely oriented in the x direction. Utilizing a cubic crystal lattice does not restrict the generality of the model because the successive links are considered as average components of the actual bond vectors.

In the amorphous regions the lengths of each link will be taken as ± 1, using the unit of length $l_0/\sqrt{3}$, with l_0 equal to the bond length. In the crystalline regions the lengths of each link will again be taken as ± 1 in the same units. The y and z components in the crystalline regions are taken to be zero. In actuality it is the sum of the y components in the crystalline regions that is zero because the molecular chains in these regions have a regular spiral structure. The same consideration applies to the z components.

Consider the successive x components only. They can exist in four states r_+, r_-, h_+, and h_-, where r_+ is

the state of an x component in an amorphous region pointing in the $+1$ direction, r_- is a similar state pointing in the -1 direction, h_+ is the state of an x component in a crystalline region pointing in the $+1$ direction, and h_- is the similar state pointing in the -1 direction. The successive x components form a Markoff chain [1]. The matrix of transition probabilities for successive elements in the chain is given by

$$P = \begin{array}{c|cccc} & r_+ & r_- & h_+ & h_- \\ \hline r_+ & \frac{1-p}{2} & \frac{1-p}{2} & p & 0 \\ r_- & \frac{1-p}{2} & \frac{1-p}{2} & 0 & p \\ h_+ & 1-\alpha & 0 & \alpha & 0 \\ h_- & 0 & 1-\alpha & 0 & \alpha \end{array} \quad (1)$$

The probability for an x component in the r_+ state to be followed by an x component in the h_+ state is equal to p. The probability that an x component in the h_+ is followed by one in the same state is given by α. The other transition probabilities are all shown in the matrix P. The mathematical methods of the Markoff chain permit the calculation of many important properties of the molecular chain in terms of the quantities p and α. The principal ones will now be presented.

The fraction of the x components that exist in the h_+ and h_- states can be regarded as the fractional degree of crystallinity, which is given by the formula

$$\text{Fractional crystallinity} = p/(1-\alpha+p) \quad (2)$$

The fraction of the x components that exist in the r_+ and r_- states can be regarded as the fractional degree of amorphicity, which is given by the formula

$$\text{Fractional degree of amorphicity} = (1-\alpha)/(1-\alpha+p) \quad (3)$$

A sequence may be defined as an unbroken succession of components in the same state. The average size of the h_+ or h_- sequences can be regarded as the sequence length in the crystalline regions.

$$\text{Average sequence length in crystalline regions} = 1/(1-\alpha) \quad (4)$$

Similarly the average size of an amorphous sequence can be obtained from a succession of components in either the r_+ or r_- states, and it may be calculated from the following formula

$$\text{Average sequence length in amorphous regions} = 1/p \quad (5)$$

Finally, the mean square length of a chain of n links in the x direction is given by

$$\bar{R}_x^2 = \left[\frac{2p(2-\alpha)}{(1-\alpha)(1-p)(1-\alpha+p)} + \frac{1+p}{1-p}\right]\frac{nl_0^2}{3} \quad (6)$$

By comparison, the value of $\bar{R}_x^2$ if p is equal to zero, i.e., if the chain does not enter into a crystalline state is

$$\bar{R}_{x^2(p=0)} = \frac{nl_0^2}{3} \quad (7)$$

The ratio of $\bar{R}_x^2$ to $\bar{R}_{x^2(p=0)}$ can be interpreted as the ratio of the square of the length of the oriented fiber to the square of the length of the fiber after being raised above its melting temperature

$$\left(\frac{\bar{R}_x^2}{\bar{R}_{x^2(p=0)}}\right)^{\frac{1}{2}} = \frac{\text{length of oriented fiber}}{\text{length of shrunk fiber}} = \left[\frac{2p(2-\alpha)}{(1-\alpha)(1-p)(1-\alpha+p)} + \frac{1+p}{1-p}\right]^{\frac{1}{2}} \quad (8)$$

Equations 2, 4, and 8 give three physically measurable quantities, the fractional degree of crystallization, the sequence length in the crystalline regions, and the shrink ratio in terms of two molecular parameters, α and p. The self consistency of these relations can, therefore, be checked experimentally.

Ultimately it may be possible to describe fibers and fiber properties in terms of these two molecular parameters, α and p. By using Equations 2, 4, and 8, values of α and p can be determined for fibers and correlated with the method of orientation and drawing.

The help of Professor W. Feller is deriving Equation 8 is deeply appreciated. The support of the Office of Naval Research, Contract No. Nonr-09000 and Nonr-09001, is gratefully acknowledged.

A mathematical appendix to this paper will be published elsewhere.

Literature Cited

1. Feller, W., "An Introduction to Probability Theory," 2nd edition, New York, John Wiley and Sons, Inc., 1957, pp. 338–349, 380–385.

A. V. TOBOLSKY
V. D. GUPTA

Action of Hypochlorite on Resin-Treated Cotton

Ahmedabad Textile Industry's
Research Association
Navrangpura, Ahmedabad 9, India
June 6, 1961

To the Editor
Textile Research Journal

Dear Sir:

Recently, the Piedmont Section of AATCC published an account of their very interesting work on the chlorine retention of resin-treated cotton fabrics [4]. We have been studying this problem along similar lines for the last two years and would like to supplement the published observations with our data. The aim of our investigation was to study the kinetics of chlorine retention, a subject which has received little attention.

The resin-treated cotton fabric was treated with hypochlorite (2.5 g./l.) at pH 9.5 at 35° C. for different periods of time. Dimethylol urea (DMU) was selected first because, with its high chlorine retention, experimentation was expected to be simpler.

The results (Table I) show that during treatment with hypochlorite, there is a rapid loss of nitrogen from the fabric and of active chlorine from the hypochlorite bath. Activation of hypochlorite solutions by urea and other nitrogenous compounds has been reported [5]. Nitrogenous decomposition products of DMU as well as formaldehyde, liberated through decomposition of DMU in the hypochlorite treatment, may account for the accelerated loss of active chlorine. The possibility of oxycellulose formation in the redox system formaldehyde–hypochlorite was also investigated. Several examples of such oxidation of cellulose with other redox systems have been published [2]. The cotton fabric after hypochlorite treatment was washed thoroughly, treated with 0.1 *N* HCl at 65° C. for 30 min. to remove the resin (and retained chlorine), washed, and then tested for carboxyl content. No significant increase was found over the corresponding control sample. The test sample also did not show a discoloration on scorching, which is a qualitative test for oxycellulose.

Due to the rapid decomposition of DMU on hypochlorite treatment, dimethylol ethylene urea (DMEU) was studied next, using magnesium chloride as catalyst for curing at 150° C. for 5 min. The DMEU-treated cotton fabric was also treated with hypochlorite as before. A material:liquor ratio of 1:500 was used, however, to minimize variations in bath concentration due to possible activation of the hypochlorite. Table II shows that even DMEU is quite unstable to prolonged hypochlorite treatments, resulting in a loss of nitrogen and of fabric crease recovery accompanied by decomposition of the hypochlorite. Corresponding treatment with alkali alone at pH 9.5 does not produce either nitrogen loss or fall in crease recovery.

In spite of the large decrease in nitrogen content, chlorine retention steadily increases with increasing time of hypochlorite treatment. NCH_2OH content, determined by the method published earlier [1] first decreases and then increases (Table III). If one takes into account the following reactions, occurring

TABLE I. Treatment of DMU-Treated Cotton with Hypochlorite

Time of treatment	Loss of nitrogen from fabric, %	Conc. of available chlorine in bath, g./l.
0	00.0	2.50
10 min.	—	2.21
15 min.	18.2	1.71
30 min.	—	1.44
60 min.	—	0.84
3 hr.	36.4	—
8 hr.	48.8	—
26 hr.	74.0	—

TABLE II. Treatment of DMEU-Treated Cotton with Hypochlorite

Time of treatment, hr.	Decomposition of bath, %	Loss of fabric crease recovery, %	Loss of nitrogen from fabric, %
0	—	—	—
1	1.4	10.8	—
3	2.1	8.1	2.5
6	3.6	4.1	7.7
24	11.7	10.9	18.0
96	23.4	22.2	15.5
192	48.1	41.4	28.2

simultaneously

$$\text{Cell–OCH}_2\text{N–C} \longrightarrow \text{Cell} + \text{>N·CH}_2\text{OH}$$

$$\text{>N·CH}_2\text{OH} \xrightarrow{\text{OH}^-} \text{>NH} + \text{HCHO}$$

$$\text{>NH} \xrightarrow{\text{OCl}^-} \text{>N·Cl}$$

and estimates the total NCH_2OH produced as free NCH_2OH (experimentally determined) + NCH_2OH equivalent to N·Cl (calculated from values of retained chlorine) one obtains the values given in column 5 of Table III, which show a steady increase in NCH_2OH formation. The progressive fall in crease recovery shown in Table II would indicate an extensive rupture of the cellulose–DMEU cross-links, which should result in a continuous increase in $N{\cdot}CH_2OH$ formation as observed here.

The mechanism by which these cross-links are broken is not clear. Oxidative attack of the hypochlorite on DMEU or cellulose or both may be taking place. Cyclic ethylene urea (CEU) itself may, like N-chlorohydantoins [3], undergo the following reactions:

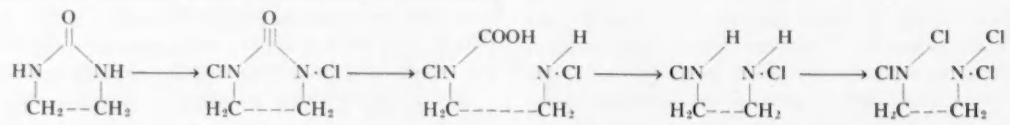

Some evidence for such a reaction is obtained from the observation that when CEU is reacted with hypochlorite, the chlorine consumption is much greater than that calculated for chloramine formation. In the case of DMEU-treated cellulose, however, such a reaction can operate only with the small proportion of DMEU which has reacted with, but not cross-linked, cellulose.

Further work is in progress and will be reported later.

TABLE III. Treatment of DMEU-Treated Cotton with Hypochlorite; Increase in NCH_2OH Content and Retained Chlorine

Time of treatment, hr.	NCH_2OH content	Retained chlorine	NCH_2OH equivalent of retained chlorine	Corrected NCH_2OH
0	0.324	—	—	0.324
1	0.235	0.0809	0.0736	0.309
3	0.247	0.1031	0.0938	0.341
6	0.257	0.1210	0.1100	0.367
24	0.314	0.1569	0.1427	0.457
96	0.392	0.1479	0.1345	0.527
192	0.363	0.2824	0.2568	0.620

Literature Cited

1. Mehta, P. C. and Modi, J. R., TEXTILE RESEARCH JOURNAL **30**, 532 (1960).
2. Nabar, G. M., Scholefield, F., and Turner, H. A., *J. Soc. Dyers Colourists* **53**, 5 (1957).
3. Petterson, R. C. and Grzeskowiak, U., *J. Org. Chem.* **24**, 1414 (1959).
4. Wayland, R. L., Jr., *Am. Dyestuff Reptr.* **49**, 55 (1960).
5. Zakoschikor et al., *Zhur. Priklad. Khim.* **10**, 36 (1937).

M. K. GOKHALE
P. C. MEHTA

In Coming Issues

Theoretical Aspects of Hook Removal at Drafting Operations. *V. B. Merchant*

The Use of Coreactant Curing Agents with a Diepoxide to Impart Wrinkle Resistance to Cotton Fabrics. *Robert M. Reinhardt, Russell M. H. Kullman, Harry B. Moore, and J. David Reid*

The Effect of Radial Heterogeneity on Fiber Properties. *R. W. Singleton and M. A. Sieminski*

Studies on the Chlorine Retention of Fabrics Treated with Dimethylol Ethylene Urea. *P. C. Mehta and J. R. Mody*

The Accelerotor as a Test Machine for Felting Shrinkage. *G. L. Stott*

Some Studies on the Formation of Hooks in Carding. *V. A. Wakankar, S. N. Bhaduri, B. R. Ramaswamy, and G. C. Ghosh*

The Physical Properties of Wool Fibers at Various Regains.

Part IV: Mechanical Changes due to "Incorporated" Water. *M. Feughelman and I. C. Watt*

Part V: The Nature of Birefringence. *A. R. Haly and O. A. Swanepoel*

Relaxation Shrinkage of Wool Fabrics: Its Occurrence in Worsteds, and Dependence upon Cloth Structures. *K. Baird*

A Modification of the Method for Defining and Measuring Crimp of Textile Fibers. *M. Shiloh, J. Goldstein, D. Mejzler, and E. Alexander*

Boundary Friction of Textile Fibers. *Tomlinson Fort, Jr. and J. S. Olsen*

Fiber Configuration in Sliver and Roving and its Effect on Yarn Quality. *A. R. Garde, V. A. Wakankar, and S. N. Bhaduri*

FIBER PHYSICIST

Position is now available in the Charlotte Developement Laboratories for a Senior Physicist, Physical Chemist or Engineer with a strong academic background in physics and physical chemistry, and a zest for challenging assignments. The opening requires a minimum of 3 years experience in man-made fibers or other field involving properties of visco-elastic elements.

Excellent opportunity for advancement and personal recognition. Send resume, including salary requirements, to E. C. Johnson.

Celanese

CORPORATION OF AMERICA

P. O. Box 1414 Charlotte 1, N. Carolina